StructuralComponents7.0

A study of rigid frames behaviour and a computational tool prototype
for the early design of mid-rise buildings

by

David Arturo Niño Romero
November 2019

TU Delft Delft University of Technology

StructuralComponents7.0

A study of rigid frames behaviour and a computational tool prototype
for the early design of mid-rise buildings

by

David Arturo Niño Romero
Student number: 4745000

in fulfilment of the requirements for the degree of

Master of Science
in Structural Engineering

at the Delft University of Technology
in coordination with White Lioness technologies,
to be defended publicly on the 15th of November 2019.

Thesis committee:	Prof. dr. ir. J.G. Rots (Chairperson)	TU Delft
	Dr. ir. J. Coenders (Supervisor)	White Lioness technologies
	Dr. ir. M.A.N Hendriks (Supervisor)	TU Delft
	Ir. R. Crielaard (Supervisor)	TU Delft
	Ir. B. Hohrath (Daily Supervisor)	White Lioness technologies

PREFACE

This is the final Master's thesis report of David Arturo Niño Romero for the degree in Structural Engineering from the Delft University of Technology. This research project contributes to the ongoing development of "Structural-Components" that addresses the early-stage design computational tools for buildings.

The work in this thesis was made in the:

Department of Structural Mechanics
Faculty of Civil Engineering & Geo-sciences
Delft University of Technology
in cooperation with White Lioness technologies

Graduation committee:

Prof. dr. ir. J.G. Rots (Chairperson)
E-mail: J.G.Rots@tudelft.nl
Affiliation: Delft University of Technology
Faculty of Civil Engineering and Geo-sciences.

Dr. ir. J. Coenders (Supervisor)
E-mail: jeroencoenders@white-lioness.com
Affiliation: Founder and CEO of White Lioness technologies

Dr. ir. M.A.N Hendriks (Supervisor)
E-mail: M.A.N.Hendriks@tudelft.nl
Affiliation: Delft University of Technology
Faculty of Civil Engineering and Geo-sciences.

Ir. R. Crielaard (Supervisor)
E-mail: R.Crielaard@tudelft.nl
Affiliation: Delft University of Technology
Faculty of Civil Engineering and Geo-sciences.

Ir. B. Hohrath (Daily Supervisor)
E-mail: babettehohrath@white-lioness.com
Affiliation: White Lioness technologies

ACKNOWLEDGEMENTS

There are many people that gave me support during the development and writing of my thesis. I am very grateful with all of them.

I want to sincerely thank my graduation committee: Prof. dr. ir. J.G. Rots, Dr. ir. J. Coenders, Dr. ir. M.A.N Hendriks, Ir. R. Crielaard and Ir. B. Hohrath. Thanks again to Jeroen Coenders that shared with me and introduced me to "StructuralComponents". I would also like to thank Ir. J.W. (Hans) Welleman who provided me with his guidance on many occasions.

Thanks to my friends that took the time to repeatedly check my report, and to the ones that shared their ideas and support. Special thanks to my friends that gave me their support during the most challenging times of my Master.

And finally, thanks to my family, in spite of the distance, I could always feel their support during this stage of my life.

SUMMARY

During the early stages of the construction process of a building, the potential impact of design decisions is at its greatest. Paradoxically, design freedom is maximum at this stage and continuously decreases from then onwards, while the opposite pattern occurs with the volume of available information. This paradox is based on the MacLeamy curve (MacLeamy, 2004) . One of the reasons for the reduced volume of available information at preliminary stages is the lack of computational tools and that the available ones are not being used to their full potential (Coenders, 2011) . To address this, StructuralComponents has been in development as a parametric and real-time preliminary design tool for building structures.

The main objective of this research project was the expansion of StructuralComponents by the development of a parametric real-time computational tool prototype to quickly determine the feasibility of mid-rise buildings designs with rigid frames as stability members. This was done by means of the research on the analytical representation of rigid frames under lateral loads.

The study of rigid frames behaviour was performed to define a range of applicability of the existing analytical representation and to develop two new methods to analytically represent rigid frames behaviour: a correction method for the shear beam representation and a method based on the Timoshenko beam theory. To allow for vertical connections of different rigid frame geometries, an analytical method to consider a different stiffness along the height was developed. The results showed that the analytical shear beam representation of rigid frames has a reduced range of applicability for parametric purposes. This reduced applicability is due to the combined shear and bending behaviour, which depends mainly on the beam-to-column inertia ratio and the overall slenderness.

The correction method follows from the prediction of the error when using the shear beam representation. In addition to the correction of the shear beam representation, the prediction of the error was defined as a parameter to classify the behaviour of a rigid frame as a shear, flexural or combined type. It was defined that, if the error is less than 20 percent, the shear beam solution is accurate enough for the preliminary design and that if the error is greater than 40 percent the bending effects are predominant. Both, the applicability range and the correction method are based on analytical and numerical comparisons. The implemented software comprises Maplesoft to get the analytical solutions and Grasshopper with Karamba3D (which contains the finite element solver) to get the numerical solutions. The method based on the Timoshenko beam theory comes from the theoretical derivations of a serial system that takes into account both, bending and shear deformations. It was found that it is more appropriate to analytically represent the

general behaviour of rigid frames with the Timoshenko beam theory and by additionally considering a different stiffness calculation for the ground floor.

Also, it was shown that the vertical connections of rigid frame geometries can be addressed with the calculation of an analytical solution for each different geometry along the height, and this was achieved with the use of boundary and matching conditions. Both analytical approaches, the Timoshenko beam representation and the method for vertical connections were implemented in the tool prototype.

The computational tool prototype consists of a calculation method to assess the structural performance of a complete building by the simultaneous structural analysis of every rigid frame subjected to a lateral load. First, the lateral load is assumed to be transferred from the facade to the lateral stability members as a uniformly distributed load. Then, the displacement solutions are obtained from differential Equations 0.1 and 0.2 which are derived from the Timoshenko beam theory for static determinate schemes; for this case, the idealisation of a rigid frame as a cantilever beam. This derivation is based on the fact that the moment and shear distributions can be found through equilibrium. The subdivision of the 1D idealisation, and therefore the use of a set of differential equations to get the analytical solutions, allows taking into account a different stiffness along the height as shown in Figure 1.1. The three main characteristics of the tool prototype are the parametric adaptability, the instantaneous display of results and the stacking "Lego-type" connection between components.

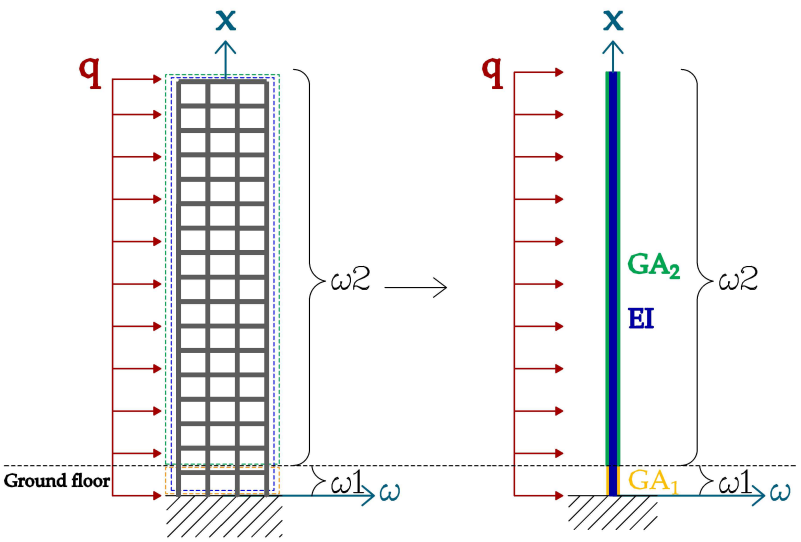

Figure 0.1: Physical structural system and the analytical Timoshenko beam representaion (Serial system)

$$\frac{\mathrm{d}^2}{\mathrm{d}x^2} w1\,(x) = -\frac{q}{GA1} - \frac{M}{EI} \tag{0.1}$$

$$\frac{\mathrm{d}^2}{\mathrm{d}x^2} w2\,(x) = -\frac{q}{GA2} - \frac{M}{EI} \tag{0.2}$$

The concepts of the applicability range, the correction method for the shear beam representation, the Timoshenko beam representation and the method for vertical connections were tested and validated with numerical calculations with the finite element solver embedded in Karamba3D. The validations in this research project show that the proposed and implemented methods are suitable for preliminary design stages because the error for the most unfavourable geometric configurations resulted in less than 15 percent.

The expansion of StrucuturalComponents was achieved through the research into rigid frames behaviour and the development of a computational tool prototype. It is recommended to conduct further research and tool development for different structural systems and, additionally, to include feasibility checks that involve other disciplines (for example architecture, environmental engineering or engineering economics). In so doing, more informed decisions can be made at the preliminary stages during the construction of a building.

CONTENTS

1 INTRODUCTION

The motivation of this research project and the background of previous works of StructuralComponents are addressed in this chapter as well as a general overview of computational tools in the building industry.

1.1 MOTIVATION

During the design, engineering and construction of a building, a paradox arises between the design freedom and the available information to make decisions. This paradox is based on the MacLeamy curve introduced in 2004, where the potential impact of decisions is compared to the cost of design changes. It is conveyed that at the preliminary stages, the design freedom is maximum but continuously decreases for the proceeding stages and that an opposite pattern occurs with the volume of available information.

The availability of computational tools can be related to the increasing pattern as shown by Rolvink (2010) . These variables and patterns are graphically presented in Figure 1.1. StructuralComponents is intended to change the pattern of the available tools by being a powerful tool for the early design stage of a building so that better-informed decisions can be made even from preliminary designs.

As presented in Figure 1.1, there exists a lack of tools for the preliminary design stage especially regarding the structural performance of such a design. This is explicitly expressed as a gap between the architecture and structural engineering disciplines by Hohrath (2018).

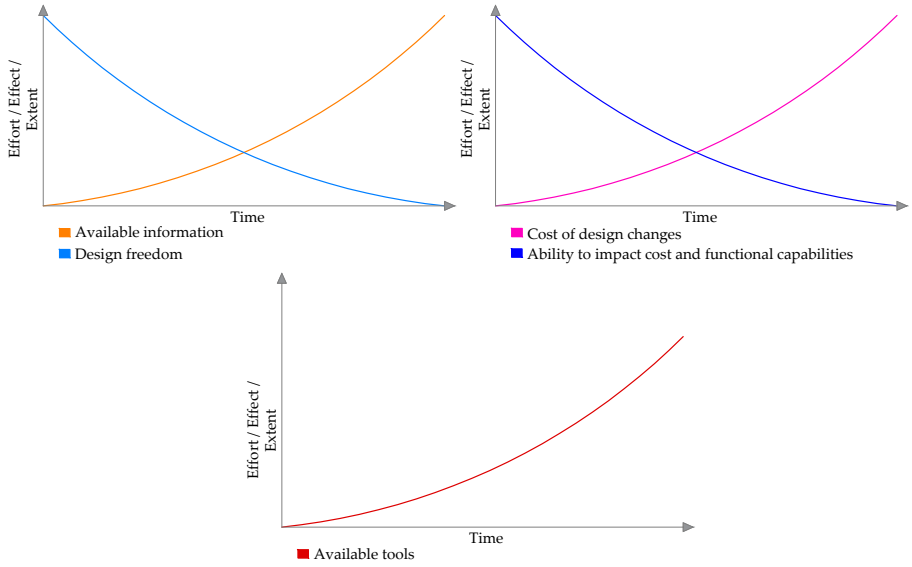

Figure 1.1: Paradox during the design, engineering and construction of a building

1.2 STRUCTURALCOMPONENTS

1.2.1 Background

There have already been previous works and contributions to the concept and development of StructuralComponents.

Structural Design Tools (SDT) approach was introduced by Coenders and Wagemans (2006) in "Structural Design Tools: The next step in modelling for structural design". This approach had the goal to guide the computational developments and strategies so that the engineer can support their design decisions. In the same line, it aimed to provide designers with the possibility of creating their own tools and not to be completely restrained to the existing solutions, in agreement with the idea that the development should not be technology-driven but user-driven as expressed by Coenders (2011)

NetworkedDesigned "Next generation for computational design" by Coenders (2011) addressed the creation of a computational infrastructure where the life cycle of a building can be followed so that the loss of information and the gaps between design engineering processes can be reduced. An important characteristic of this infrastructure is the possibility to support the development of tools, applications, frameworks and systems to provide new opportunities for the use of computation in different disci-

plines such as for structural design and engineering, so new design tools as StructuralComponents can be developed (Coenders, 2011) .

StructuralComponents1.0 (SC1.0) "Development of parametric associative design tools for the structural design of high-rise buildings" by Breider (2008) can be considered as one of the first strategies based on the SDT methodology to rapidly evaluate the structural performance of a building during the conceptual design phase (Rolvink, 2010) . SC1.0 provides the engineer with a dashboard to visualise near real-time structural analysis and design results, which are placed alongside the generated 2D structural model. This tool consists of a group of components enabled in the GenerativeComponents software tool to model, assemble, analyse and process results of several configurations of a building comprised of cores, columns and/or outriggers, with the Lego-block quality in order to provide versatility and flexibility. Breider implements the Super Element Method (SEM) where the structural behaviour can be determined by analytical expressions instead of shape functions. The following three aspects are described by Rolvink (2010) as the principal shortcomings of SC1.0: 2D models only, a limited number of components and a software code which is not set up in a modular way.

StructuralComponents2.0 (SC2.0) "A Parametric and associative toolbox for conceptual design of tall Building Structures" by Rolvink (2010) provided a framework for the toolbox with the modular setup feature based on an Object-Oriented-Programming (OOP) class language. This allowed the connection of the framework to different computational applications and the possibility to extend the functionality Rolvink (2010) . Furthermore, research into the analysis methods for the conceptual design of tall buildings was performed and implemented into the now 3D toolbox. This prototype of StructuralComponents was developed for Grasshopper which is the graphical algorithm editor integrated for Rhino3D modelling (Davidson, 2019) . Rolvink presents as limitations the following: SC2.0 is based on software applications only supported by .NET framework, analysis for elements with both bending and shear deformation have been implemented for certain cases only. The SEM is also implemented for this version.

StructuralComponents3.0 (SC3.0) "A client-server software architecture for FEM-based structural design exploration" by VandeWeerd (2013) focused on the generation of design alternatives of the synthesis phase of a building and on the provision for more versatility and flexibility for the design by using finite element analysis (FEA) instead of the SEM as in previous versions. SC3.0 implements its own Parametric and Associative Design (PAD) system in order to break the dependency with Rhino and Grasshopper, however this reduces the usability, visualisation and integration with CAD software as mentioned by Van de Weerd. It was also concluded that a higher emphasis on this phase of generation of alternatives by the use of an abstraction system can provide a better understanding of the influence of certain parameters on the overall performance of the building. Van de Weerd also states that the source code used in the system architecture is

complex, which causes difficulty for the extensibility of the tool and the easy of understanding by people with not enough programming skills.

StructuralComponents4.0 (SC4.0) "Conceptual building models with structural design justification" by Bovenberg (2015) had the main objective of representing structural design concepts not as simple analysis or modelling methods but as a complete design story or justification then, a better representation of the reasoning supporting the design is provided at the same time that an improved analysis and optimization can be accomplished by considering parallel alternatives (Bovenberg, 2015) . SC4.0 implemented a prototype that is formed by the conceptual design of a building, a parametric engine and a user interface. Based on this, high-level requirements of structural design during the conceptual stage were defined. Complete software implementation of the features of SC4.0 was not a goal, nor was the creation of a FEA analysis engine.

StructuralComponents5.0 (SC5.0) "Super element based tool for early design collaboration applied to mid-rise buildings" by Hohrath (2018) . The main objective was achieved by the development of a tool prototype consisting of three building blocks which are analysed with the SEM to immediately determine the structural feasibility of a concrete mid-rise building during the preliminary stage, as well as some architectural requirements.

The three building blocks were developed to model a complete building with concrete floors, shear walls and/or cores as structural systems. These systems, as mentioned by Ham and Terwel (2017) , are adequate to take lateral loads. At first, the loads are taken by the facades and then transferred to the floors and finally to the stability elements, which for this case are the shear walls or the cores.

One characteristic of the building blocks is that they are parametrically adaptable (Hohrath, 2018) . Another remarkable characteristic is the Lego-block connection type to stack the building blocks together to get the geometry envisioned. These blocks are capable to display specific kinematic or constitutive relations as shear forces, moments or displacements, along their length in real-time. The elements that compose a building block can change from grey to red when the elements do not fulfil the structural or architectural requirements.

To provide the building blocks with the capabilities of parametric adaptability, the displaying of real-time results and the stacking style connection, the following general software workflow was implemented for their development. First, the symbolic expressions are derived with Wolfram Mathematica or Maple, secondly, the derivations are scripted in Python, then, a parametric geometry is developed in Grasshopper and finally, the results are visualised in Rhino. This software workflow is similarly implemented in this research project, and it is shown in Figure 1.2.

One of the limitations of SC5.0 is the specific building type that can be modelled and analysed with this prototype, which is a mid-rise concrete

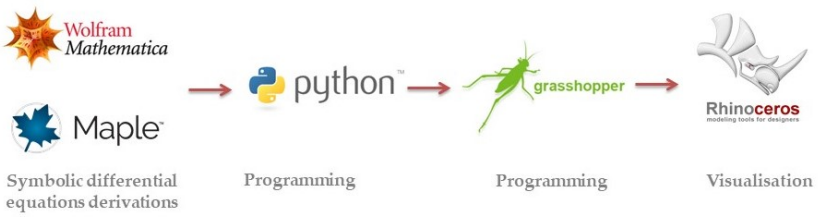

Figure 1.2: Software workflow in SC5.0 and SC7.0

building where the stability elements are shear walls or cores. Hohrath (2018) mentions that this situation critically reduces its use in practice.

StructuralComponents6.0 (SC6.0) "An early-stage design tool for flexible topologies of mid-rise concrete buildings" by Dierker (2019) consisted of the development of a tool for the conceptual design of concrete buildings where lateral stability is provided by different configurations of shear walls. Dierker describes this research project in three phases: the study of the conceptual design process, the development of a calculation method that can be used for any number and arrangement of shear walls, and the tool implementation through Python and Grasshopper. The calculation method can be understood as the simultaneously structural analysis of each stability member in the building, in this case, shear walls. A similar calculation method is implemented during this research project but for rigid frames as stability members.

In addition to the academic works on StructuralComponents, several scientific papers have been published as the following:

- "Structural Components - a parametric associative design toolbox for conceptual structural design" by Rolvink et al. (2010a)
- "StructuralComponents - a toolbox for conceptual structural design" by Rolvink et al. (2010b)
- "StructuralComponents 4: Conceptual building models with structural design justification" by Bovenberg et al. (2015)
- "Structural Components 5.0: Collaborative conceptual design tool for structural and architectural feasibility using super elements" by Hohrath et al. (2018)

1.2.2 Structural analysis methods

Many of the currently available tools, such as SAP2000 by CSI (2019) , Robot Structural Analysis by Autodesk (2019) and Karamba3D Parametric Engineering by Preisinger (2019) , perform structural analysis through the use of the finite element method (FEM) which is a numerical based method to solve partial differential equations. Its application involves a solution of very large systems of linear equations, which are arranged in a matrix form.

The FEM is very convenient for the analysis of complex geometries and it can be computationally automatised (Wells, 2006) . Conversely, some of the previous versions of StructuralComponents implement the Super Element Method (SEM) for the structural analysis phase.

It is probable that the SEM was used for the first time by the aerospace industry and implemented since the 1960s (Rolvink, 2010), but the type of analysis performed was different to the one implemented in StructuralComponents. The SEM type used for the aerospace industry, which is also referred as the Traditional Super Element Method, consisted of the condensation of nodes within a substructure, while the one implemented in StructuralComponents consists of the derivation of symbolic differential equations to obtain a closed-form solution for the displacements function. The latter was developed by Steenbergen (2007) who also defines a Super Element as a set of finite elements that together can be considered as only one element.

Steenbergen (2007) compares some aspects of the commonly used FEM with the SEM. Apart from the fact that calculation and modelling time is saved by the implementation of the SEM, a better understanding and insight into the structural behaviour is possible. This characteristic allows to easily identify the parameters governing the structural response what FEM cannot easily perform. Another advantage of the SEM is the capability to perform dynamic analysis to account for stochastic wind loads. This type of SEM consists of the derivation of symbolic differential equations for each super element. To include the boundaries and transitions of the elements, the pattern of the finite element method is adopted. Steenbergen (2007) describes this methodology as a "smart symbiosis" of the analytical method and the numerical based finite element method.

For this research project, the first phase of the SEM, which consists of the use of symbolic differential equations to represent a group of elements as a single element, is implemented. However, to include transitions between elements an analytical procedure is proposed instead of following the scheme of the FEM. This method can be defined as a complete symbolic and analytical representation of a group of elements. The reason to follow this approach is to reduce the computational effort of performing the FEM scheme and the assumption of the representation of the stability members of a building as cantilever beams.

1.3 COMPUTATIONAL TOOLS IN THE BUILDING INDUSTRY

Extensive research was performed in SC5.0 by Hohrath (2018) into existing and under development computational tools, not only in the building industry but also in the aerospace and automotive industries. Hohrath (2018) concludes that advance drawing tools are available for the Architec-

ture, Engineering and Construction industry (AEC) and that there are still several limitations for the structural analysis tools commercially available for the conceptual design phase. New tools additions to the overview presented in SC5.0 are briefly described below and supplementary comments on Karamba3D.

1.3.1 Structural analysis

Robot Structural Analysis by Autodesk. Since June 2018 the structural analysis capability of Revit was discontinued, which was due to release of Robot Structural Analysis (RSA). It is a structural analysis software based on the finite element method, with a powerful auto-meshing tool, a compilation of design codes and even the capability to perform nonlinear calculations (Autodesk, 2019) . One of the important advantages of RSA is its connection with Revit. This is convenient because of the capability of Revit to automatically reflect the changes made in the 3D-model anywhere else like in the architectural plans. However, RSA is also based on the FEM and it is mainly intended for later stages than the preliminary ones.

Karamba3D by Preisinger (2019) is a parametric tool used to evaluate the structural performance of a building in real-time. It uses the FEM and it is possible to study the structural behaviour of frames, spatial trusses and shells. Karamba3D was released in 2011 and introduced for practical use as a plugin for Grasshopper.

The capability of Karamba3D to show real-time results makes the tool attractive for the preliminary design of a building. It can be feasible to develop geometric and parametric building blocks that can be connected to the FEM solver component of Karamba3D. Then, the visualisation of specific results as internal forces, stresses or displacements can be programmed in a similar way as in StructuralComponents. Nonetheless, it also requires research on how to interpret and program the results generated by the FEM to provide insight into the behaviour of a complete building. A weak point of StructuralComponents is the limited versatility and flexibility to model different types of buildings, while this modelling freedom is higher with Karamba3D due to its embedded finite element solver. However, Karamba3D requires more detailed information and the creation of an specific set up of items to implement the finite element solver. To reach a fair comparison between the tools for the preliminary design stage, more detailed research should be performed for each of them on several aspects such as the following: computational effort, modelling freedom, the accuracy of the results, speed of real-time results and the insight of structural behaviour.

1.3.2 Optimisation

Kangaroo is a digital tool to explore shapes with form-finding procedures. It is also an engine for Grasshopper for shape optimisation. Kangaroo can computationally approximate rules imposed by nature for the shape optimisation process. There also exists Kangaroo physics which implements the particle-spring method to derive numerical solutions for complex geometries (Vanderlinden et al., 2018) . Then, Kangaroo is a convenient tool to define the optimal shape, in terms of structural performance, during the early design, but its application is intended more for membrane light-weight or shells structures.

Galapagos is a plugin for Grasshopper and an evolutionary solver to account optimisation problems. To use Galapagos it is necessary to set a specific objective obtained from a function or determined procedure. This objective can be achieved by several values combinations of the inputs to the function or procedure. Specifically, Galapagos generates a sample population of possible solutions by the variation of the inputs parameters, assign a specific score to each solution and, classify as high or low the performance of individuals samples. High-performance individuals samples are allowed to 'reproduce' and the low-performance are not. While running, Galapagos will converge in an area with the optimum solution (Vanderlinden et al., 2018) .

Octopus is also a plugin for Grasshopper and it works similarly to Galapagos. The difference relies on the allowance for more than one objective with its multi-fitness criteria characteristic. It is also useful to perform visual explorations of the range of potential solutions in a more intuitive way than Galapagos (Vanderlinden et al., 2018) .

1.3.3 Visualisation

Human UI by Heumann (2016) is a plugin for Grasshopper and can be used to create separate interfaces from the canvas in Grasshopper. It is an interactive tool of easy access and manipulation. These qualities can make the Grasshopper definitions accessible even for persons who are not familiar with the scripting processes of Grasshopper (Vanderlinden et al., 2018) . The implementation of Human UI into StructuralComponents is attractive to make the tool even easier to use. Figure 1.3 shows a possible configuration of HUMAN UI interface which is connected to a Grasshopper script.

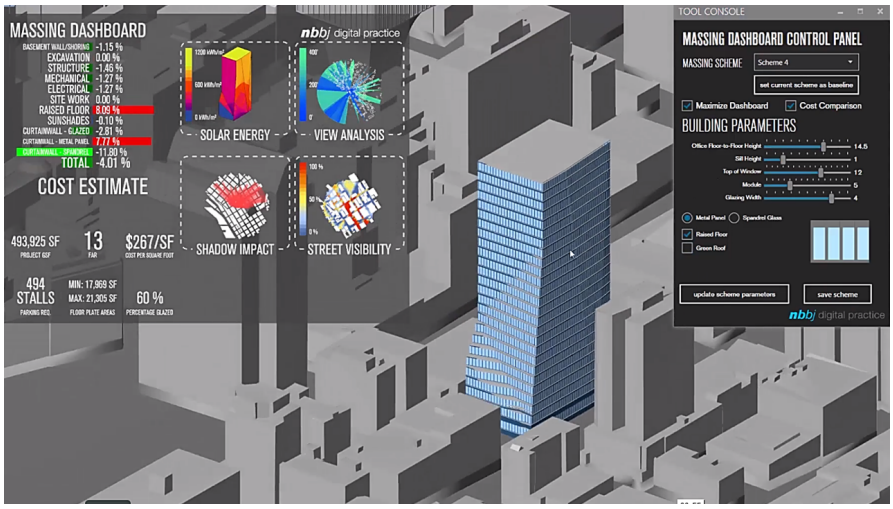

Figure 1.3: Human UI separate interface. © Copyright Performance Network 2019

Because of the necessity to define a specific objective and due to iterative features, to perform structural optimisation during the preliminary design stages can be complicated and time-consuming. However, they are presented as long term goal of including optimisation even at these early stages. Also, Robot, Karamba3D and Human UI are presented because it is considered that some of their explained features can contribute to improving StructuralComponents.

2 PROBLEM DEFINITION

In this chapter, several structural systems for mid-rise buildings are described and their already used analytical representation. A greater emphasis is given to rigid frames as structural systems. Based on the limitations of the analytical representation of rigid frames and the lack of computational tools for the preliminary design, the objectives, research questions, scope and methodology were defined and are presented in this chapter.

2.1 MID-RISE BUILDINGS STRUCTURAL SYSTEMS

The selection of an appropriate structural system to withstand lateral loads is an important process of the engineering of a building, especially to comply with structural requirements as stiffness and stability (Rolvink, 2010) . Strong determinants to choose or discard some structural systems are the intended use of the building and its total height. Depending on the height, the qualification of a building as high-rise or mid-rise is defined. The scope of this research project was limited to mid-rise buildings structures. Therefore, an overview of several structural systems in mid-rise buildings to withstand lateral loads and its analytical representation is presented. A deeper description is made for rigid frames systems.

The classification of a building as high, medium or low rise varies according to the referred literature or construction code. It is mentioned by Breider (2008) that the definition of a building as a high-rise can be relative to its location and surroundings. However, it is known that the taller and slender the building is, the more significant are the dynamic effects. For the proof of concepts, dynamic analyses are excluded, which is the foundation for the definition of a mid-rise building for this research project. In accordance to the Eurocode, dynamic analyses are required when a building exceeds the height of 100 meters and the slenderness is higher than 4:1 (NEN-EN-1991-1-4, 2005) . A list of lateral stability systems for buildings is provided in the reader of the TU Delft course: Building Structures 2 by Ham and Terwel (2017) , which consists of shear walls, cores, rigid frames, tube systems, outriggers, mega-structures and hybrid structures. Ham and Terwel recommend that shear walls, cores and rigid frames can be used for buildings no taller than 100 meters. Brief descriptions on the systems are presented together with their symbolic analytical representation already used

by Rolvink (2010) and Hohrath (2018) . The derivation of specific elements differential equations can be found in the lecture notes written by Simone (2007) and the lecture's material of the course: Analysis of Slender Structures in TU Delft by Welleman (2017) .

2.1.1 Shear walls - Infinitely rigid floors

A structural system using shear walls as main stability elements can carry both, gravity and lateral loads, their resistance is mainly provided by its plane stiffness. Breider (2008) rightly mentions that the name "Shear walls" can be misleading because they deform mainly as bending beams when subjected to lateral loads. Figure 2.1 shows as structural system conformed by shear walls, it assumed that rigid floors are infinitely rigid. Hohrath (2018) and Rolvink (2010) both represent the shear walls as Euler-Bernoulli beams to analytically describe its behaviour. The differential equation that describes an Euler-Bernoulli beam under a uniform distributed load is the following:

$$EI \frac{\mathrm{d}^4}{\mathrm{d}x^4} w(x) = q \tag{2.1}$$

where:

EI	=	Bending stiffness
$w(x)$	=	Displacement function
q	=	Uniformly distributed load

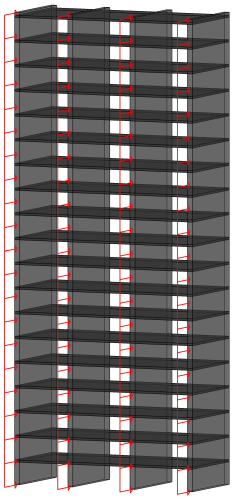

Figure 2.1: Shear walls system

2.1.2 Shear walls - Floors with finite stiffness

One of the super elements developed by Steenbergen (2007) was the one shown in Figure 2.2 which consists of 4 shear walls joined by concrete floors which are not considered to be infinitely rigid. Therefore, the floor stiffness is considered for the analytical symbolic representation with the following set of differential equations, where kf represents the floor stiffness.

$$EI \frac{\mathrm{d}^4}{\mathrm{d}x^4} w_a(x) + k_f w_a(x) - k_f w_b(x) = q_a \tag{2.2}$$

$$EI \frac{\mathrm{d}^4}{\mathrm{d}x^4} w_b(x) + k_f w_b(x) - k_f w_a(x) = q_b \tag{2.3}$$

where:
k_f = Floor stiffness

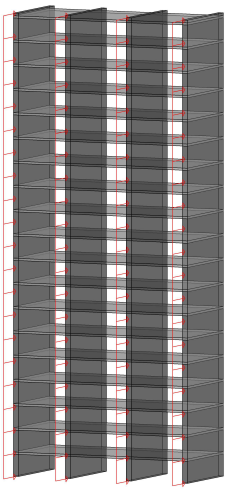

Figure 2.2: Coupled shear walls system

2.1.3 Cores - Infinitely rigid floors

A core structure is commonly known as a box formed by shear walls, Figure 2.3. The main difference with respect to a shear walls system is the provision of torsional resistance Breider (2008) . The cores are commonly located in the centre of the building which also facilitates a space for stairs or elevators. Rolvink (2010) presented three types of cores structures: the bending core, the framed core, and the perforated core. If only the bending is taken into consideration it is also possible to describe the behaviour of the core as Euler-Bernoulli beam with a hollow cross-section.

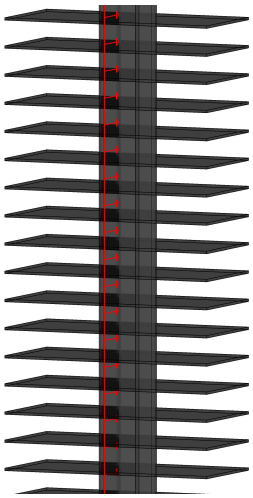

Figure 2.3: Core system

Furthermore, Steenbergen (2007) derived the symbolic analytical representation for other structural systems as a core coupled to a shear wall, or a core coupled to two shear walls in an asymmetric arrangement. These analytical representations take into account more than two degrees of freedom. The complete derivations are presented by Steenbergen (2007) .

2.1.4 Rigid frames

A rigid frame consists of a set of columns and girders provided with moment-resisting joints, as shown in Figure 2.4. The absence of braces and its commonly orthogonal configurations make this system an attractive one (Breider, 2008) . A rigid frame can be represented as a shear beam as implemented in SC2.0 by Rolvink (2010) . The differential equation of a shear beam is presented below as well as the equivalent shear stiffness expression used by Rolvink (2010) and other literature research papers such as the one by Olowokere et al. (1991) .

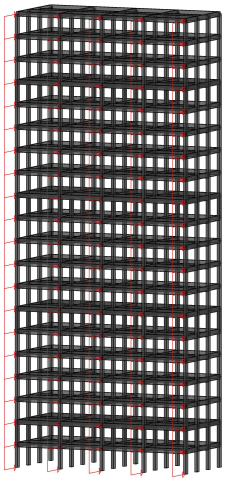

Figure 2.4: Rigid frame system

$$GA \frac{\mathrm{d}^2}{\mathrm{d}x^2} w(x) = -q \tag{2.4}$$

where:
GA = Shear stiffness

$$GA = 12 \frac{E}{h} \left(\left(\sum_{columns} \frac{Ic}{h} \right)^{-1} + \left(\sum_{beams} \frac{Ib}{b} \right)^{-1} \right)^{-1} \tag{2.5}$$

where:
E = Modulus of elasticity
h = Floor height
b = Beam length
Ic = Moment of inertia of a column
Ib = Moment of inertia of a beam

2.1.5 Shear wall and/or cores with frames

In these type of systems, shear walls and cores behave as cantilever beams with only bending deformations, and the frame accounts for the shear deformations. Breider (2008) emphasises that this model can only be valid if the shear-to-bending stiffness ratio (GA/EI) is the same along the height of the building. The governing equation of this system is presented in the lecture notes by Simone (2007) and it is shown below.

$$EI \frac{\mathrm{d}^4}{\mathrm{d}x^4} w(x) - GA \frac{\mathrm{d}^2}{\mathrm{d}x^2} w(x) = q \tag{2.6}$$

Previous structural systems and their analytical representations have been already studied and implemented in previous versions of StructuralComponents as by Rolvink (2010) and Hohrath (2018) . However, the representation of a rigid frame as shear beam is not always accurate enough for parametric purposes. Then, a deeper literature review about rigid frames behaviour is presented in the following section.

2.2 ANALYTICAL REPRESENTATION OF RIGID FRAMES

Olowokere et al. (1991) and Rolvink (2010) , implement the shear beam analytical representation for the behaviour of rigid frames. However, rigid frames lateral deformation does not always exhibit a pure shear behaviour. Ham and Terwel (2017) addressed this situation by explaining that the total lateral deformation of rigid frames consists of both, shear and bending contributions. The shear contribution is caused by the local bending in columns and beams, and the bending contribution is caused by the axial strains in the columns. Then, the behaviour of specific configurations of rigid frames can lead to a combined global behaviour with bending and shear deformations.

The idealisation of a rigid frame as a shear beam requires the representation of all columns and beams as a 1D element. The structural scheme is defined as a vertical cantilever shear beam, which implies fixed supports at the bottom. This idealisation is shown in Figure 2.5.

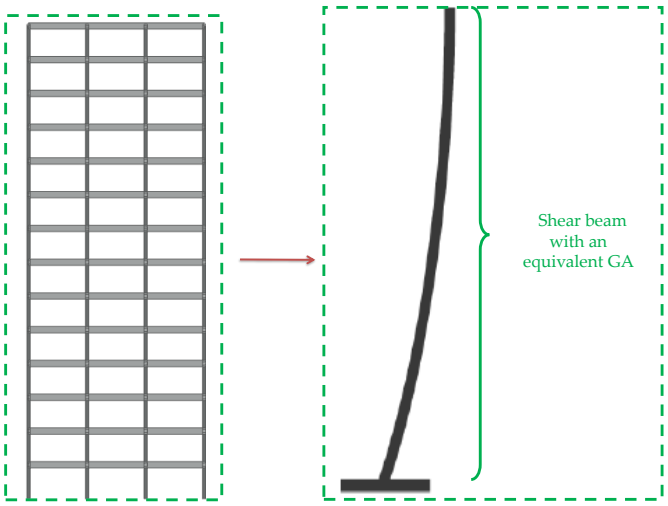

Figure 2.5: 2D rigid frame idealisation as a 1D shear beam

An essential part of the analytical representation is the calculation of an equivalent shear stiffness which depends on geometric parameters of the rigid frames, shown in Equation 3.25. The same expression is implemented by Olowokere et al. (1991) . Nonetheless, they state that such a representation is based on the assumption that the points of contraflexure of all elements occur exactly at mid-length. The point of contraflexure is where the

flexural moment is zero. Also, Eroğlu and Akkar (2011) say that the shear beam representation can work with sufficient accuracy but for dual structural systems. Rolvink (2010) also mentions that some analysis methods implemented in her research only apply to certain cases because to account for elements with shear and bending deformations is more time-consuming and complex.

Caterino et al. (2013) mention that the distinction between a shear or a bending type depends on the beam-to-column stiffness. They defined the coefficient alpha as a real value which tends to be 0.25 when flexural behaviour is predominant and that tends to be 1 when shear behaviour is predominant. The expression of the coefficient alpha is a function that depends on the elasticity modulus, the inertia of the cross-sections, the height of the columns, the length of the beams and the position of the points of contraflexure in the columns. Caterino et al. (2013) used the procedure Muto (1965) to predict the point of contraflexure in columns and for beams, it seems, it was assumed to be always at the mid-length. They also acknowledged that special attention is needed for the ground and roof levels of the rigid frame where the stiffness changes are more drastic, especially at the ground level, so they provided a different expression to calculate the coefficient alpha for the ground level.

Eroğlu and Akkar (2011) also developed a formulation to determine the qualification of a rigid frame as shear type or flexural type. They defined the coefficient alpha as a function which depends on the Blume's parameter (Blume, 1968) and the story level. To acknowledge drastic stiffness changes for the ground and roof floors, they provided three different formulations for the coefficient alpha. Eroğlu and Akkar (2011) consider the Blume's parameter as an indicator of the shear or flexural type and as the parameter that takes into account the relevant variables for determining the lateral stiffness for continuum systems. Akkar et al. (2004) present the formulation of the Blume's parameter which is described as the ratio of the beam to column rigidities. They mention that for extreme cases the Blume's parameter is zero when a pure flexural-type occurs and infinity when a pure shear-type occurs. The Blume's parameter is calculated as shown below.

$$\rho = \sum_{beams} \frac{Ib}{lb} \left(\sum_{columns} \frac{Ic}{lc} \right)^{-1} \tag{2.7}$$

where:

ρ	=	Blume's parameter
Ib	=	Moment of inertia of individual beam
lb	=	Beam length
Ic	=	Moment of inertia of individual column
lc	=	Column length (Floor height)

Then, the following statements can be drawn:

- The analytical representation of a rigid frame as a shear beam is not applicable for all cases.
- A combination of shear and flexural behaviour can occur in rigid frames.
- There is a stiffness variation along the height of the rigid frame, especially at the ground and top floor when the combined behaviour occurs.
- There are parameters such as the one by Blume (1968) or the alpha coefficient by Caterino et al. (2013) to determine the type of behaviour based on material and geometric properties.

2.3 OBJECTIVES

2.3.1 Main objective

The main objective of this research project was the expansion of StructuralComponents by means of research on the analytical representation of rigid frames under lateral loads, as well as the development of a parametric real-time computational prototype tool to quickly determine the feasibility of mid-rise buildings designs with rigid frames as stability members. This general objective was divided into 3 objectives.

2.3.2 Objective 1: Investigate rigid frames behaviour and its analytical representation

Research question 1: How can the behaviour of rigid frames, either shear, bending or combined type, be represented analytically?

Rolvink (2010) and Olowokere et al. (1991) used the analytical representation of a rigid frame as a shear beam, as well as the specific equivalent shear stiffness (Equation 3.25), but it is also acknowledged that this is not applicable for all cases due to the combined bending and shear behaviour. In order to parametrically implement the shear beam representation, it is necessary to define a range of applicability, which is dependent on geometric parameters, and to determine if a correction can be used to account for bending effects. Also, there are theories that can analytically account for both, bending and shear deformations, as the Timoshenko beam theory. The ideal scenario would be if a theory can be used so it can be parametrically implemented for all possible geometric configurations of rigid frames.

Then, it is necessary to explore both alternatives, a correction method and a theoretical approach to increase the applicability of the analytical representation of rigid frames behaviour.

2.3.3 Objective 2: Implement an analytical method for vertical connections

Research question 2: How can different rigid frames geometries be connected in an analytical way instead of following the scheme of the finite element method?

As an example, the Super Element Method by Steenbergen (2007) is a combination of the analytical and numerical approaches. This is because the super elements are connected following the finite element method scheme. However, there also exists the possibility to account for the element's transitions with the derivations of several analytical solutions with the definition of intermediate matching conditions. This alternative connection method must be explored to determine its suitability for the preliminary design.

2.3.4 Objective 3: The development of a real-time tool prototype of rigid frames solved analytically

Research question 3: What are the software features and framework to develop a real-time tool prototype of rigid frames?

It is necessary to determine if the software framework already implemented in previous versions of StructuralComponents is suitable for the tool prototype for rigid frames structural systems. It also must be explored the possibility to include new features that can make the tool easier to manipulate for the user.

2.4 SCOPE

This research project was limited to the determination of the structural feasibility of reinforced concrete rigid frames as stability members under lateral loads. The stability members were assumed to be clamped at the bottom so they can be represented as cantilever beams. Stafford Smith and Coull (1991) state that rigid frames as structural systems are suitable for buildings with moderate slenderness and an average maximum of 30 floors. For the tool prototype, maximum slenderness of 5:1 and a maximum amount of floors equal to 30 were adopted as limitations. Following the height restriction, dynamic analyses were excluded. To firstly solve the analytical representation to account for the combined shear and bending behaviour of rigid frames, this research project was focused on the 2D structural behaviour of rigid frames that can be parametrically adjusted with nine different geometric parameters.

2.5 METHODOLOGY

The methodology for this research project is presented per objective. The structure of the methodology consists of three steps: approach, data collection and the justification of methodological choice.

2.5.1 Objective 1: Investigate rigid frames behaviour and its analytical representation

To analytically represent rigid frames behaviour, the applicability range of the shear beam representation was determined and the following two approaches were explored:

- A correction method of the shear beam representation
- Timoshenko beam representation

To determine the applicability range of the shear beam representation and to develop the correction method, a quantitative approach was followed based on the identification of patterns to categorise the behaviour of rigid frames and its analytical representation. To collect data, tests were made to compare the numerical with the analytical solutions; the numerical solution by the use of the finite element method is considered as the most exact solution available for structural analysis. This quantitative approach was chosen due to the possibility of using powerful parametric tools; specifically, Grasshopper-Rhino, GhPython (McNeel, 2019) and Karamba3D (which contains the finite element solver), to produce, collect and manipulate an extensive amount of data. The derivation of the analytical solutions was performed with Maplesoft (Maplesoft, 2019) , and the surface polynomial interpolations with the Matlab curve fitting tool (MathWorks, 2019) .

Also, a quantitative and theoretical approach was followed by studying the derivations of the shear beam and the Timoshenko beam theories to analytically represent the behaviour of rigid frames. The theoretical expressions were obtained from the lecture notes by Simone (2007) and the lecture material by Welleman (2017) . The aim of this quantitative and theoretical approach was justified with the idea of the derivation of expressions that are applicable to all cases. The validations were performed by comparing the analytical with numerical solutions. The derivation of the analytical solutions was performed with Maplesoft and the numerical solutions with Grasshopper-Rhino and Karamba3D.

2.5.2 Objective 2: Implement an analytical method for vertical connections

A quantitative approach was followed which consisted of the derivation of analytical solutions that include one geometric change along the height. The validations of this method were performed with the same methodology as

in objective 1. This approach was chosen to provide a generic and analytical way to address the transitions of elements instead of using the finite element scheme.

2.5.3 Objective 3: The development of a real-time tool prototype of rigid frames solved analytically

The tool implemented the validated formulations from previous objectives, therefore, the foundations for the prototype tool are based on a quantitative approach. The software implemented for the tool development were Grasshopper-Rhino, GhPython and Telepathy (NBBJ, 2019) as an advantageous plugin for scripting in Grasshopper because it allows to send and receive information without wires to anywhere in the Grasshopper canvas. These software tools were chosen mainly because of their parametric characteristics and their visual scripting advantages.

3 STUDY AND RESULTS OF RIGID FRAMES BEHAVIOUR

This chapter contains the study and results of the analytical representation of rigid frames. To collect data in order to find patterns and to categorise the behaviour of rigid frames based on its geometric properties, a parametric study is performed to compare analytical to numerical solutions for 480 models. The definition of the range of applicability, a proposed correction method for the shear beam representation, the implementation of the Timoshenko theory, and the method to analytically account for vertical connections are presented in this chapter.

3.1 APPLICABILITY OF THE SHEAR BEAM REPRESENTATION

3.1.1 Derivation of the analytical solution of the shear beam

As the Euler-Bernoulli beam theory takes into account only bending deformations, the shear beam theory accounts only for shear deformations. The derivation of the analytical solution of a shear beam is shown below. This derivation is presented by Simone (2007) and Welleman (2017) . In this research project, analyses and studies were made idealising the stability members of a building as a clamped cantilever beam under a uniformly distributed lateral load. The derivation consists of the following steps:

1. Derivation of the ordinary differential equation (ODE)
    - Free body diagram
    - Kinematic relation
    - Constitutive relation
    - Equilibrium
2. Derivation of the ordinary differential equation (ODE)
    - Solution of the ODE
    - Boundary conditions
    - Solution for the unknown constants
    - Substitution in ODE solution, kinematic and constitutive relations

Now, brief descriptions for each of the steps are shown.

1. Derivation of the ordinary differential equation (ODE)

   I Free body diagram
   In Figure 3.1, the free body diagram for an infinitesimal section of the beam is shown.

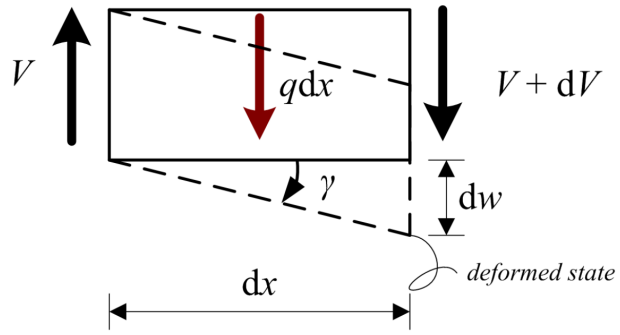

Figure 3.1: Free body diagram for shear beam model by Welleman (2017)

   II Kinematic relation
   In the previous figure, the shear distortion is represented as gamma and it related to the deflection by:

$$\gamma = \frac{dw}{dx} \tag{3.1}$$

   III Constitutive relation
   As explained by Simone (2007) , the constitutive relation comes from Hooke's law which results in:

$$V = GA\,\gamma \tag{3.2}$$

   IV Equilibrium
   Vertical equilibrium of the forces represented in the body diagram shown before is performed, followed by the substitution of the kinematic and constitutive relation to obtaining the ODE for a shear beam.

$$-V + qdx + V + dV = 0 \tag{3.3}$$

$$GA\,\frac{\mathrm{d}^2}{\mathrm{d}x^2} w\,(x) = -q \tag{3.4}$$

2. Derivation of the analytical solution of the shear beam (ODE)

   I Solution of the ODE

   The shear beam ODE is of second order, so its solution contains two unknown constants

$$w = -1/2\,\frac{qx^2}{GA} + \_C1\,x + \_C2 \tag{3.5}$$

The deflection, or displacement solution is substituted into the kinematic and constitutive relations.

II Boundary conditions

To find the unknowns, the following boundary conditions are defined for the case of a cantilever shear beam, which implies a fixed support at the bottom (x=0).

$w = 0$ at $x = 0$ and $V = 0$ at $x = L$

III Solution of the unknown constants

The system of 2 equations and 2 unknowns is solved.

$\_C1 = qL/GA$ and $\_C2 = 0$

IV Substitution of the kinematic and constitutive relations in the ODE.

Once the unknowns are found, the analytical solutions for the displacement, the shear deformation and the shear force are obtained.

$$w = 1/2\,\frac{xq\,(-x + 2\,L)}{GA} \tag{3.6}$$

$$\gamma = \frac{q\,(L - x)}{GA} \tag{3.7}$$

$$V = q\,(L - x) \tag{3.8}$$

It can be seen that because a static determinate case is chosen, the function of the shear force can be found by equilibrium and the same occurs for the bending moment function.

$$M = -1/2\,q\,(L - x)^2 \tag{3.9}$$

3.1.2 Tests of the shear beam representation

A step of performing an analytical symbolic representation of a stability member is the validation with finite element models. In order to verify the use of the shear beam theory to represent rigid frames behaviour, four different configurations of rigid frames were initially tested. The analytical

solution was obtained by the use of Equation 3.6 where the equivalent shear stiffness was calculated with the expression previously introduced and also shown below. The physical structural system and the analytical shear beam model are shown in Figure 3.2, as well as the definition of the coordinate system used in this research project. The four models specifications are shown in Tables 3.1-3.4. These models are called as the initial four models throughout this research project.

$$GA = 12\frac{E}{h}\left(\left(\sum_{columns}\frac{Ic}{h}\right)^{-1} + \left(\sum_{beams}\frac{Ib}{b}\right)^{-1}\right)^{-1} \tag{3.10}$$

The numerical solution is obtained by means of the finite element method with the finite element solver embedded in Karamba3D. Both solutions, numerical and analytical are shown for different frames configurations in Figures 3.3-3.6 where the variables to define the four different models are the overall slenderness and the beam-to-column inertia ratio. However, each model can be described by five different variables as shown in the table of each figure.

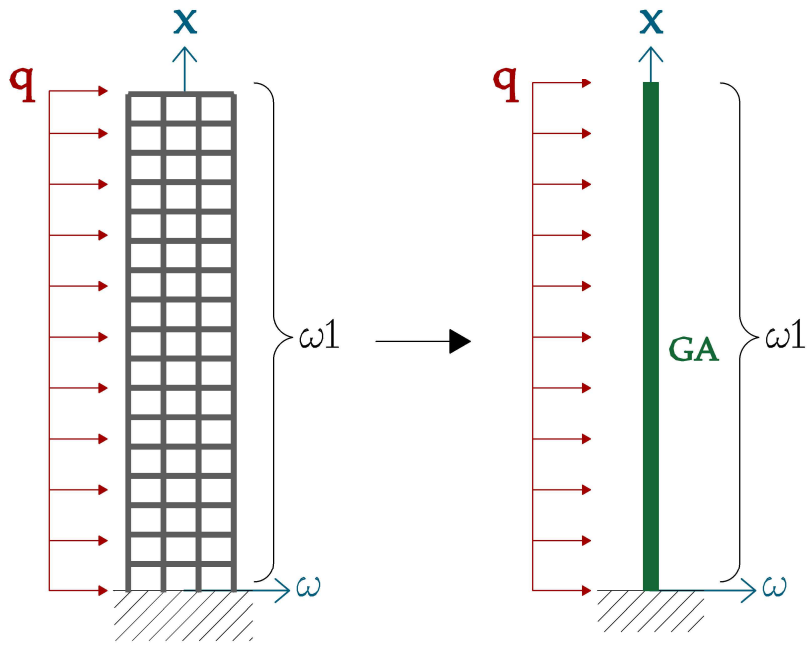

Figure 3.2: Physical structural system and analytical shear beam model

Table 3.1: Geometric properties

GEOMETRIC PROPERTIES				
	Model 1	Model 2	Model 3	Model 4
Beams height (m)	0.50	0.23	0.99	0.45
Beams width (m)	0.30	0.30	0.30	0.30
Columns height (m)	0.23	0.50	0.45	0.99
Columns width (m)	0.30	0.30	0.30	0.30
Floor hieght (m)	3.5	3.5	3.5	3.5
# Floors	4	4	4	4
Bay widht (m)	4	4	4	4
# Bays	6	6	6	6

Table 3.2: Finite elements properties

FINITE ELEMENT PROPERTIES	
Type of analysis	Linear
Element type	Beam elements
Degrees of freedom	uz, ux and phiy
Support conditions	Columns fixed at ground floor uz=0, ux=0 and phiy=0

Table 3.3: Load specifications

LOAD		
Wind pressure [P]	2.25	kN/m2
Uniformly distribubted load [q]	11.25	kN/m

Table 3.4: Material properties

MATERIAL PROPERTIES		
Concrete C25/C30		
Modulus of elasticity [E]	3100	kN/cm2
Density [gamma]	25	kN/m3

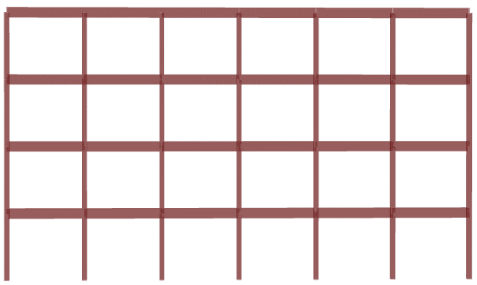

Inertia ratio	10.65	Unitless
Slenderness ratio	0.58	Unitless
Inertia magnitude	39.01	x10-4 m4
Module aspect ratio	1.14	Unitless
Overall size	336.00	m2
Error of max displacement	-1.01%	
Stiffness unity check	0.94	

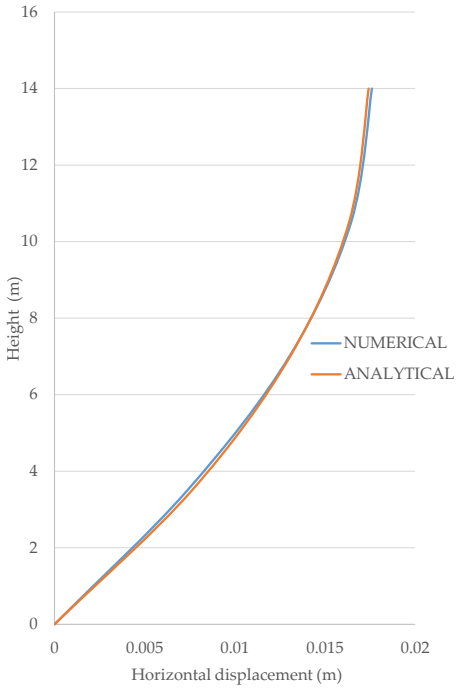

Figure 3.3: Model l: High inertia ratio and low slenderness

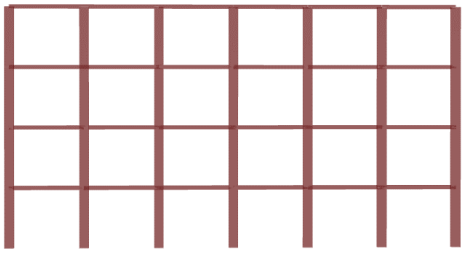

Inertia ratio	0.09	Unitless
Slenderness ratio	0.58	Unitless
Inertia magnitude	33.17	x10-4 m4
Module aspect ratio	1.14	Unitless
Overall size	336.00	m2
Error of max displacement	76.06%	
Stiffness unity check	0.79	

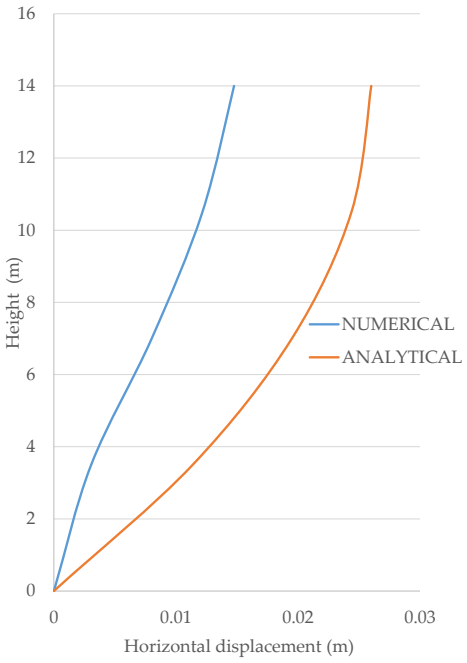

Figure 3.4: Model 2: Low inertia ratio and low slenderness

Inertia ratio	10.65	Unitless
Slenderness ratio	3.65	Unitless
Inertia magnitude	265.36	x10-4 m4
Module aspect ratio	1.14	Unitless
Overall size	2100.00	m2
Error of max displacement	-36.67%	
Stiffness unity check	1.35	

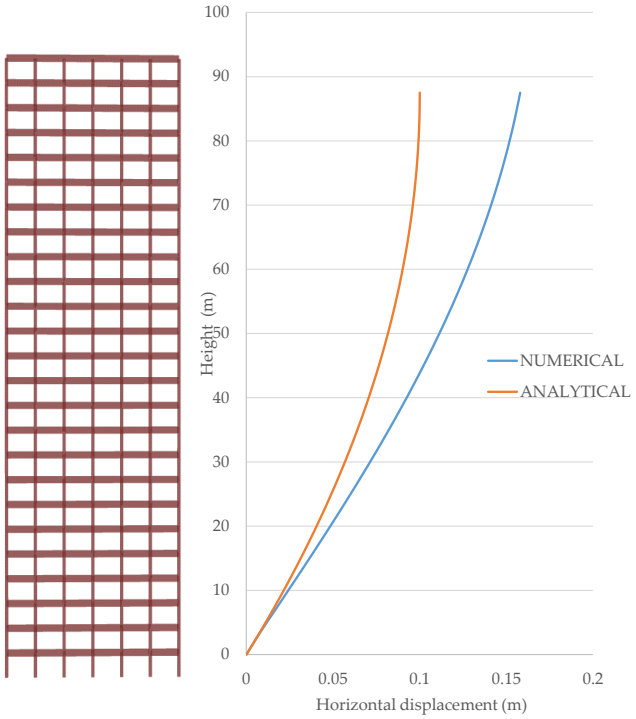

Figure 3.5: Model 3: High inertia ratio and high slenderness

Inertia ratio	0.09	Unitless
Slenderness ratio	3.65	Unitless
Inertia magnitude	265.36	x10-4 m4
Module aspect ratio	1.14	Unitless
Overall size	2100.00	m2
Error of max displacement	-13.10%	
Stiffness unity check	1.25	

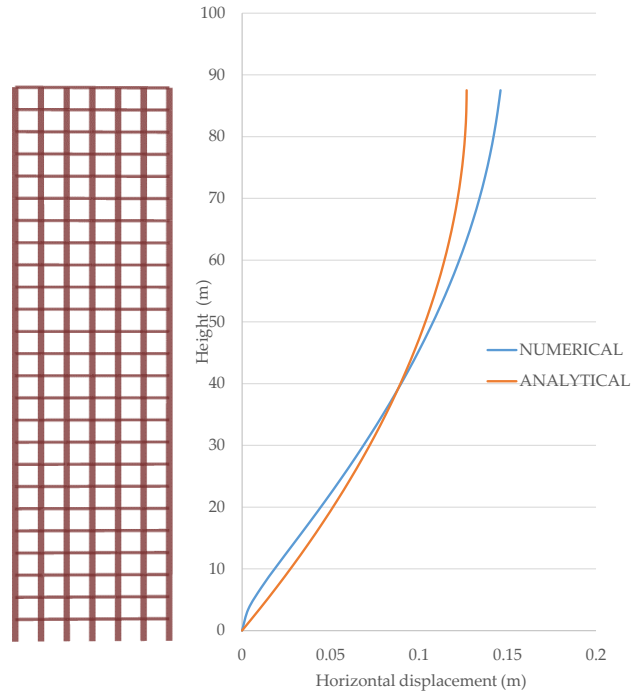

Figure 3.6: Model 4: Low inertia ratio and high slenderness

In previous figures, the inertia ratio value is shown instead of the Blumes parameter. It is useful to remember that the Blume's parameter is a ratio of the beams and columns rigidities which depends on the inertia, length of the elements and the amount of them and, if a regular rigid frame is considered, the Blume's parameter can also be rearranged and interpreted as the product of the beam-to-column inertia ratio, the column-to-beam length ratio and the beam-to-column number of elements. This is shown in the derivation shown below.

$$\rho = \sum_{beams} \frac{Ib}{lb} \left(\sum_{columns} \frac{Ic}{lc} \right)^{-1} \tag{3.11}$$

$$\rho = \frac{Ib}{Ic} \frac{lc}{lb} \frac{nb}{nc} \tag{3.12}$$

where:
nb = Number of beams
nc = Number of columns

From the rearrangement of the Blume's parameter, it can be seen that if there is the same amount of columns and beams along the cross-section of the rigid frame, and the lengths of the elements are the same, the Blume's parameter becomes only the beam-to-column inertia ratio.

Eroğlu and Akkar (2011) use the Blume's parameter as a measure to classify the rigid frame behaviour as shear or flexural type; however, from the Figures 3.3-3.6 the following observations can be made:

- In Figure 3.3 the analytical symbolic representation is accurate because the slenderness is low and the Blume's parameter is high (Large beams).
- In Figure 3.4 the analytical symbolic representation is not accurate because the slenderness is low and the Blume's parameter is low (Large columns). The displacements are small relative to the total height of the frame. The analytical approximation is conservative in terms of displacements.
- In Figure 3.5 the value of the Blume's parameter suggests shear-type rigid frame but from the numerical plot, some bending effects can be seen. The analytical approximation is not conservative in terms of displacements.
- In Figure 3.6 the value of the Blume's parameter suggests flexural-type rigid frame but from the numerical plot, an overall shear-type behaviour can be seen with some bending effects at the bottom. The

analytical approximation is not conservative in terms of the maximum displacement.

Then, it has been shown that the analytical shear beam representation of rigid frames is not applicable to all cases. Moreover, an almost opposite pattern occurs with low and high slenderness configurations, in terms of the fitting error between analytical and numerical solutions.

3.1.3 Study of rigid frames behaviour

With the aim to find patterns to explain the error of the analytical representation of rigid frames, the following output results from finite element analyses were studied:

- Points of contraflexure
- The axial forces in the columns
- The maximum displacement at the top

Points of contraflexure

The point of contraflexure is the location along the length of the element where the bending moment has zero value; it can also be described as the location where the bending moment changes sign. It is explained by Olowokere et al. (1991) that the analytical representation of a rigid frame as shear beam it is based on the assumption that the points of contraflexure are located at mid-length and mid-height of all the beams and columns.

The same four models with different configurations of rigid frames under the same lateral load were studied. The bending moment diagrams for all the beams and all the columns are shown in Figures 3.7-3.10; from these, the location of the point of contraflexure can be observed. In Figures 3.7 and 3.8, sub-figures in the middle show the bending moment diagrams of the beams and the sub-figures at the bottom the bending moment diagrams of the columns. In Figures 3.9 and 3.10 the bending moment diagrams for the beams are shown in the left sub-figures and for the columns in the right sub-figures. The second and four sub-figures represent the same bending moment diagrams as the first and third, respectively, but with a higher scale factor for visualisation purposes.

- Model l: High inertia ratio and low slenderness.
- Model 2: Low inertia ratio and low slenderness.
- Model 3: High inertia ratio and high slenderness.
- Model 4: Low inertia ratio and high slenderness.

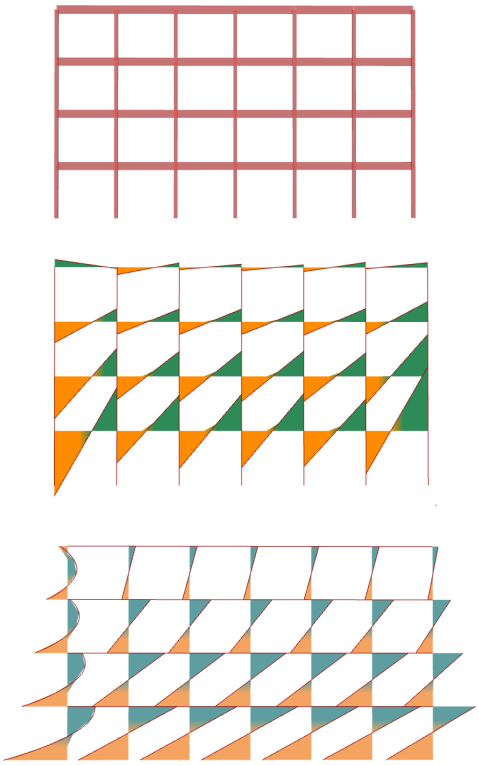

Figure 3.7: Model 1. Bending moment diagrams

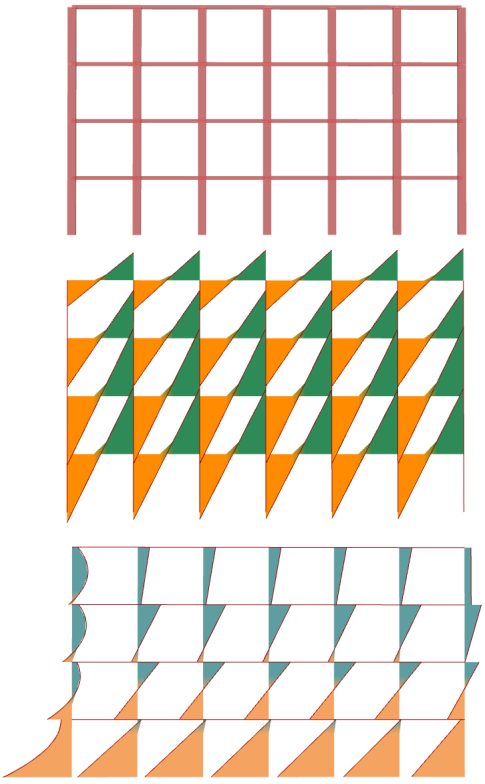

Figure 3.8: Model 2. Bending moment diagrams

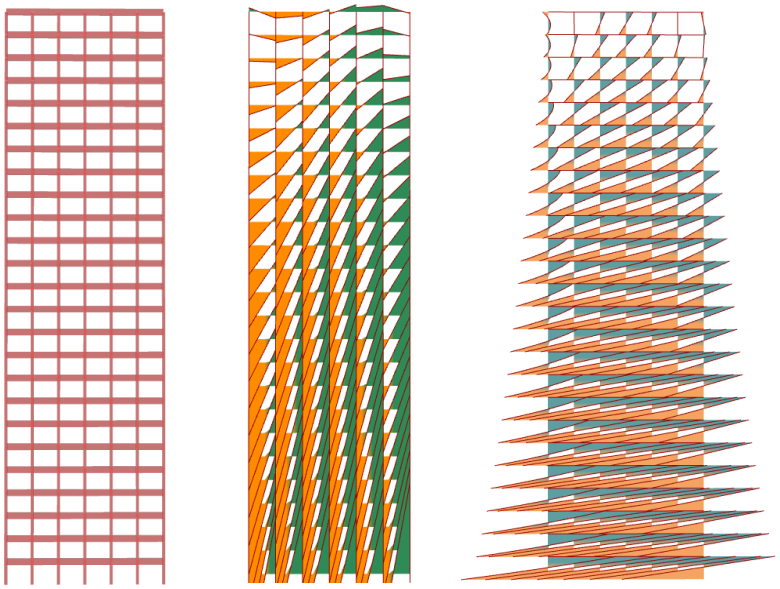

Figure 3.9: Model 3. Bending moment diagrams

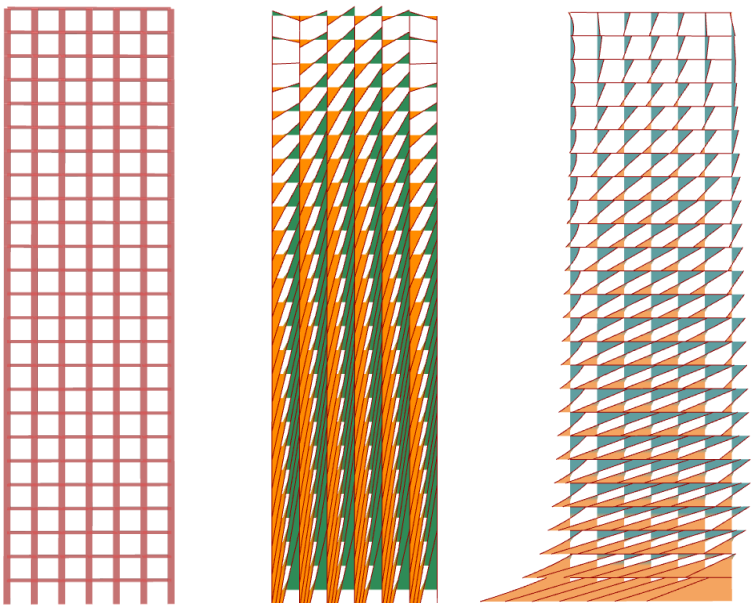

Figure 3.10: Model 4. Bending moment diagrams

Based on previous results the following situations are observed:

- Model 1: For almost all beams and columns the point of contraflexure is located in the middle.
- Model 2: For all beams the point of contraflexure is located in the middle, but not for the columns.
- Model 3: For almost all columns the point of contraflexure is located in the middle. Only at low floors, the point of contraflexure in beams

is located in the middle. At high floors, the bending moment diagrams follow a pattern where the point of contraflexure tends to be not in the middle of each beam element but in the middle of the total width.

- Model 4: For all beams the point of contraflexure is located in the middle. For the columns, only for a few intermediate floors the point of contraflexure is in the middle.

Then, the assumption of the location of the points of contraflexure at mid-length and mid-height of all the beams and columns is only met for model 1, where the beam-to-column inertia ratio is large and the slenderness is low.

The axial forces in the columns

In the same way, the variations of the axial forces in the columns are studied with the aim to find a pattern to explain the error of the analytical representation. Ham and Terwel (2017) , present the portal method with which an approximation for the analysis of a rigid frame can be made. In this method, it is assumed that the interior columns of the rigid frame tend to have zero axial forces which is a good approximation for rigid frames that deform mainly by shear. Figures 3.11 and 3.12 show the axial force diagrams for the four models described in the previous section.

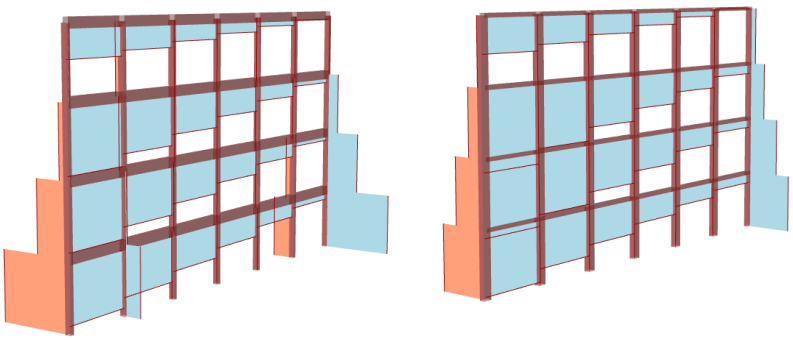

Figure 3.11: Models 1 and 2: Axial force diagrams

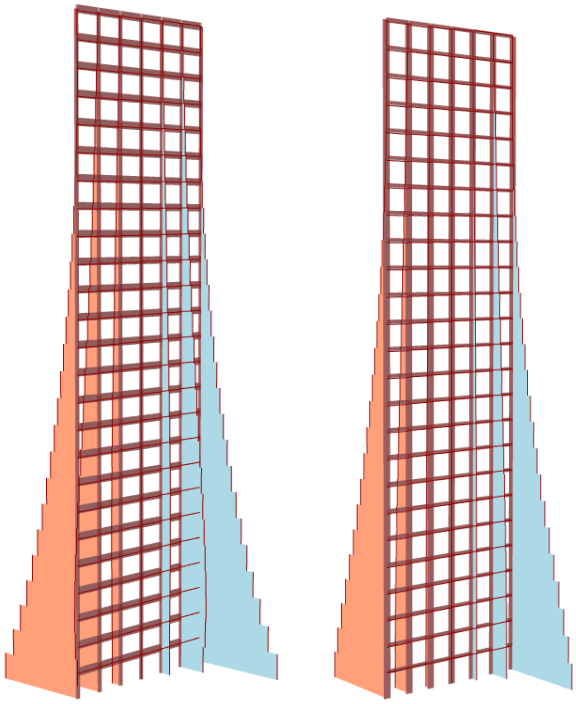

Figure 3.12: Models 3 and 4: Axial force diagrams

The following observations are made from the output results presented in Figures 3.11 and 3.12.

- Model 1: The axial forces of the interior columns do not tend to zero.
- Model 2: The axial forces of the interior columns tend to zero.
- Model 3: The axial forces of the interior columns do not tend to zero.
- Model 4: The axial forces of the interior columns tend to zero.

Under the premise that rigid frames deform mainly by shear when the axial forces of the interior columns tend to zero, models 2 and 4 would deform mainly by shear, however this does not happen for model 2, as can be seen in Figure 3.4. Moreover, the pattern of the axial forces in the columns as a parameter to predict behaviour type would differ from the Blume's parameter because the beam-to-column inertia ratios of models 2 and 4 are low which would suggest a bending behaviour, according to the Blume's parameter. Ham and Terwel (2017) acknowledge the situation that for taller buildings with stiffer beams than columns, the rigid frame can behave as a flexural cantilever beam.

From the initial tests, the point of contraflexure and the column axial forces studies, it can be observed that the distinction between shear, combined or bending behaviour of a rigid frame is strongly dependent on two variables: the beam-to-column inertia ratio and the overall slenderness; and that the error of the shear beam analytical representation is related to

the cases where the bending deformations are significant as can be seen in the deformed shape comparisons of numerical and analytical solutions from Figures 3.3-3.6.

The maximum displacement at the top

To understand the two-variable dependency regarding the classification of rigid frames behaviour, the maximum displacement at the top of rigid frames under lateral load was studied deeply in this research project to compare the shear beam analytical representation with the numerical solution.

First, the four studied models can be represented as points in a 2D space where the horizontal axis is the inertia ratio and the vertical axis is the slenderness as shown in Figure 3.13.

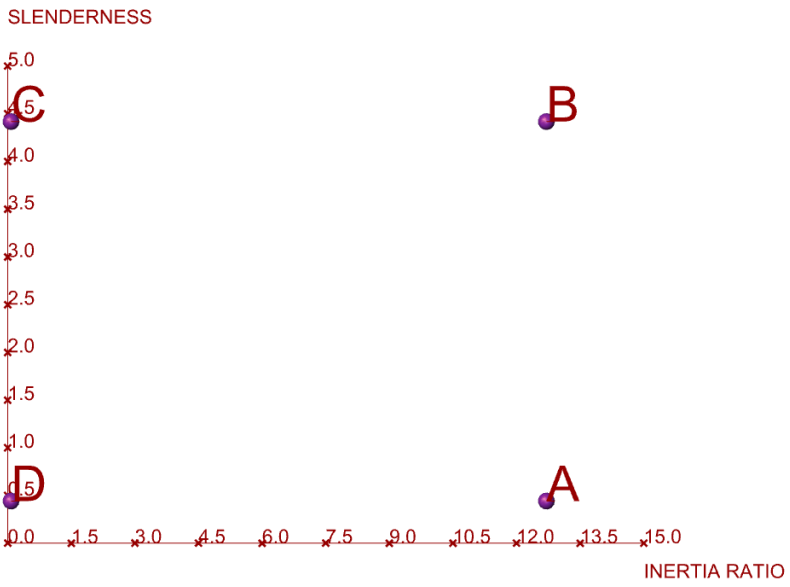

Figure 3.13: Studied models described in a 2D coordinate space. Model 1: A, Model 2: D, Model 3: B and Model 4: C.

To visualise the two-variable dependency of the percentage error between the analytical and numerical solutions, the maximum displacement was obtained for 40 rigid frames configurations and plotted in a 3D space where the third axis is the error percentage. Then, a surface interpolation was generated, this process is shown in Figures 3.15-3.18.

The geometric specifications of each of the 40 models are presented in Figure 3.14. The uniformly distributed load applied to each of the models comes from a wind pressure of 1.25 kN/m2 factored by a safety factor of 1.5 and a factor of 1.2 for second-order effects. The structural scheme for the 1D analytical representation is a cantilever beam, so the solution can be obtained from Equation 3.6. The finite element models consist of 'beam' elements with three degrees of freedom on each node (two translations and one rotation), and the columns are assumed to have fixed supports. The defined

geometric properties and applied wind load for the models are based on the recommendations of Ham and Terwel (2017) and Caterino et al. (2013) for their studies on common geometries for rigid frames.

Beams cross-section		Columns cross-section		Floor height	Floors	Bays width	Bays	Inertia ratio	Slender-ness	Inertia magni-tude	Module aspect ratio	Overall size
h (m)	w(m)	h (m)	w(m)	hf (m)	Amount	bw (m)	Amount	IR	S	IM (x10-4 m4)	AR	A (m2)
0.21	0.30	0.49	0.30	3.5	3	4	6	0.08	0.44	31.73	1.14	252
0.25	0.30	0.46	0.30	3.5	3	4	6	0.16	0.44	27.23	1.14	252
0.26	0.30	0.44	0.30	3.5	3	4	6	0.22	0.44	25.46	1.14	252
0.28	0.30	0.42	0.30	3.5	3	4	6	0.30	0.44	24.01	1.14	252
0.30	0.30	0.40	0.30	3.5	3	4	6	0.40	0.44	22.88	1.14	252
0.32	0.30	0.39	0.30	3.5	3	4	6	0.55	0.44	22.08	1.14	252
0.35	0.30	0.35	0.30	3.5	3	4	6	1.00	0.44	21.44	1.14	252
0.39	0.30	0.32	0.30	3.5	3	4	6	1.83	0.44	22.08	1.14	252
0.46	0.30	0.25	0.30	3.5	3	4	6	6.41	0.44	27.23	1.14	252
0.49	0.30	0.21	0.30	3.5	3	4	6	12.70	0.44	31.73	1.14	252
0.21	0.30	0.49	0.30	3.5	7	4	6	0.08	1.02	31.73	1.14	588
0.25	0.30	0.46	0.30	3.5	7	4	6	0.16	1.02	27.23	1.14	588
0.26	0.30	0.44	0.30	3.5	7	4	6	0.22	1.02	25.46	1.14	588
0.28	0.30	0.42	0.30	3.5	7	4	6	0.30	1.02	24.01	1.14	588
0.30	0.30	0.40	0.30	3.5	7	4	6	0.40	1.02	22.88	1.14	588
0.32	0.30	0.39	0.30	3.5	7	4	6	0.55	1.02	22.08	1.14	588
0.35	0.30	0.35	0.30	3.5	7	4	6	1.00	1.02	21.44	1.14	588
0.39	0.30	0.32	0.30	3.5	7	4	6	1.83	1.02	22.08	1.14	588
0.46	0.30	0.25	0.30	3.5	7	4	6	6.41	1.02	27.23	1.14	588
0.49	0.30	0.21	0.30	3.5	7	4	6	12.70	1.02	31.73	1.14	588
0.21	0.30	0.49	0.30	3.5	21	4	6	0.08	3.06	31.73	1.14	1764
0.25	0.30	0.46	0.30	3.5	21	4	6	0.16	3.06	27.23	1.14	1764
0.26	0.30	0.44	0.30	3.5	21	4	6	0.22	3.06	25.46	1.14	1764
0.28	0.30	0.42	0.30	3.5	21	4	6	0.30	3.06	24.01	1.14	1764
0.30	0.30	0.40	0.30	3.5	21	4	6	0.40	3.06	22.88	1.14	1764
0.32	0.30	0.39	0.30	3.5	21	4	6	0.55	3.06	22.08	1.14	1764
0.35	0.30	0.35	0.30	3.5	21	4	6	1.00	3.06	21.44	1.14	1764
0.39	0.30	0.32	0.30	3.5	21	4	6	1.83	3.06	22.08	1.14	1764
0.46	0.30	0.25	0.30	3.5	21	4	6	6.41	3.06	27.23	1.14	1764
0.49	0.30	0.21	0.30	3.5	21	4	6	12.70	3.06	31.73	1.14	1764
0.21	0.30	0.49	0.30	3.5	34	4	6	0.08	4.95	31.73	1.14	2856
0.25	0.30	0.46	0.30	3.5	34	4	6	0.16	4.95	27.23	1.14	2856
0.26	0.30	0.44	0.30	3.5	34	4	6	0.22	4.95	25.46	1.14	2856
0.28	0.30	0.42	0.30	3.5	34	4	6	0.30	4.95	24.01	1.14	2856
0.30	0.30	0.40	0.30	3.5	34	4	6	0.40	4.95	22.88	1.14	2856
0.32	0.30	0.39	0.30	3.5	34	4	6	0.55	4.95	22.08	1.14	2856
0.35	0.30	0.35	0.30	3.5	34	4	6	1.00	4.95	21.44	1.14	2856
0.39	0.30	0.32	0.30	3.5	34	4	6	1.83	4.95	22.08	1.14	2856
0.46	0.30	0.25	0.30	3.5	34	4	6	6.41	4.95	27.23	1.14	2856

Figure 3.14: Geometric properties of each model

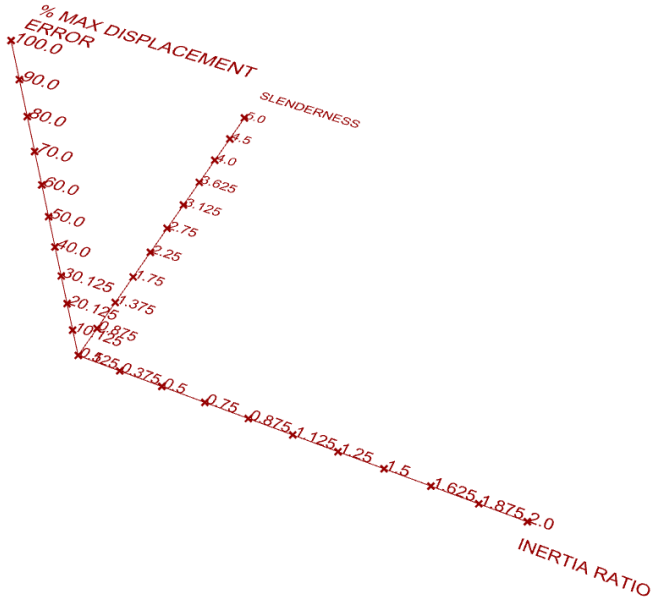

Figure 3.15: Process to obtain the surface interpolation of the percentage error

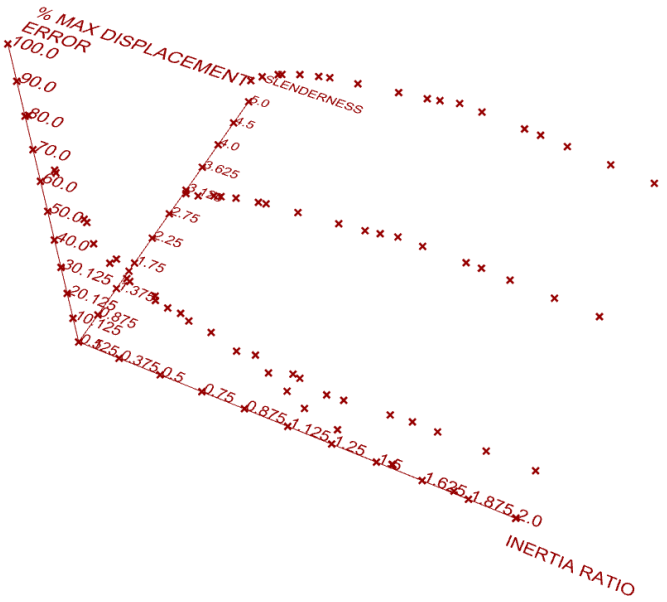

Figure 3.16: Process to obtain the surface interpolation of the percentage error

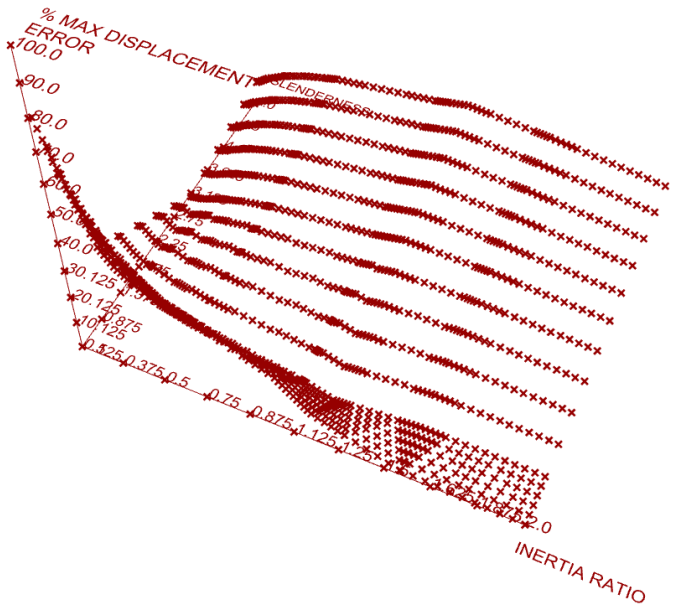

Figure 3.17: Process to obtain the surface interpolation of the percentage error

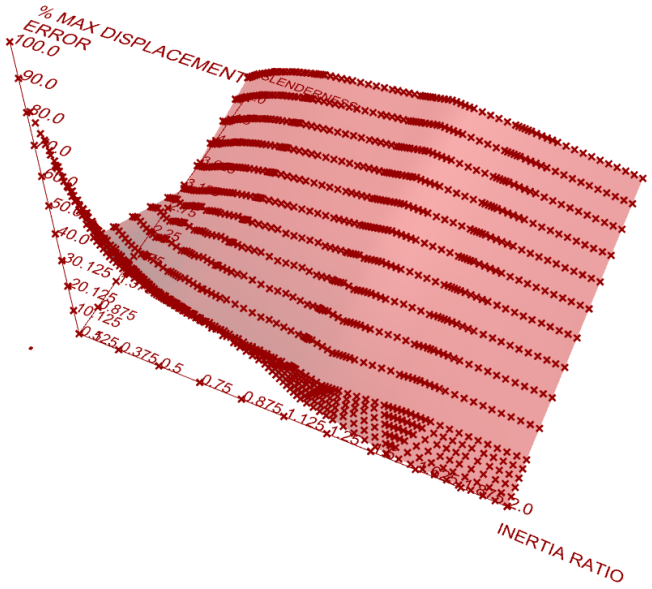

Figure 3.18: Percentage error interpolated surface

In Figures 3.15 and 3.18, the x-axis was adjusted to visualise in half of the axis inertia ratios where the columns are larger than the beams, and in the other half the opposite: where the beams are larger than the columns.

If an allowable percentage error for the preliminary design is defined, then a plane can be plotted as shown in Figure 3.19. If seen from the top, the green area will define a safe range of applicability for the analytical representation for several combinations of inertia ratio and slenderness. For this research project, a 20 percent error is defined as allowable for prelim-

inary design purposes, this is based on personal communications with the graduation committee members of this master's thesis.

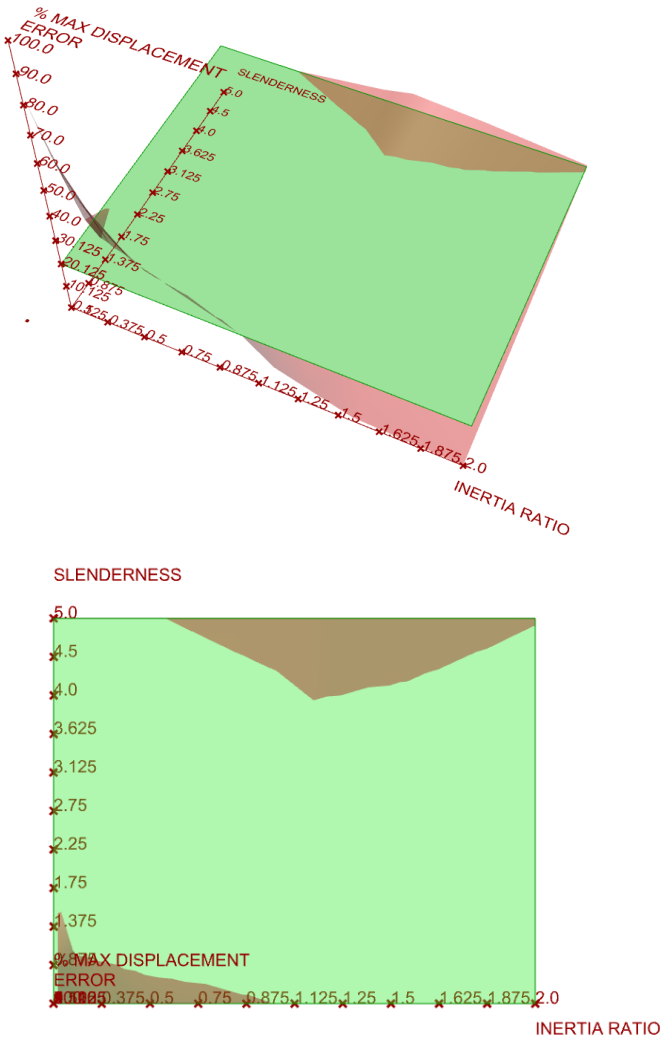

Figure 3.19: Plane to represent an allowable error of 20 percent

Tests were performed by changing parameters of the rigid frames to check if, for the specific values of inertia ratios and slenderness, the error remains the same by modifying other parameters as the cross-size. The specific geometric properties of each test are presented in Appendix A as well as the systematic procedure to define the 480 models, this shown in Figures A.5-A.7 and Table A.1. Some of these tests failed because of, even if the inertia ratio and slenderness are kept with specific values within the safe range, the cross-section size changes result in a different error as the predicted one by the surface interpolation. There is a pattern that can be described as follows: if the cross-section size increases, then the error increases. Figure 3.20 shows two rigid frames with the same inertia ratio and slenderness but a different cross-section size. The observed pattern can be summarised as: the larger the cross-sections the larger the error.

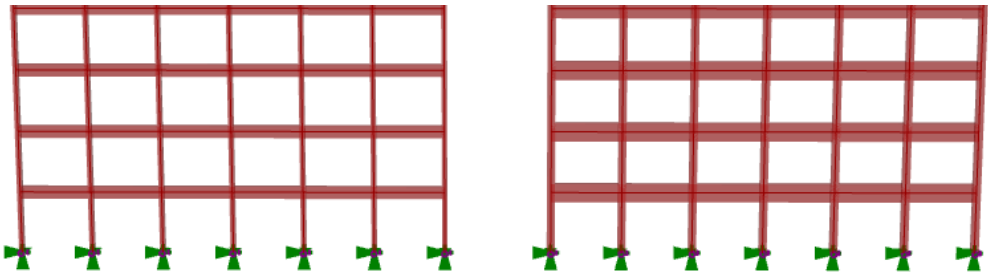

Figure 3.20: Different cross-section sizes

The previous situation can be seen as a third variable dependency to predict the error by inputting only geometric properties of the rigid frame. In this research project, this third variable is defined as the inertia magnitude which consists of the sum of the inertia of a beam and the inertia of a column. The increasing or decreasing of the error due to this variable can be seen as a vertical extrapolation of the previously generated surface, which is shown in Figure 3.21. Such extrapolated surfaces are obtained with the same process shown in Figure 3.15 by the generation of another 80 models.

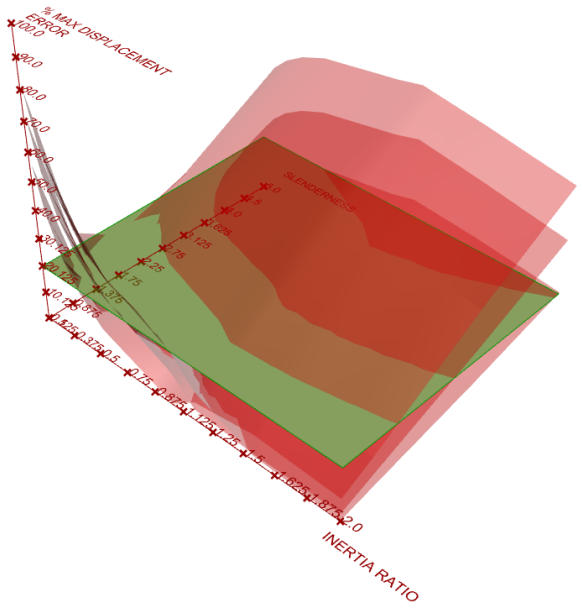

Figure 3.21: Surfaces to account for the inertia magnitude

Also in Figure 3.21, the allowable error plane is plotted for a value of 20 percent. It can be observed that the applicability range is drastically reduced, which is again visualised as the green area.

Tests were performed by changing parameters of the rigid frames to check if, for the specific values of inertia ratio, slenderness and the inertia magnitude, the error remains the same by modifying other parameters as the length of the elements. Some of these tests failed because, even if the inertia ratio, slenderness, and the inertia magnitude are kept with specific values,

the changes in the module aspect ratio result in a different error. Figure 3.22 shows two frames with the same inertia ratio, slenderness, inertia magnitude but, a different module aspect ratio. The following pattern was observed: the larger the module aspect ratio is the smaller the error. The consideration of this pattern and the one of the inertia ratio observed in Figure 3.18, are the reasons to use these variables in a separate way instead of as their product as in the Blume's parameter as shown in Equation 3.12. To observe this pattern, another 240 models were performed.

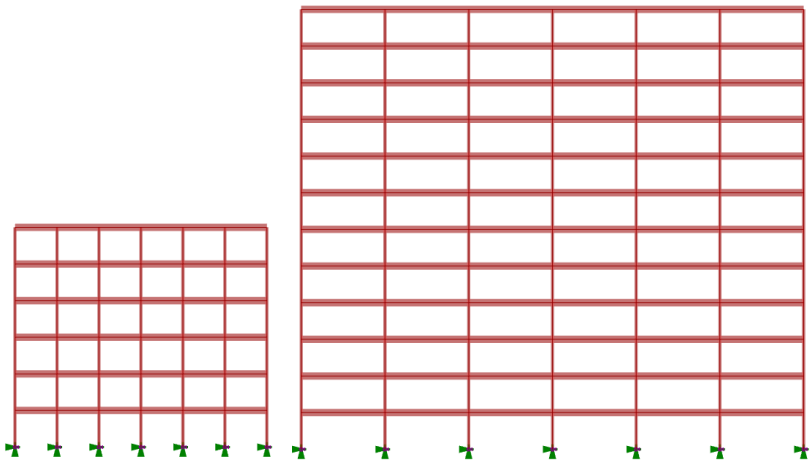

Figure 3.22: Different module aspect ratio

The previous situation can be seen as a fourth variable dependency of the percentage error. In this research project, this fourth variable was defined as the module aspect ratio.

Once more, tests were performed by changing parameters of the rigid frames in order to check if for specific values of inertia ratio, slenderness, inertia magnitude and module aspect ratio, the error remains the same by modifying other parameters as the number of floors or bays. Some of these tests failed because of, even if the inertia ratio, slenderness, inertia magnitude and the module aspect ratio are kept with specific values, the change of the overall size of rigid frames results in a different error. Figure 3.23 shows two frames with the same inertia ratio, slenderness, inertia magnitude, module aspect ratio but a different overall size of the rigid frame. The following pattern was observed: the larger the overall size the larger the error. The overall size of was defined as the area obtained by the product of the total height with the total width. To observe the pattern involving this variable, another 120 models were performed.

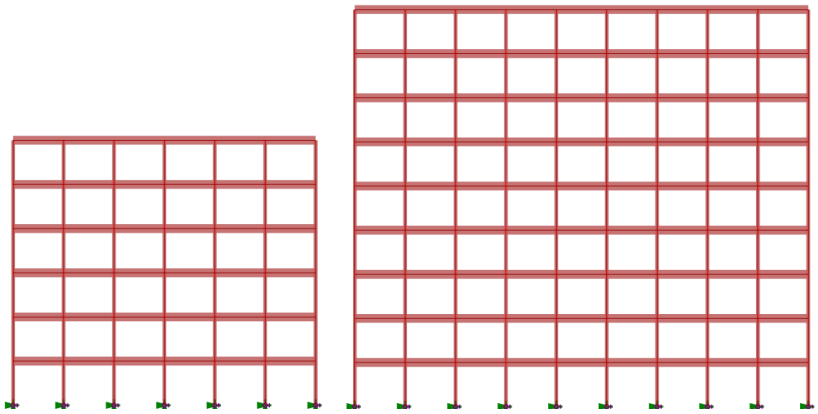

Figure 3.23: Different overall size

Then, after the study just presented it can be seen that error of the shear beam analytical representation depends on multiple geometric variables.

3.1.4 Applicability range

An applicability range can be defined from an interpolated surface generated with a combination of the most unfavourable values for the five variables shown before; that surface is shown in Figure 3.24 as a top view where the allowable percentage error for the preliminary design is defined as 20 percent and plotted as a green plane.

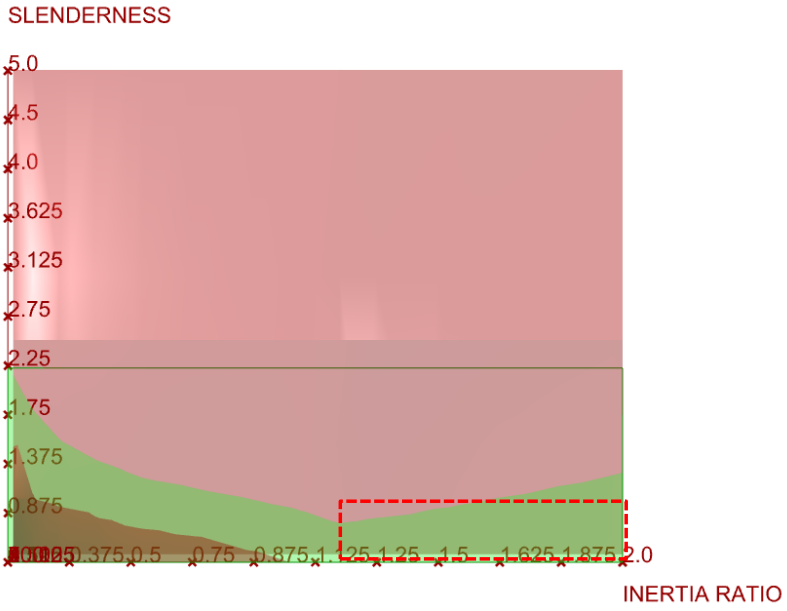

Figure 3.24: Range of applicability of the shear beam analytical representation

From a top view, the green area will define a safe range of applicability for the parametric implementation of the analytical shear representation of rigid frames. For now, for parametric purposes and simplicity on the delimiters, the range of applicability is defined in terms of the inertia ratio and the slenderness which is indicated with the red box in Figure 3.24. Eroğlu and Akkar (2011) use the coefficient alpha as behaviour type indicator and, they present a surface interpolation in a 3D space for the coefficient alpha which depends on the Blume's parameter and the number of stories; further on, they present several error surfaces of the top displacement which are also a function of the Blume's parameter and the number of stories. This literature reference, together with the study of the five variables dependency presented before, are the reasons to define the inertia ratio and the slenderness as the most relevant variables with which the behaviour type can be determined for this research project.

Then, the shear beam representation is applicable when the beam-to-column inertia ratio is greater than one and the overall slenderness is less than 1.

$$IR > 1 \qquad and \qquad S < 1 \tag{3.13}$$

where:
IR = Beam-to-column inertia ratio
S = Overall rigid frame slenderness

3.1.5 Rigid frames zones classification

Based on the applicability range definition and the initial tests shown in Figures 3.3-3.6 a zones division for the most unfavourable interpolated error surface is proposed and shown in Figure 3.25.

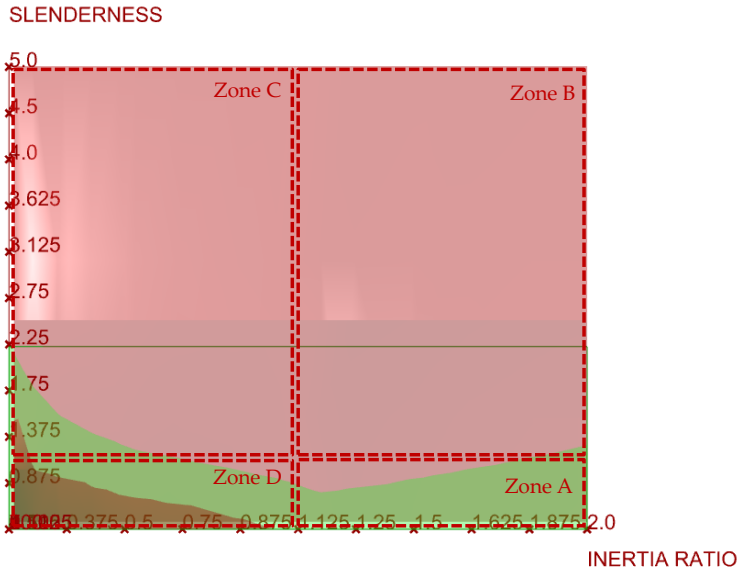

Figure 3.25: Rigid frames zones classification

In the following lines, a brief description for each zone is presented where:

High slenderness is defined as $S > 1$
High inertia ratio is defined as $IR > 1$

1. **Zone A** ($1 < IR < 12.7$ and $0 < S < 1$)
   - Low slenderness and high inertia ratio
   - Mostly shear behaviour (the applicability range falls in this zone
   - The shear beam representation is accurate

2. **Zone B** ($1 < IR < 12.7$ and $1 < S < 5$)
   - High slenderness and high inertia ratio
   - Combined behaviour
   - The shear beam representation is not accurate and non-conservative.

3. **Zone C** ($0 < IR < 1$ and $1 < S < 5$)
   - High slenderness and low inertia ratio
   - Combined behaviour
   - The shear beam representation is only conservative when the inertia value ratio is less than 0.05, for the other cases is not conservative.

4. **Zone D** ($0 < IR < 1$ and $0 < S < 1$
   - Low slenderness and low inertia ratio
   - Mostly flexural behaviour
   - The shear beam representation is not accurate but conservative.

Then, the range of applicability of the shear beam representation is defined as the zone A. This zone can also be related to the points of

contraflexure study, because it is in this zone where the position of the contraflexure does occur at mid-length and mid-height of the elements.

From this study it is observed that the error of the analytical representation is linked to the cases where the combined shear and bending behaviour occurs. To address this, a correction method for the shear beam representation was developed and the Timoshenko beam theory was explored and implemented.

3.2 CORRECTION METHOD FOR THE SHEAR BEAM REPRESENTATION

Because of the applicability range presented before is small for parametric purposes, a different approach, which consisted of the correction of the shear beam analytical solution, was explored. Figure 3.6 shows that even with bending effects, the overall deformation can be more related to a shear beam than to a bending beam. Then, it was proposed to correct the analytical shear beam representation by the prediction of the error based on data interpolations.

The prediction of the error comes from a procedure of a series of sequential polynomial interpolations that take inputs from the five geometric variables described before. The polynomial interpolations functions are based on data obtained from 480 rigid frames tests that vary geometrically to take into account the patterns related to each of the five variables. The range of values for the geometric properties of the models was chosen so the commonly feasible rigid frames geometries were included.

Out of the four zones classification, the correction procedure was focused on zones B and A because of the following reasons:

1. Indicators, as the Blume's parameter, would predict a shear behaviour type for zone B and this can be misinterpreted as a good analytical shear beam representation.

2. The analytical solution is not accurate and non-conservative for zone B. As shown in the Figure 3.5 the deformed shape of the analytical solution is less than the numerical solution. The zone A is where the analytical shear beam representation is accurate even with no correction.

Then, the procedure to predict the error of the analytical shear beam representation for zone B was developed and explained below.

If the error had a dependency on only one variable, a fitting function could be approximated based on several representative points, as shown if Figure 3.26. Then, the way to obtain a prediction of the error would be by entering the fitted function with an specific value for the variable. This

process is represented graphically in the left side of Figure3.26. In a similar way, if there is a dependency on two variables the graphical process can be seen as surface function with two inputs as shown in the right side of Figure 3.26.

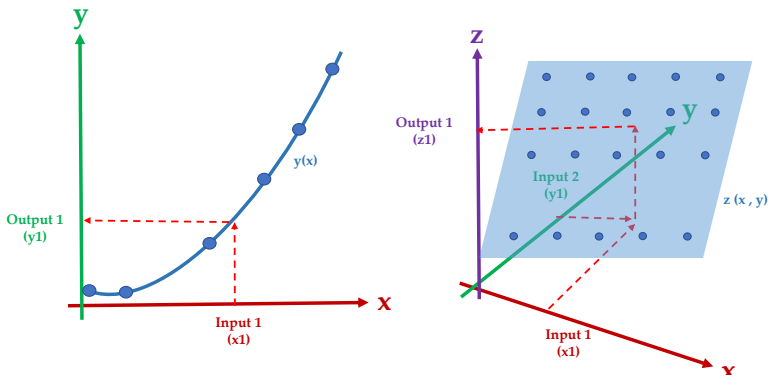

Figure 3.26: Fitting curves general procedure

For the case of predicting the error of the analytical representation of rigid frames this approach is more complex due to the multiple variable dependencies. Then, the following procedure based on polynomial interpolations was developed. The procedure consists of two stages each with specific steps. A diagram of stage one is shown in Figure 3.27.

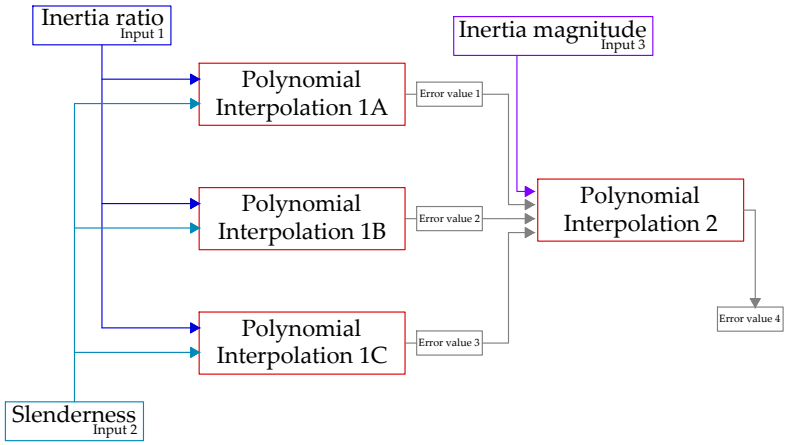

Figure 3.27: Prediction of the error procedure: Stage 1

Stage 1 A two variable dependency can be represented with an interpolated surface as shown in Figure 3.18. To consider a third variable, multiple surfaces were obtained. In this procedure, each of the surfaces represent a specific value for the inertia magnitude. The polynomial equations to approximate the surfaces are of a degree 3x3 and were obtained with the curve fitting tool of Matlab, as shown in Figure 3.28.

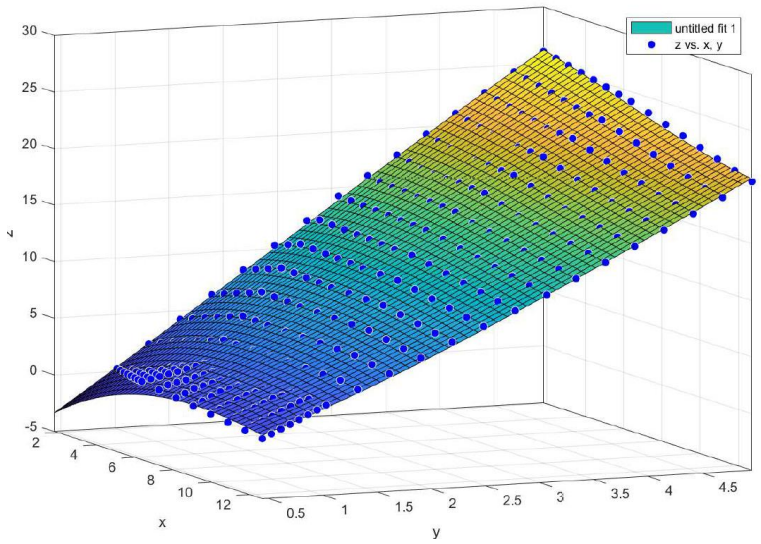

Figure 3.28: Matlab curve fitting tool

By having three interpolated surfaces, three variables are considered to predict the error: the inertia ratio, the slenderness and the inertia magnitude. The steps involved in this stage are presented below.

1. Obtain three error values (Errors 1, 2 and 3) from the three interpolated surfaces.

   These error values are obtained by simultaneously entering the three interpolated surfaces with the specific values of the inertia ratio and slenderness.

2. Obtain an interpolated error (Error 4) from the three previous errors.

   A Lagrange polynomial interpolation is generated based on three points, where the x values are the inertia magnitudes of each of the three interpolated surfaces and the y values are the obtained errors. Then, the error 4 is obtained by entering the Lagrange polynomial with the specific value of the third variable which is the inertia magnitude. The procedure to obtain error 4 is represented graphically in Figure 3.29.

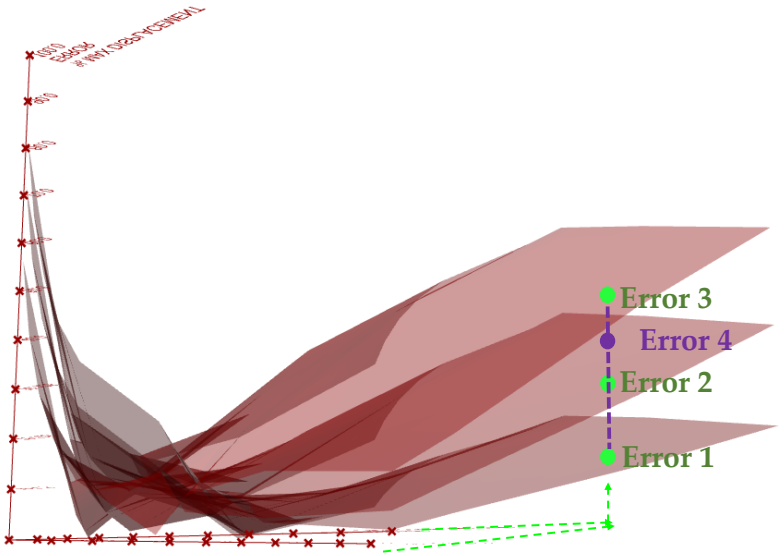

Figure 3.29: Procedure to obtain error 4

Stage 2

Once the error is approximated based on the dependency of the first three variables: inertia ratio, slenderness and inertia magnitude, the error is factored to considered the left two variables which are the module aspect ratio and the overall size. The steps involved in this stage are presented below. This stage is represented with the diagram shown in Figure 3.30.

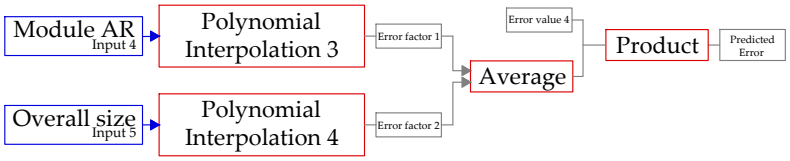

Figure 3.30: Prediction of the error procedure: Stage 2

1. Obtain Error factor 1 by entering a Lagrange polynomial based on three points for three different module aspect ratios. The Langrange polynomial is generated with the following three points, where AR stands for aspect ratio:

	X values	Y values
Point 1	Module AR 1	1
Point 2	Module AR 2	Average decrease sub-factor 1
Point 3	Module AR 3	Average decrease sub-factor 2

2. Obtain factor 2 by entering a Lagrange polynomial based on three points for three different overall sizes.

	X values	Y values
Point 1	Overall size 1	1
Point 2	Overall size 2	Average increase sub-factor 1
Point 3	Overall size 3	Average increase sub-factor 2

3. Calculate a final factor as the geometric mean of factors 1 and 2.

$$GM = \sqrt{F1\,F2} \tag{3.14}$$

4. Calculate the predicted error by multiplying the mean factor and the Error 4.

With the described procedure, the error can be predicted so the analytical solution can be corrected as shown in Figure 3.31. Due to the time limitation of this research project, the procedure to predict the error was only developed for zones B and A. The same procedure can be developed for zones C and D, however, the bending effects can be larger for zone D so it might be more appropriate to represent the behaviour with the bending beam theory and the correction of it for the cases with combined behaviour. More detailed explanations on the developed method to predict the error are presented in appendix A of this report.

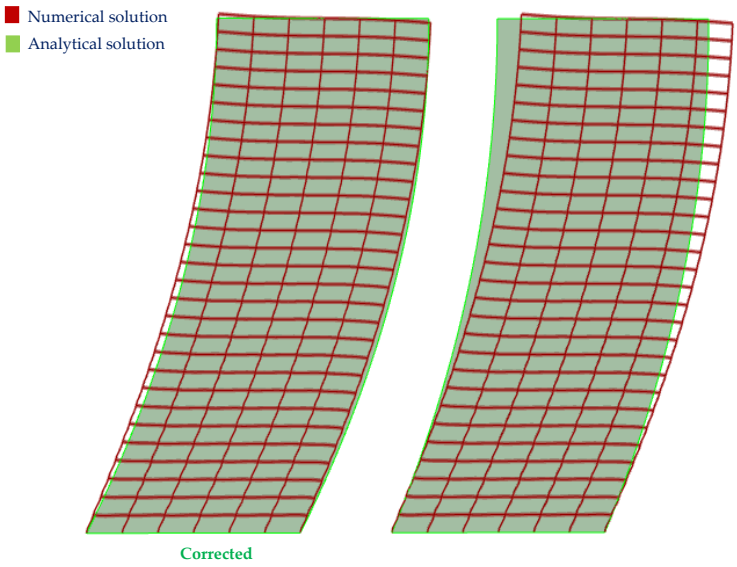

Figure 3.31: Correction of the analytical solution

Then, the displacement function of the shear beam representation can be corrected by means of the procedure just described. The moment and shear forces can be obtained by equilibrium due to the assumption of the static determinate scheme. Also, the prediction of the error can be used as a parameter to classify the behaviour of a rigid frame. The larger the error the larger the bending effects. This parameter differs from the Blume's parameter due to five variables dependency.

The correction method was developed only for the zones B and A. Therefore, different theories based on mechanics that can account for both bending and shear deformations were explored.

The Timoshenko beam theory is described by Simone (2007) as an expansion of the Euler-Bernoulli beam theory that also takes into account shear deformations. In a similar way as the derivation of the ordinary differential equation of the shear beam, Equation 3.16 is derived based on the Timoshenko theory and for the specific case of a static determinate beam. This derivation comes by adding the rotation due to bending in the kinematic relation for the shear deformation, as shown in Equation 3.15. The complete derivation is presented in the lecture material of the TU Delft course: "Analysis of Slender Structures" by Welleman (2017) .

$$\gamma = \frac{\mathrm{d}}{\mathrm{d}x} w\left(x\right) + \phi \tag{3.15}$$

$$\frac{\mathrm{d}^2}{\mathrm{d}x^2} w\left(x\right) = -\frac{q}{GA} - \frac{M}{EI} \tag{3.16}$$

where:
M = Moment function for the static determinate case

For the bottom clamped beam case, the analytical solution is the following:

$$w = 1/24\, \frac{qx\left(6\,GA\,L^2x - 4\,GA\,Lx^2 + GA\,x^3 + 24\,EI\,L - 12\,EI\,x\right)}{GA\,EI} \tag{3.17}$$

The complete procedure to derive the analytical solution is shown in appendix B: Timoshenko beam - One field - Static.

From equation 3.16, it can be observed that if the bending stiffness goes to infinity, the resulting equation is the shear beam ordinary differential equation (ODE), and in the opposite case, if the shear stiffness goes to infinity the resulting expression would be the Euler-Bernoulli ODE. Then, this theory looks very attractive to represent the general behaviour of rigid frames. Figure 3.32 shows three different deformed shapes for a general model of a cantilever Timoshenko beam, the variations are due to the increasing or decreasing of the stiffnesses values.

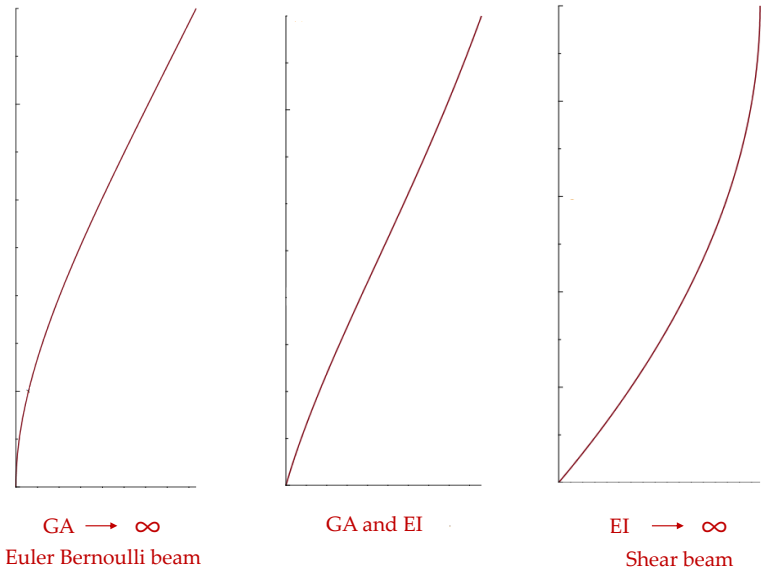

Figure 3.32: Possible deformed shapes of a Timoshenko cantilever beam

To test this theory to represent rigid frames behaviour, an equivalent shear and bending stiffness must be defined. Then, the equivalent shear stiffness is defined as presented in Equation 3.25, and the bending stiffness is defined as presented by Hoenderkamp (2005) which is shown below.

$$EI\,frame = \sum_{columns} EI_{ci} + \sum_{columns} EAc^2{}_{ci} \tag{3.18}$$

where:
A = Cross sectional area of column i
c = Distance from column i to the centroid of the columns

Tests were performed to check the implementation of Equation 3.17 with the use of the shown expressions for the shear and bending stiffnesses. As before, these tests consisted of the comparison of analytical and numerical results. Some tests failed mainly due to the assumption of constant stiffness (shear and bending stiffnesses) along the height. Even when a rigid frame has a regular geometry along the height, the total lateral stiffness of the rigid frame varies, especially at the ground and top floors. By inspection of Equations 3.25 and 3.23 to determine the equivalent stiffnesses, it can be noticed that these will be constant along the height of all the rigid frame.

However, it is known that the shape of the solution of Timoshenko differential equation changes depending on the numerical value of the shear and bending stiffnesses as shown in Figure 3.32. Based on this, an iterative procedure was performed to determine if a specific combination of values for the bending and shear stiffnesses can accurately approximate the exact

numerical displacement solution. To do this, the evolutionary solver Galapagos (Rutten, 2019) , was used. Such iterative procedure struggles on finding the specific values that would make the Timoshenko analytical solution accurate compared to the numerical solution; specifically, the overall best combination of the shear and bending stiffnesses values fails to give a good approximation at the lowest levels of the rigid frame. Figure 3.33 shows the implementation of Galapagos.

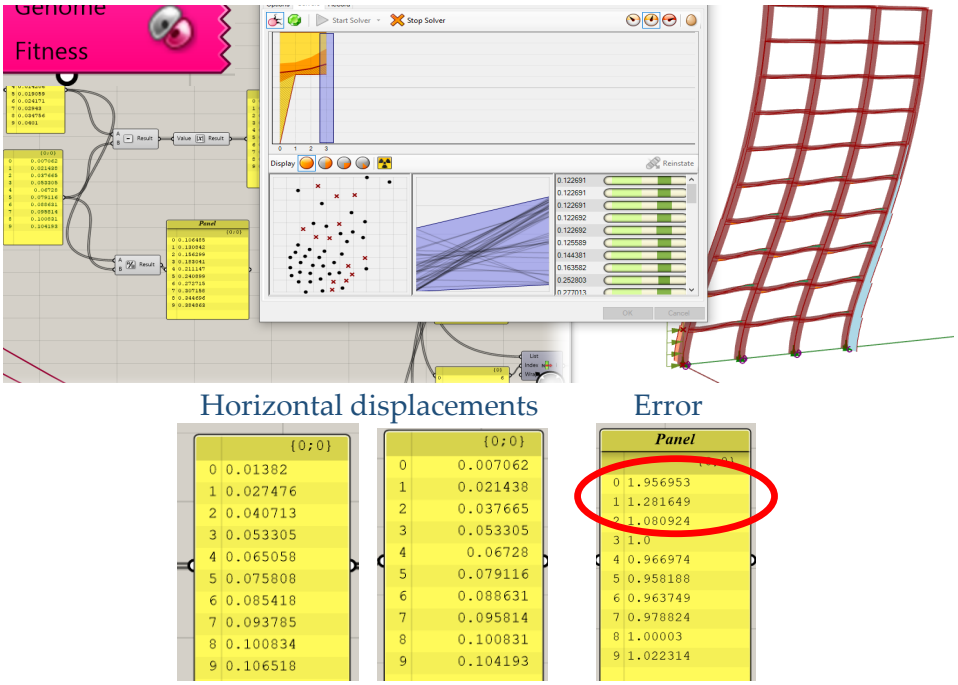

Figure 3.33: Iterative procedure using Galapagos

The observation of a greater error at the lower levels can be related to the stiffness variation along the height. Caterino et al. (2013) and Eroğlu and Akkar (2011) define different factors and formulations for the stiffness of the ground and top floors of a rigid frame. However, from the procedure performed with Galapagos, it can be seen that the greater error occurs at the bottom of the rigid frame.

Besides the Timoshenko theory, there are other analytical theories to account for both bending and shear deformations. The following differential equation is used for a combined system, also presented by Simone (2007) and Welleman (2017) .

$$EI\frac{\mathrm{d}^4}{\mathrm{d}x^4}w\left(x\right)-GA\frac{\mathrm{d}^2}{\mathrm{d}x^2}w\left(x\right)=q \tag{3.19}$$

The analytical solution of the previous equation for the case when the combined system is clamped at the bottom is shown below. The complete derivation is shown in Appendix B - Combined system - one field.

$$w = \frac{qL^2}{GA}\left(-\frac{1+\alpha\, L\sinh(\alpha\, L)}{\alpha^2 L^2\cosh(\alpha\, L)} + \frac{\cosh(\alpha\, x)+\alpha\, L\sinh(\alpha\ (L-x))}{\alpha^2 L^2\cosh(\alpha\, L)} + \frac{x}{L} - 1/2\,\frac{x^2}{L^2}\right) \tag{3.20}$$

where:
$\alpha^2 \quad = \quad GA/EI$

Both Timoshenko and the combined system theories take into account shear and bending deformations. However, there is a relevant difference between them, Timoshenko theory is derived on the basis of a serial system and the combined system as parallel. From the initial tests presented in section 3.1.2, it can be seen that the bending effects on a rigid frame make the total deflection to increase, this can clearly be seen in Figure 3.5. Then, it can be stated that rigid frames behave as a serial system and that the use of theory as Timoshenko can be implemented. But, the variable stiffness along the height for rigid frames still remain.

The previous theories descriptions and findings on the combined behaviour of rigid frames can be summarised with the following sentences.

- The behaviour of rigid frames displays a total deformation similar to a serial system and the Timoshenko theory is derived on the basis of a serial system.
- The combined behaviour of rigid frames exhibits a variable stiffness along its height and especially at the bottom.

Based on previous premises, it was proposed to represent the behaviour of rigid frames by splitting the 1D analytical representation into two fields and use the Timoshenko theory for each of them. The separation into fields is proposed in order to consider a different shear stiffness for the first floor where the bending effects are high due to the fixed support conditions. This proposed method is represented in Figure 3.34.

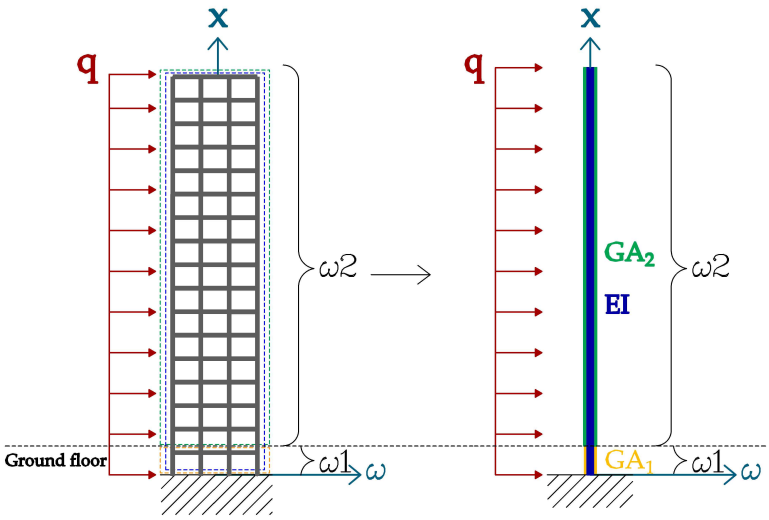

Figure 3.34: Physical structural system and analytical Timoshenko beam representation (Serial system).

Then, the following set of differential equations are proposed as a method to represent the combined behaviour of rigid frames with fixed support conditions.

$$\frac{\mathrm{d}^2}{\mathrm{d}x^2} w1\,(x) = -\frac{q}{GA1} - \frac{M}{EI} \tag{3.21}$$

$$\frac{\mathrm{d}^2}{\mathrm{d}x^2} w2\,(x) = -\frac{q}{GA2} - \frac{M}{EI} \tag{3.22}$$

The analytical displacement solution for the first differential equation which accounts for the first field is shown as Equation 3.17. And for the second field, the analytical displacement solution, as well as the boundary and matching conditions, moment, shear and deformations equations are presented in Appendix B: Timoshenko beam - three fields - static.

The equivalent stiffness expressions are defined as follows.

- Equivalent bending stiffness as presented by Hoenderkamp (2005)

$$EI\,frame = \sum_{columns} EI_{ci} + \sum_{columns} EAc^2{}_{ci} \tag{3.23}$$

- Equivalent shear stiffness for the first floor, as presented by Hoenderkamp (2005) .

$$GA1 = \frac{12\,E\left(1 + 1/6\sum_{columns}\frac{Ic}{h}\left(\sum_{beams}\frac{Ib}{b}\right)^{-1}\right)}{h\left(\left(\sum_{columns}\frac{Ic}{h}\right)^{-1} + 2/3\left(\sum_{beams}\frac{Ib}{b}\right)^{-1}\right)} \tag{3.24}$$

- Equivalent shear stiffness from second to top floor, as presented by Hoenderkamp (2005) , Rolvink (2010) and Olowokere et al. (1991) .

$$GA2 = 12\,\frac{E}{h}\left(\left(\sum_{columns}\frac{Ic}{h}\right)^{-1} + \left(\sum_{beams}\frac{Ib}{b}\right)^{-1}\right)^{-1} \tag{3.25}$$

The same initial tests as in section 3.1.2 were performed but now with the method just described based on the Timoshenko beam theory. The structural scheme for the analytical representation changes and is shown in Figure 3.34. The results are shown in Figures 3.35 to 3.38.

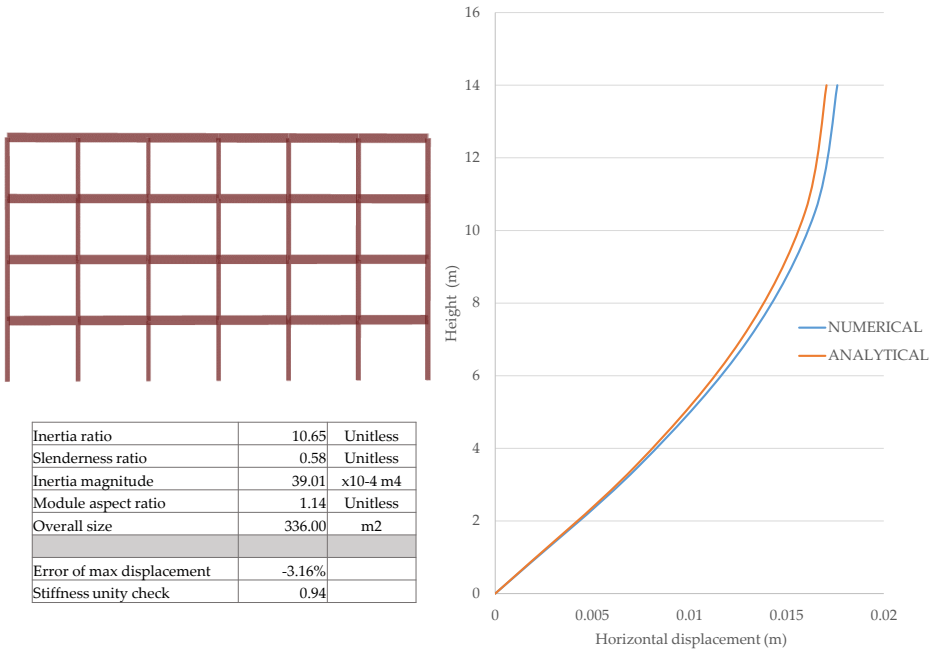

Figure 3.35: Model lB: High inertia ratio and low slenderness

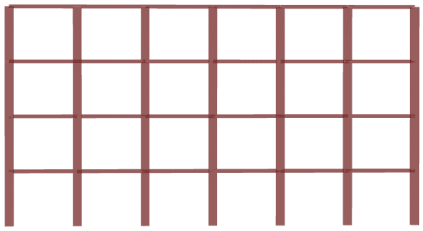

Inertia ratio	0.09	Unitless
Slenderness ratio	0.58	Unitless
Inertia magnitude	33.17	x10-4 m4
Module aspect ratio	1.14	Unitless
Overall size	336.00	m2
Error of max displacement	14.97%	
Stiffness unity check	0.79	

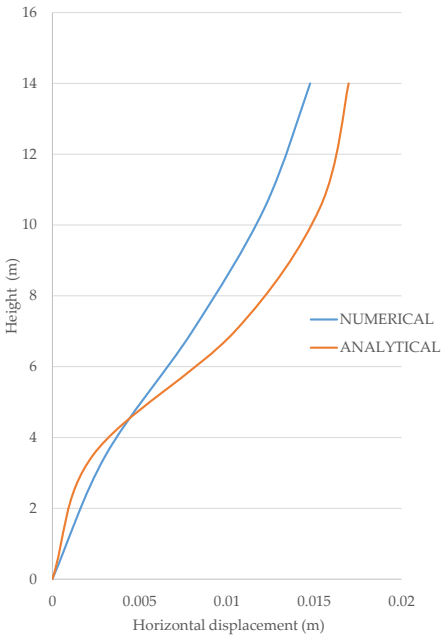

Figure 3.36: Model 2B: Low inertia ratio and low slenderness

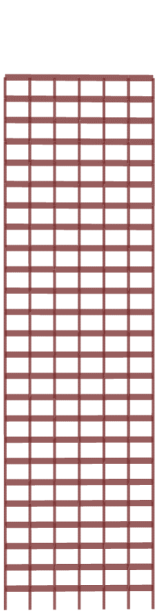

Inertia ratio	10.65	Unitless
Slenderness ratio	3.65	Unitless
Inertia magnitude	265.36	x10-4 m4
Module aspect ratio	1.14	Unitless
Overall size	2100.00	m2
Error of max displacement	-9.14%	
Stiffness unity check	1.35	

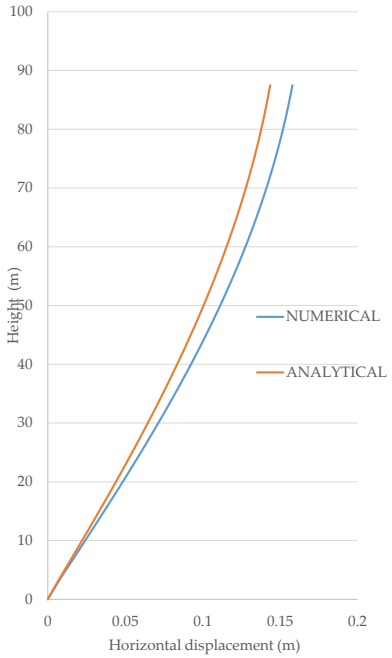

Figure 3.37: Model 3B: High inertia ratio and high slenderness

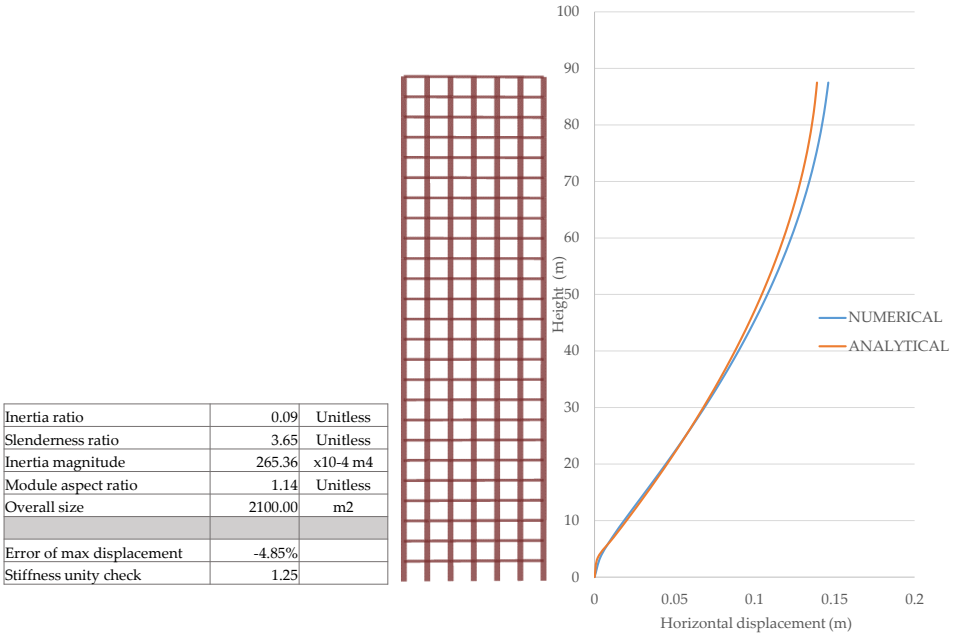

Inertia ratio	0.09	Unitless
Slenderness ratio	3.65	Unitless
Inertia magnitude	265.36	x10-4 m4
Module aspect ratio	1.14	Unitless
Overall size	2100.00	m2
Error of max displacement	-4.85%	
Stiffness unity check	1.25	

Figure 3.38: Model 4B: Low inertia ratio and high slenderness

From Figure 3.35 to 3.38, the following observations can be made.

- In Figure 3.35 the error of the analytical symbolic representation is mainly because a different shear stiffness for the top floor is not considered. The analytical approximation is not conservative but sufficiently accurate for preliminary design because the error is less than 5 percent.
- In Figure 3.36 the error of the analytical symbolic representation is mainly because a different shear stiffness for the top floor is not considered and also because significant bending effects due to the fixed support extend farther than only the ground floor. The analytical approximation is conservative and the error is considered as allowable for the preliminary design because it is less than 20 percent.
- In Figure 3.37 the error of the analytical symbolic representation is mainly because a different shear stiffness for the top floor is not considered. The analytical approximation is not conservative but sufficiently accurate for preliminary design because the error is less than 10 percent.
- In Figure 3.38 the error of the analytical symbolic representation is mainly because a different shear stiffness for the top floor is not considered. The analytical approximation is not conservative but sufficiently accurate for preliminary design because the error is less than 5 percent.

Then, by the implementation of Timoshenko theory with a different shear stiffness for the ground floor to represent the behaviour of rigid frames,

the bending effects are considered and the applicability is larger than the correction method because it includes the four defined zones.

3.4 ANALYTICAL METHOD FOR VERTICAL CONNECTIONS OF COMPONENTS

The three aimed and most important characteristics for the tool prototype are the parametric adaptability quality, the real-time displaying of results and the stacking of rigid frames geometries to create a complete building geometry. On StructuralComponents5.0 by Hohrath (2018) , the stacking of the building blocks was solved with the procedure described by Steenbergen (2007) as part of the Super Element Method (SEM). This stage of the SEM follows the scheme of the Finite Element Method (FEM). During this research project, a different approach was proposed and implemented for the connection of rigid frames geometries. Instead of the derivations of stiffness matrices for each component, different analytical solutions are derived for specific parts (fields) along the height of the building. Figure 3.39 shows how a 2D frame with a drastic change in its vertical geometry can be represented as a 1D analytical model with the Timoshenko beam theory.

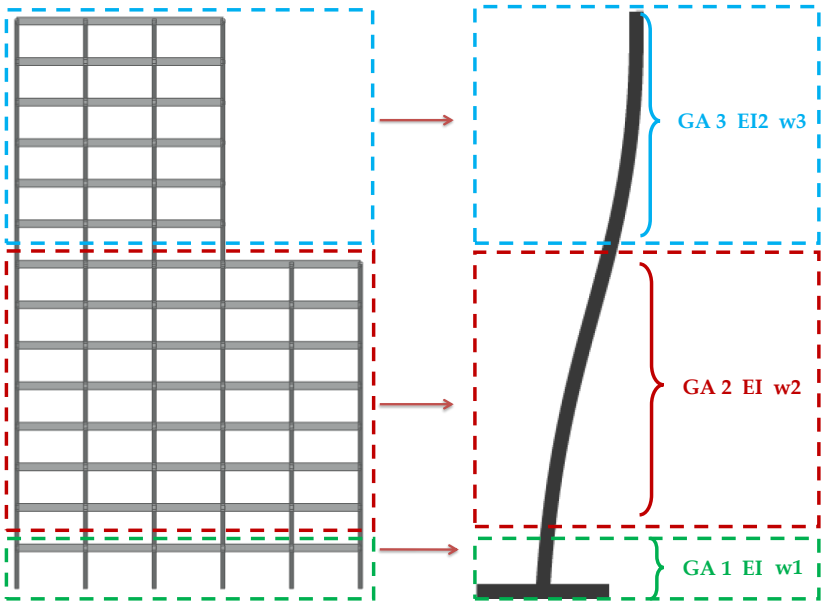

Figure 3.39: Analytical representation of drastic geometric change along the height

Then, the set of differential equations to allow for a drastic change of stiffness along the height of the rigid frame are the following.

$$\frac{\mathrm{d}^2}{\mathrm{d}x^2} w1\,(x) = -\frac{q}{GA1} - \frac{M}{EI1} \tag{3.26}$$

$$\frac{\mathrm{d}^2}{\mathrm{d}x^2} w2\,(x) = -\frac{q}{GA2} - \frac{M}{EI1} \tag{3.27}$$

$$\frac{\mathrm{d}^2}{\mathrm{d}x^2} w3\,(x) = -\frac{q}{GA3} - \frac{M}{EI2} \tag{3.28}$$

To obtain the analytical solutions, it was necessary to also define matching conditions instead of only boundary conditions. The analytical solutions, as well as the boundary and matching conditions, moment, shear and deformations equations, are presented in Appendix B: Timoshenko beam - three fields - static.

Then, with this analytical method to represent drastic changes on stiffness along the height of the building, the scheme of the Finite Element Method is not necessary to allow for connections between different geometries of rigid frames.

4 TOOL PROTOTYPE FOR RIGID FRAMES STRUCTURAL SYSTEMS

The structural calculation method and design feasibility checks, as well as the features and capabilities of the tool prototype, are presented in this chapter.

4.1 STRUCTURAL CALCULATION METHOD

The implemented calculation method consists of the simultaneous linear structural analysis of every rigid frame subjected to a lateral load on a building. First, the lateral load is assumed to be transferred from the facade to the lateral stability members as a uniformly distributed load as shown in Figure 4.1.

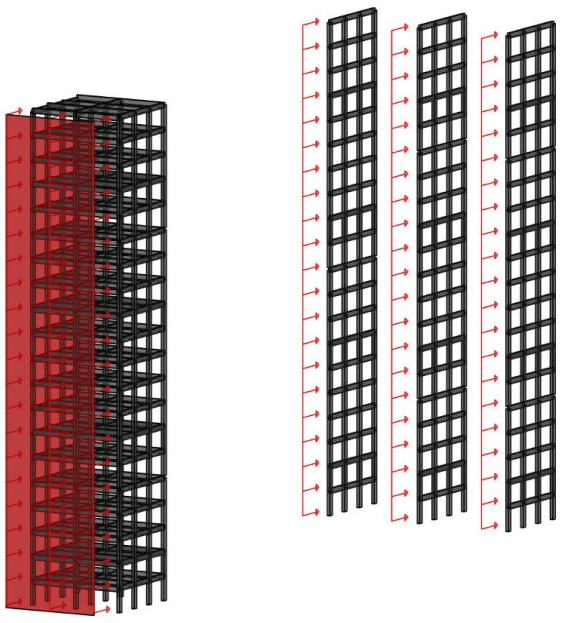

Figure 4.1: Load distribution

Then, the analytical solution is obtained with the differential equations from the Timoshenko beam theory for the static case of a cantilever

beam. The structural scheme is shown in Figure 4.2. This derivation is based on the fact that the moment and shear distributions can be found by equilibrium. The subdivision of the 1D idealisation, and therefore the use of a set of differential equations to get the analytical solution, allows taking into account different stiffness along the height.

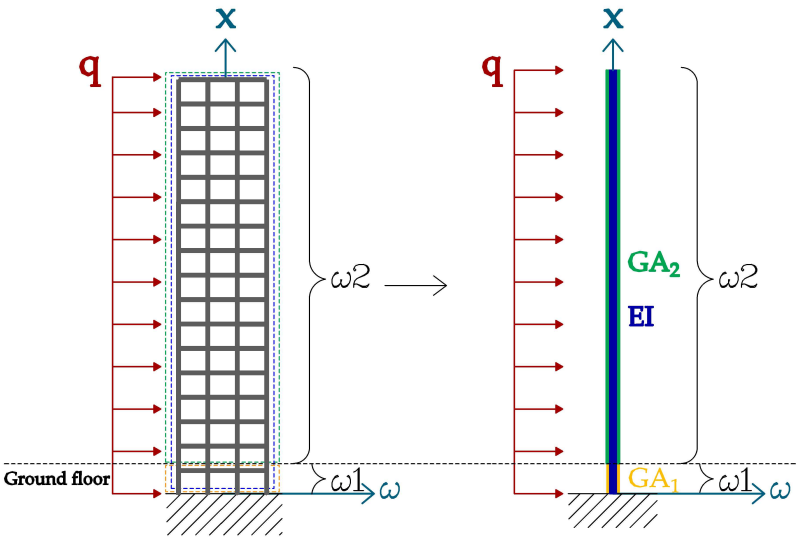

Figure 4.2: Physical structural system and analytical Timoshenko beam representaion (Serial system).

4.2 STRUCTURAL FEASIBILITY CHECKS

Breider (2008) mentions that for buildings where the lateral loads will be governing, the structural feasibility during the preliminary design stage can be based on quick stability, stiffness and strength checks. The structural feasibility checks implemented in StructuralComponentes5.0 are the ones shown in Equations 4.1-4.5. These equations were adopted from the recommendations of the reader of the course Building Structures 2 from TU Delft by Ham and Terwel (2017) and the Eurocode 2 (BS-EN-1992-1-1, 2004) .

STABILITY

$$ULS : \frac{\gamma Q \, c_d \, M_{\mathrm{q,k}}}{x} < \gamma G \;_{,inf} \, Ndead_{\mathrm{R,k}} \tag{4.1}$$

STIFFNESS

- Maximum displacement

$$SLS : c_d \, u_{\max} < \frac{H}{750} \tag{4.2}$$

- Inter-storey drift

$$SLS : c_d \, u_{interstorey} < \frac{h_{storey}}{300} \tag{4.3}$$

STRENGTH

- Compression

$$ULS : -\frac{\gamma Q \, M_{\mathrm{q,k}}}{W} - \frac{\gamma G \,_{,inf} \, Ndead_{\mathrm{R,k}}}{A} < fcd \tag{4.4}$$

- Tension

$$ULS : \frac{\gamma Q \, M_{\mathrm{q,k}}}{W} - \frac{\gamma G \,_{,inf} \, Ndead_{\mathrm{R,k}}}{A} < 0 \tag{4.5}$$

4.2.1 Feasibility checks for rigid frames

To quickly determine the structural feasibility of rigid frames systems, the feasibility checks showed in Equations 4.1-4.5 are adopted, except for the tension-strength that would severely limit the feasibility of rigid frames, even for preliminary design stages.

Also, if a rigid frame is idealised analytically with a one-dimensional element, the results from the structural analysis are global and not specifically for each element, in this case for each column and each beam. In the reader of the course: "Building Structures 2" at TU Delft by Ham and Terwel, two methods are provided to determine the internal forces acting on each element of a rigid frame when idealised as a cantilever beam. The first one is called the portal method and the second one the cantilever method. The portal method is more suitable for rigid frames that deform mainly as a shear beam and the cantilever method when it deforms more closely to a Euler-Bernoulli beam. The description of both methods is presented below and implemented in this research project to obtain the maximum tension and compression stresses in the beams and columns.

PORTAL METHOD

The portal method is implemented in this research project assuming that the greatest stresses in columns and beams occur at the ground level. This method consists of the following steps.

1. Shear force at mid-height of the first storey

   $$V_{total} = q\left(L - h_{storey}/2\right)$$

2. Shear force per bay

   $$V_{bay} = \frac{V_{total}}{n_{bays}}$$

3. Shear force in each column

   $$V_{\text{exterior-columns}} = V_{bay}/2$$

   $$V_{\text{exterior-columns}} = V_{bay}$$

4. Column bending moment

   $$M_{columns} = 1/2\, V_{columns}\, h_{storey}$$

5. Beam bending moment

   These moments are obtained through equilibrium between columns and beams bending moments. Then, it is necessary to repeat steps 1 to 4 to obtain the columns bending moments for the second floor.

   $$M_{beamfloor1} = M_{columnfloor1} + M_{columnfloor2}$$

6. Axial force in external columns

   First, the total moment is calculated and then the axial force in each of the exterior columns is obtained.

   $$M_{total} = 1/2\, qH^2$$

   $$F_{exteriorcolumns} = \frac{M_{total}}{W_{totalwidth}}$$

CANTILEVER METHOD

1. Location of the neutral axis

2. Moment of inertia of the rigid frame structure

$$\sum_{columns} A_{ci}\, {c_i}^2 = \sum_{columns} A_{ci}\, {c_i}^2$$

where c represents the distances of every column to the neutral axis.

3. The axial force in a column

$$\frac{M_i\, C_i\, A_i}{Inertia} = \frac{M_i\, C_i\, A_i}{Inertia}$$

Where the moments are calculated with the procedure explained for the portal method.

4. Shear force in the beams

$$V_{beam} = F_{columnfloor1} - F_{columnfloor2}$$

5. Beam bending moment

$$M_{beam} = 1/2\, V_{beam}\, h_{storey}$$

6. Shear force in the column

$$V_{beam} = \frac{M_{column}}{h_{storey}/2}$$

Once the critical bending moments in beams and columns, as well as the maximum axial forces in the columns are calculated, the strength feasibility checks can be defined again and are shown below in Equation 4.6 and 4.7. The compression-strength check is the one shown in 4.4 with small variations. For this research project, it is proposed to define the tension-strength feasibility check considering the maximum amount of reinforcement bars in a concrete cross-section. The maximum area of reinforcement for concrete beams and columns is 4 percent of the gross-area of cross-section according to "Concrete Buildings Scheme Design Manual" by Brooker (2006) . For this research project, the strength checks are provided only for the columns.

STRENGTH

- Compression

$$ULS: -\frac{\gamma Q\, F_{\mathrm{k,column}}}{A_{column}} - \frac{\gamma Q\, M_{\mathrm{k,\ column}}}{W_{column}} - \frac{\gamma G_{,inf}\, Ndead_{\mathrm{R,k}}}{A_{column}} < f_{cd} \tag{4.6}$$

- Tension

$$\frac{\gamma Q \left(F_{\mathrm{k,column}} - 0.04\, f_{by}\, A_c\right)}{A_{column}} + \frac{\gamma Q\, M_{\mathrm{k,\ column}}}{W_{column}} - \frac{\gamma G_{,inf}\, Ndead_{\mathrm{R,k}}}{A_{column}} < 0 \tag{4.7}$$

4.3 SPECIFICATIONS OF THE TOOLBOX

The tool prototype consists of two rigid frame components to perform real-time structural evaluations of a building. The three main characteristics of the tool are the parametric adaptability, the instantaneous display of the results and the stacking type connection between components. For each of the components the following stages are scripted: modelling, analysis, design and visualisation. The analysis is performed with the analytical solutions shown in Appendix B: Timoshenko beam - three fields - static. The design stage refers to the feasibility checks for rigid frames defined in section 4.2.1.

4.3.1 General specifications

Similarly to StructuralComponents5.0 by Hohrath (2018) , the software interface for this tool prototype is Rhino-Grasshopper with the use of GhPython component to store the analytical expressions and derivations. This software interface is chosen due to the parametric adaptability quality of the plug-in Grasshopper. Specifically, Grasshopper with GhPython are used for the modelling and analysis part, and Rhino is used for the visualisation of both, the model and the results.

4.3.2 Rigid frames components

For this project, two rigid frame components have been developed. The first one is called the initial rigid frame component (**Initial-RFC**) and the second one the connecting rigid frame component (**Connecting-RFC**). To obtain the structural analysis results, the analytical solution is obtained for every 2D portal frame according to the inputs parameter of the Initial-RFC or the combination of both the Initial-RFC and the Connecting-RFC.

The **initial-RFC** component consists of a parametric 3D arrangement of columns and beams as shown in Figure 4.3. The modelling, analysis, design and visualisation scripts are inside the same cluster, which is a compilation of Grasshopper and GhPython components; for this research project, this cluster together with its corresponding inputs and outputs integrate the

Initial-RFC. The inputs are the numerical sliders and yellow panels to the left of the main cluster and the outputs are the containers to its right.

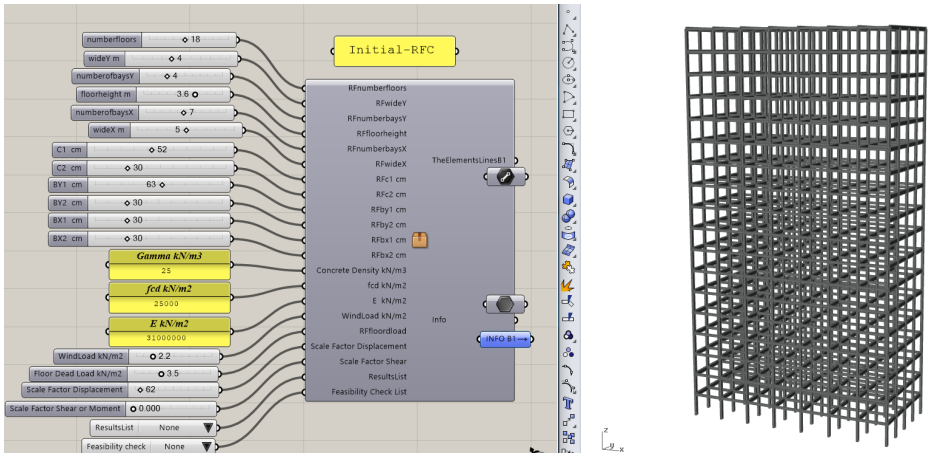

Figure 4.3: Initial-RFC (Right side: Grasshopper canvas. Left side: Rhino interface).

To allow for more geometric flexibility, especially to account for drastic stiffness changes along the height of a building the **Connecting-RFC** was developed which in a similar way consists of a parametric 3D arrangement of columns and beams shown in Figure 4.3. The modelling, analysis, design and visualisation scripts are inside the same cluster which is a compilation of Grasshopper and GhPython components. This component is meant to be vertically connected to the Initial-RFC. The vertical stacking process is done by connecting the "ElementLines" and "Info" outputs of the Initial-RFC as inputs for the Connecting-RFC, this process is shown in Figure 4.4.

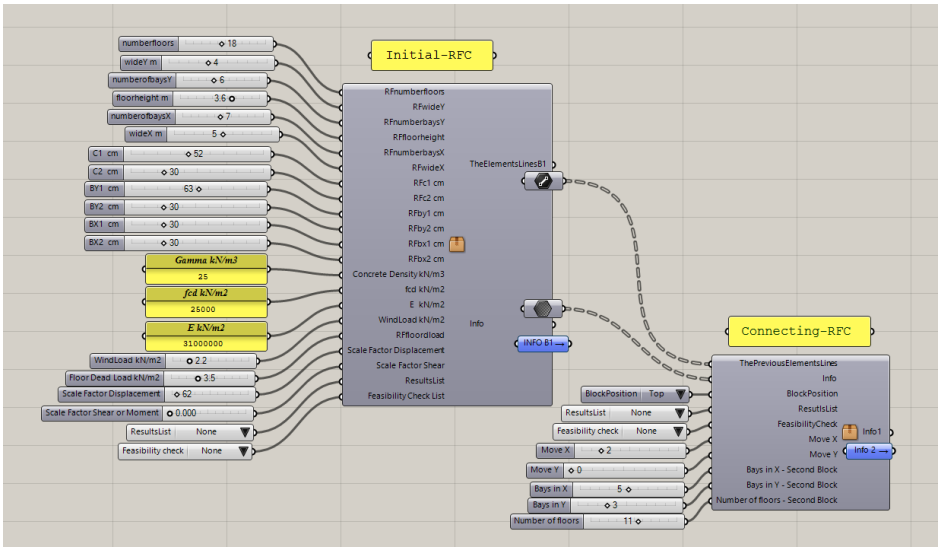

Figure 4.4: Connection of Initial-RFC and Connecting-RFC (Grasshopper canvas)

The connections of the physical structural systems of each component can be seen as the stacking of 'boxes' one on top the other. This is represented in Figure 4.5. Several building possible geometries can be model with the two rigid frames components as the ones shown in Figure 4.6. The load distribution, for the connection of rigid frames components, is illustrated in Figure 4.7.

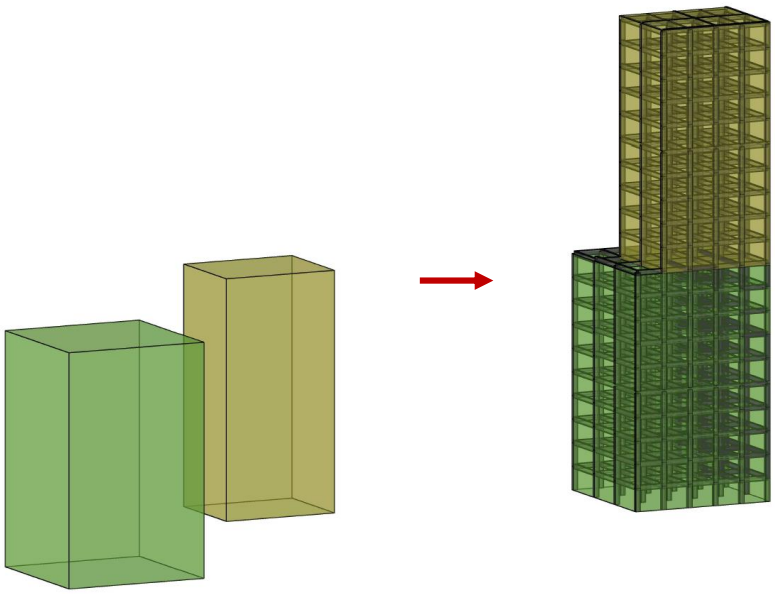

Figure 4.5: Connecting rigid frames components

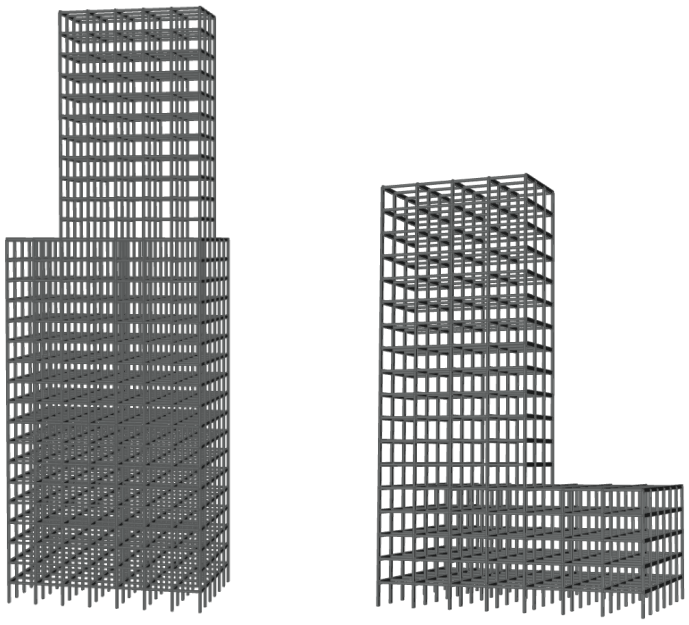

Figure 4.6: Building geometries using the rigid frames components

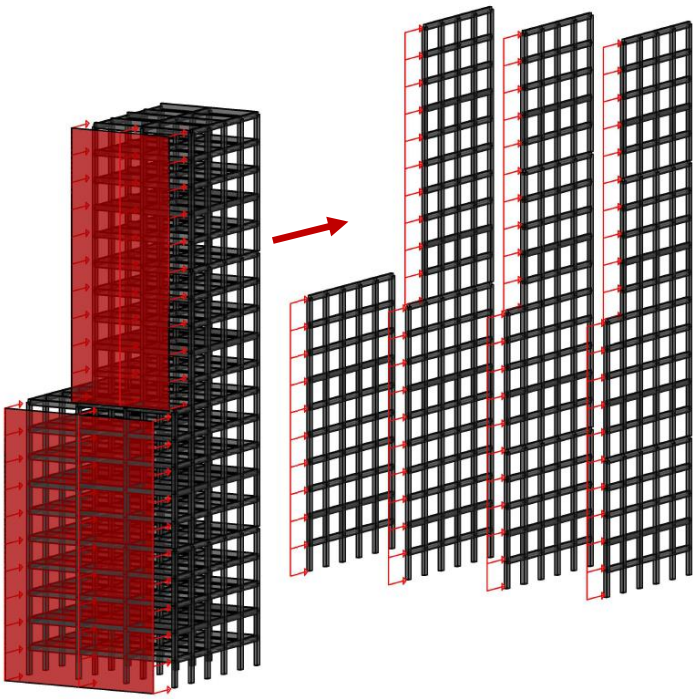

Figure 4.7: Load distribution when connecting rigid frames components

4.3.3 Data flow

The data flow of the tool prototype can be described with the following steps:

- Parameters inputs
- Geometric modelling
  - Modelling
  - Geometry visualisation
- Structural analysis
  - Calculation of analytical solution for each portal frame and each field
- Design
  - Calculation of element forces
  - Feasibility checks
- Outputs
  - Analytical results
  - Visualisation of the results

Due to the real-time capability of the components, it can be considered that all the stages run simultaneously when the input parameters are adjusted. This data flow is the same for both cases: the use of only the Initial-RFC or the use of the two components. For the second case, the final displayed analysis and design results are calculated inside the Connecting-RFC by considering every 2D rigid frames geometries composed by the two components.

4.3.4 Analysis results and design capabilities

The analysis results that the tool performs in real-time are the following:

1. The lateral deformation for the complete rigid frame
2. The shear and moment diagrams for the complete rigid frame
3. The maximum element forces of the critical elements at the ground floor: maximum axial, shear forces and moments.
4. The feasibility checks: stability, stiffness and strength.

In Figure 4.8 the displaying of the displacement, shear and moment diagram results are shown for an example geometry by the implementation of the tool. Also, the elements turn red when one or several feasibility requirements are not met, which is shown in Figure 4.9. The displaying of results by the use of both components can be seen in Figures 4.10 and 4.11 .

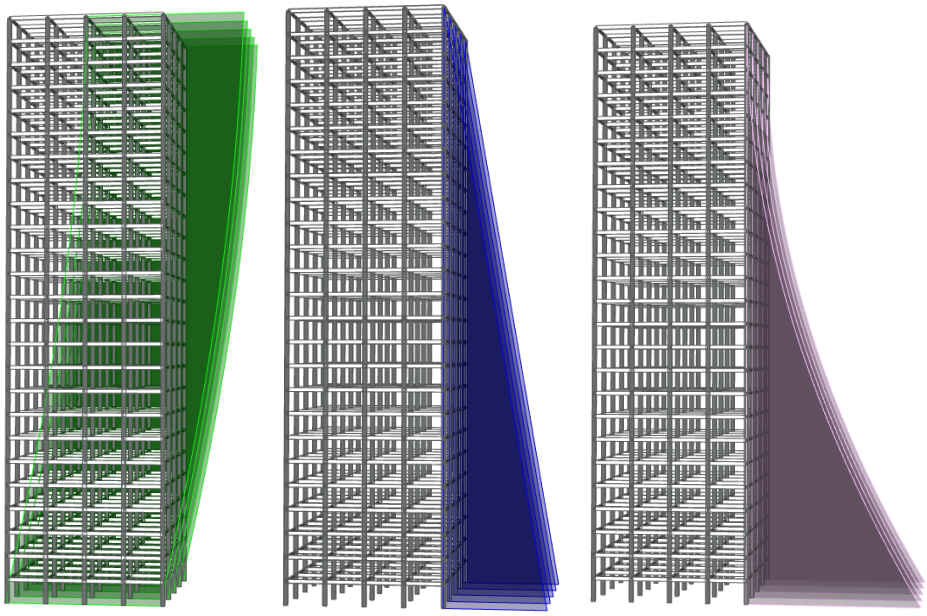

Figure 4.8: Display of results of the Initial-RFC

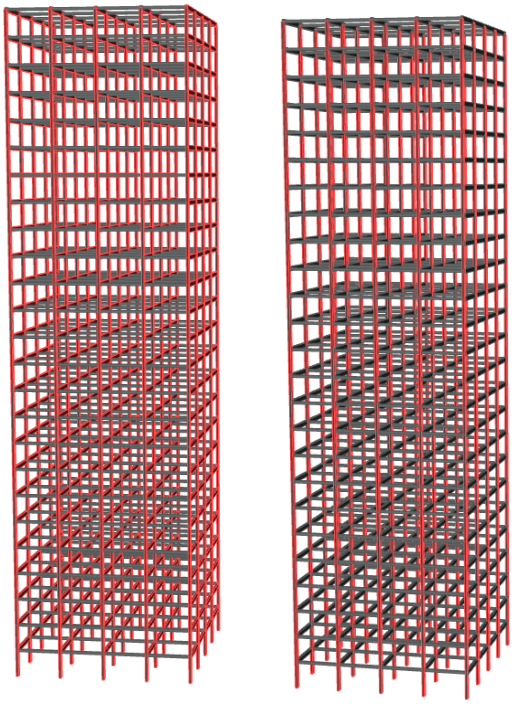

Figure 4.9: Non-compliant elements indicated in red

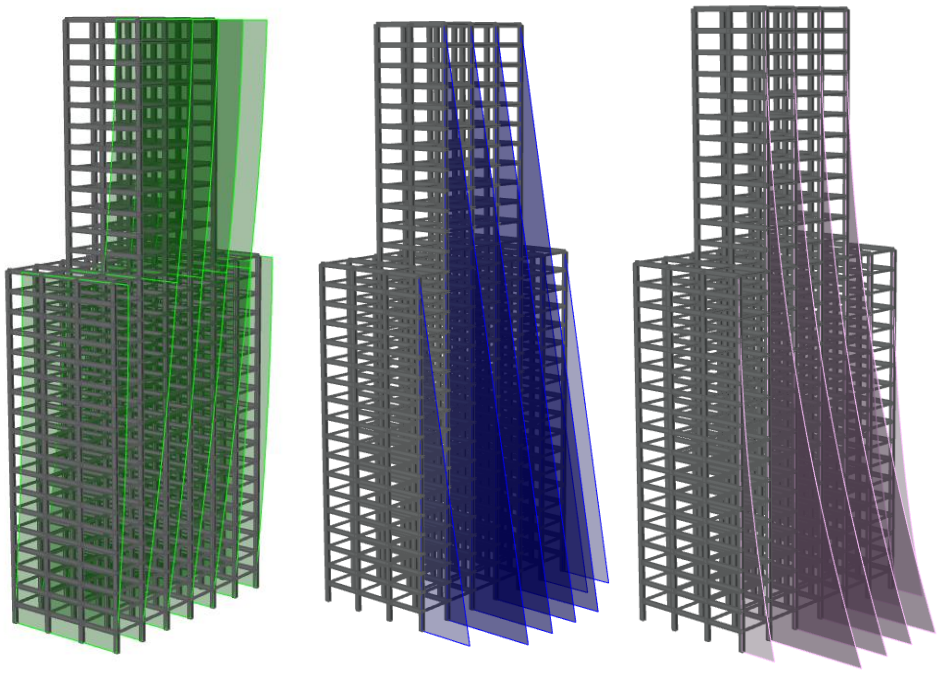

Figure 4.10: Display of results using both components

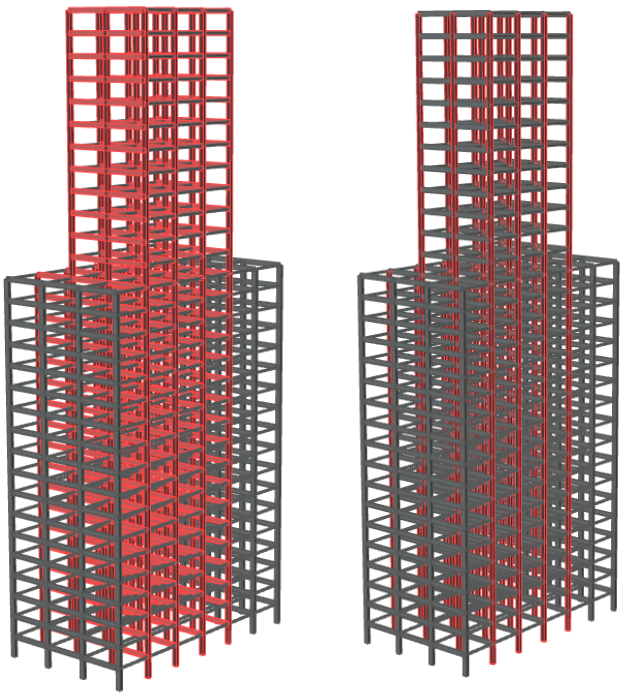

Figure 4.11: Display of results using both components

4.4 USE PROCESS

The final arrangement of the tool prototype was designed with the goal to make it simple for the user. With the use of only the Initial-RFC, the feasibility of a complete building can be assessed. From the user's perspective, the use of the tool with only the Initial-RFC consists of only 2 steps: the input of the parameters and the interpretation of the results. In the case of a different geometry along the height, the component connection step is needed as well as the input of the parameters for the second components. The frameworks just described are also presented in Figure 4.12.

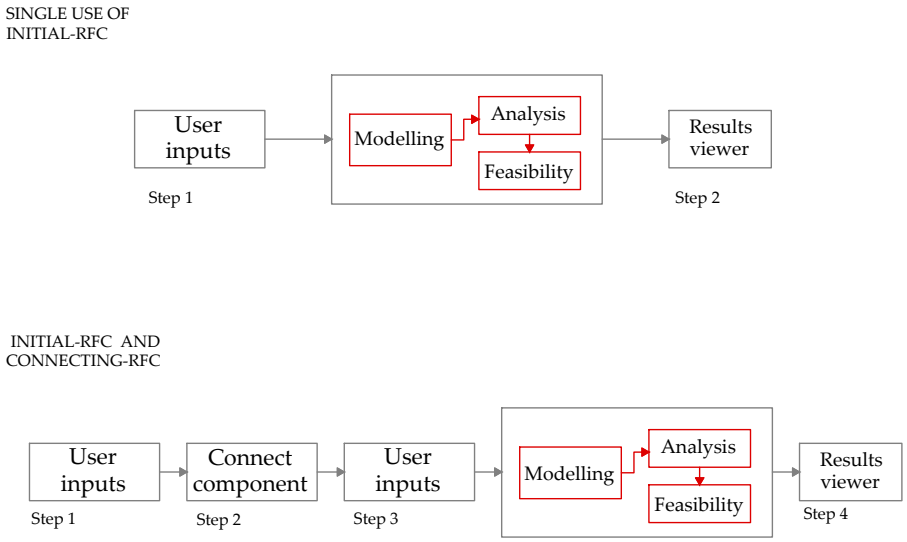

Figure 4.12: Use process of the tool prototype

5 VALIDATION OF RESULTS AND DEVELOPED METHODS

Tests were performed to validate the implemented methods. The validations are carried out by comparing the analytical and numerical solutions for common dimensions of rigid frames. The software used to derive the analytical solution was MapleSoft, and to implement Grasshopper with GhPython components was used. The numerical solutions are obtained with Grasshopper and the finite element solver embedded in Karamba3D.

5.1 APPLICABILITY OF THE ANALYTICAL SHEAR BEAM REPRESENTATION

The geometry properties of the models tested in this section are chosen within the defined range of applicability of the shear beam representation to check that the error is less than defined as allowable for the preliminary design. The analytical solution in this section is obtained from the shear beam representation with no correction. Figures 5.1 and 5.2 are the defined models to validate the range of applicability.

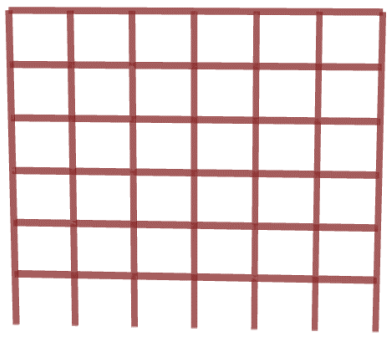

Inertia ratio	1.24	Unitless
Slenderness ratio	0.88	Unitless
Inertia magnitude	35.88	x10-4 m4
Module aspect ratio	1.14	Unitless
Overall size	504.00	m2
Error of max displacement	2.33%	
Stiffness unity check	0.53	

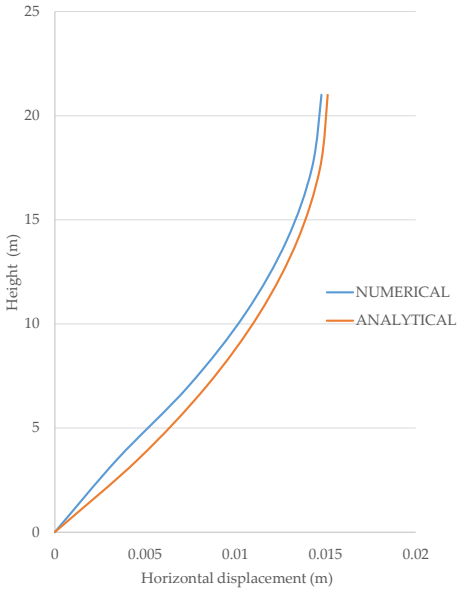

Figure 5.1: Applicability range - test 1

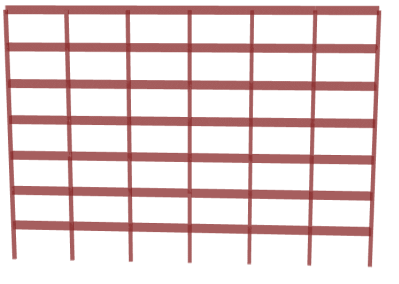

Inertia ratio	12.70	Unitless
Slenderness ratio	0.70	Unitless
Inertia magnitude	92.50	x10-4 m4
Module aspect ratio	1.67	Unitless
Overall size	630.00	m2
Error of max displacement	-4.91%	
Stiffness unity check	0.55	

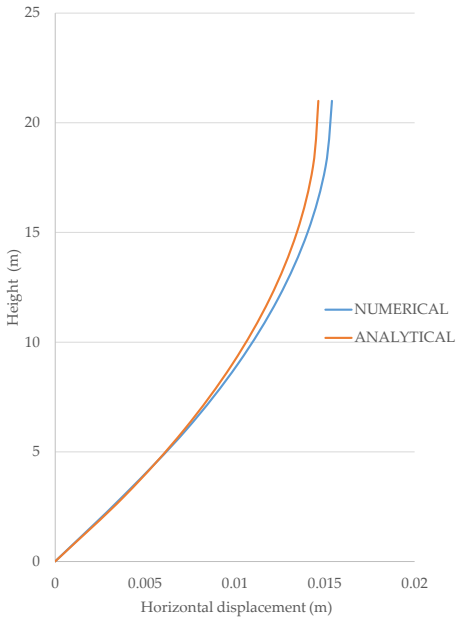

Figure 5.2: Applicability range - test 2

From Figures 5.1 and 5.2, it is shown that the error of the different models is less than 20 percent defined as the allowable for the preliminary design.

5.2 CORRECTION METHOD FOR THE SHEAR BEAM REPRESENTATION

The correction method for the shear beam representation was tested for several models within the defined zone B. The not corrected and the corrected analytical solutions are shown for every model. The properties for the models were chosen so a representative sample of zone B was covered. The results are shown in Figures 5.3-5.8.

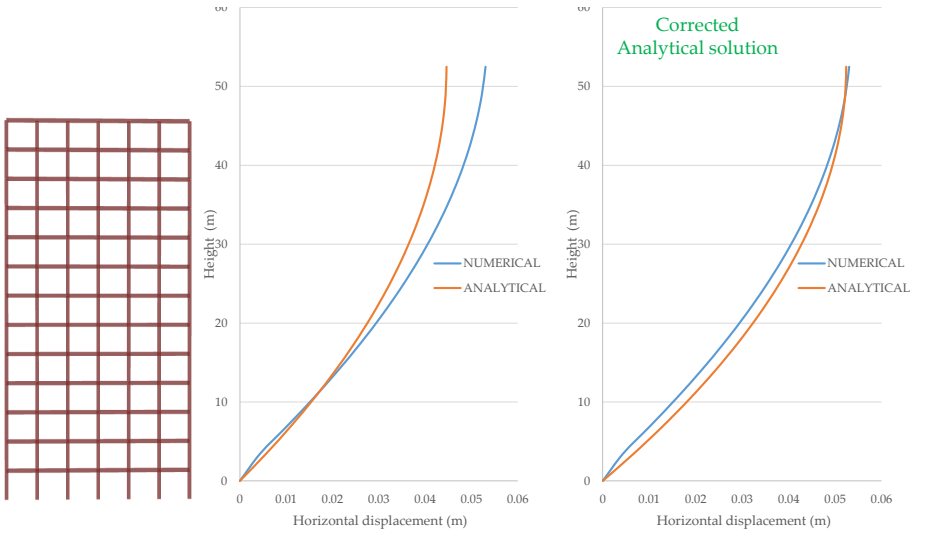

Inertia ratio	1.16	Unitless
Slenderness ratio	2.19	Unitless
Inertia magnitude	75.84	x10-4 m4
Module aspect ratio	1.14	Unitless
Overall size	1260.00	m2
Error of max displacement	-15.83%	
Stiffness unity check	0.76	

Inertia ratio	1.16	Unitless
Slenderness ratio	2.19	Unitless
Inertia magnitude	75.84	x10-4 m4
Module aspect ratio	1.14	Unitless
Overall size	1260.00	m2
Error of max displacement	-1.18%	
Stiffness unity check	0.76	

Figure 5.3: Corrected analytical solution - test 3

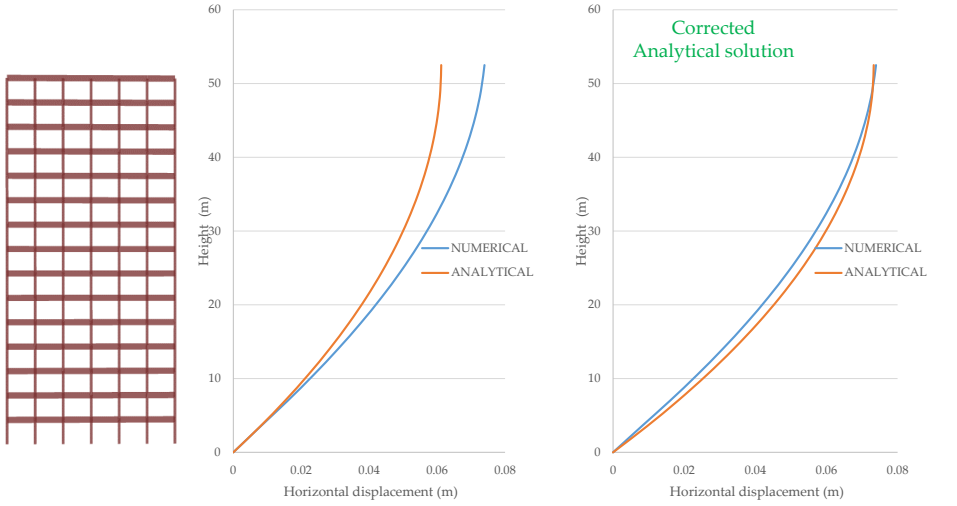

Inertia ratio	12.49	Unitless
Slenderness ratio	2.19	Unitless
Inertia magnitude	177.81	x10-4 m4
Module aspect ratio	1.14	Unitless
Overall size	1260.00	m2
Error of max displacement	-17.21%	
Stiffness unity check	1.06	

Inertia ratio	12.49	Unitless
Slenderness ratio	2.19	Unitless
Inertia magnitude	177.81	x10-4 m4
Module aspect ratio	1.14	Unitless
Overall size	1260.00	m2
Error of max displacement	-0.93%	
Stiffness unity check	1.06	

Figure 5.4: Corrected analytical solution - test 4

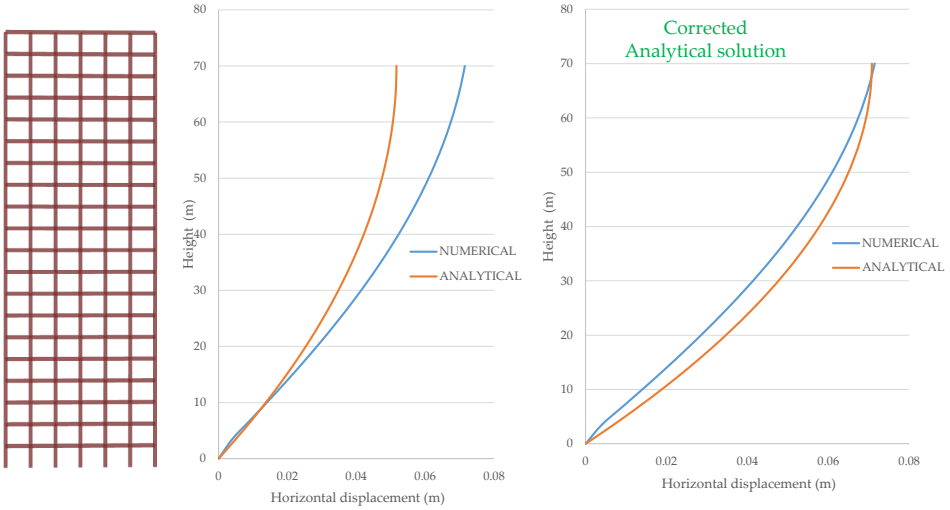

Inertia ratio	1.16	Unitless
Slenderness ratio	2.92	Unitless
Inertia magnitude	116.51	x10-4 m4
Module aspect ratio	1.14	Unitless
Overall size	1680.00	m2
Error of max displacement	-27.74%	
Stiffness unity check	0.77	

Inertia ratio	1.16	Unitless
Slenderness ratio	2.92	Unitless
Inertia magnitude	116.51	x10-4 m4
Module aspect ratio	1.14	Unitless
Overall size	1680.00	m2
Error of max displacement	-0.96%	
Stiffness unity check	0.77	

Figure 5.5: Corrected analytical solution - test 5

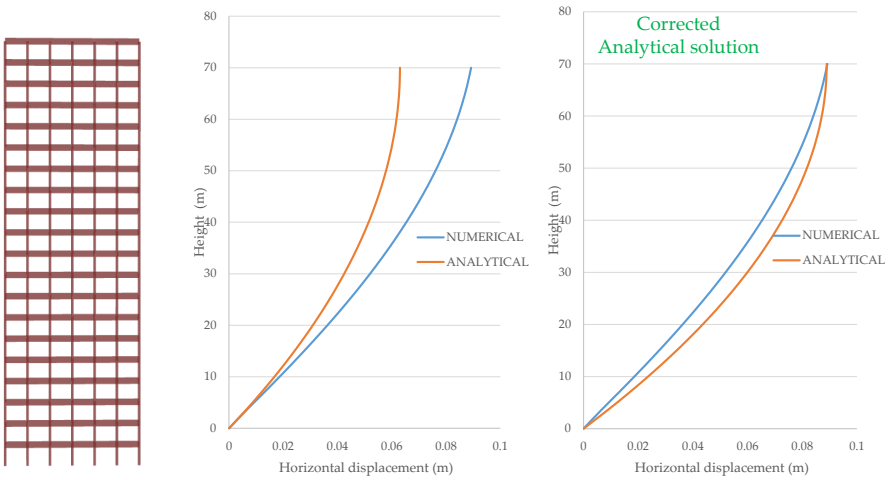

Inertia ratio	12.49	Unitless
Slenderness ratio	2.92	Unitless
Inertia magnitude	307.25	x10-4 m4
Module aspect ratio	1.14	Unitless
Overall size	1680.00	m2
Error of max displacement	-29.38%	
Stiffness unity check	0.96	

Inertia ratio	12.49	Unitless
Slenderness ratio	2.92	Unitless
Inertia magnitude	307.25	x10-4 m4
Module aspect ratio	1.14	Unitless
Overall size	1680.00	m2
Error of max displacement	-0.29%	
Stiffness unity check	0.96	

Figure 5.6: Corrected analytical solution - test 6

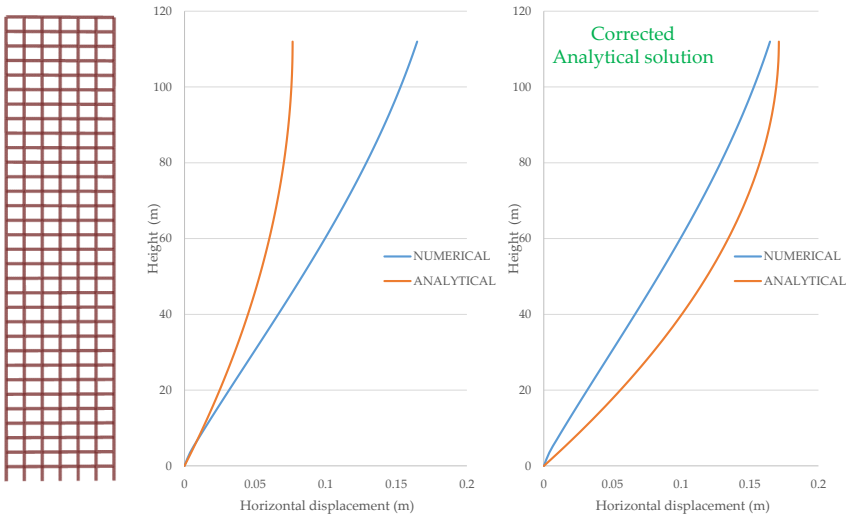

Inertia ratio	1.16	Unitless
Slenderness ratio	4.67	Unitless
Inertia magnitude	201.33	x10-4 m4
Module aspect ratio	1.14	Unitless
Overall size	2688.00	m2
Error of max displacement	-53.54%	
Stiffness unity check	1.10	

Inertia ratio	1.16	Unitless
Slenderness ratio	4.67	Unitless
Inertia magnitude	201.33	x10-4 m4
Module aspect ratio	1.14	Unitless
Overall size	2688.00	m2
Error of max displacement	3.91%	
Stiffness unity check	1.10	

Figure 5.7: Corrected analytical solution - test 7

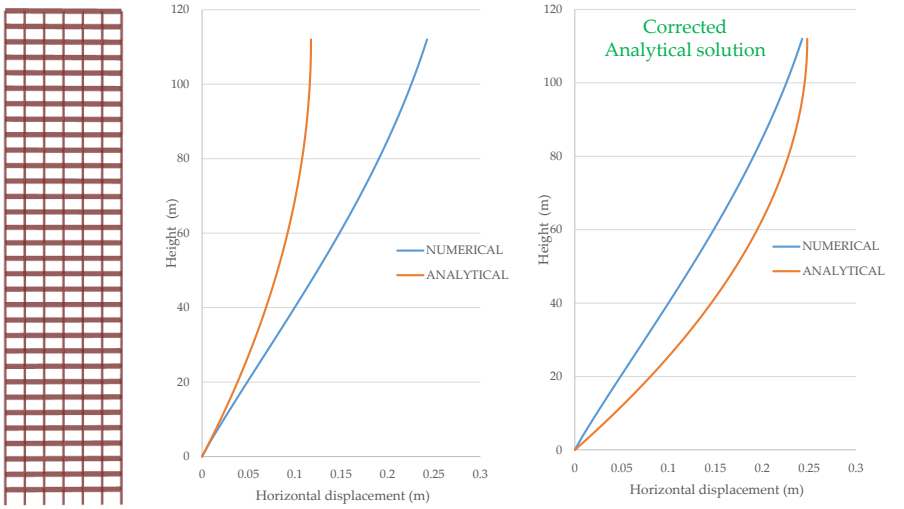

Inertia ratio	12.49	Unitless
Slenderness ratio	4.67	Unitless
Inertia magnitude	421.47	x10-4 m4
Module aspect ratio	1.14	Unitless
Overall size	2688.00	m2
Error of max displacement	-51.53%	
Stiffness unity check	1.62	

Inertia ratio	12.49	Unitless
Slenderness ratio	4.67	Unitless
Inertia magnitude	421.47	x10-4 m4
Module aspect ratio	1.14	Unitless
Overall size	2688.00	m2
Error of max displacement	2.23%	
Stiffness unity check	1.62	

Figure 5.8: Corrected analytical solution - test 8

From Figures 5.3-5.8, it is shown that the maximum displacement error percentage of the different models is less than 20 percent and even less than 5 percent. It can also be observed that for specific values for the five geometric variables (also shown in the tables of each figure), as for example

high inertia ratio and slenderness values, the corrected analytical solution is a good approximation only for the top displacement, which is again related to the bending effects as shown in tests 7 and 8. From this observation, it can be defined that when the predicted error is greater than 40 percent, the corrected analytical solution is not a good approximation due to the impact of bending deformations. The 40 percent is defined as a midpoint between tests 5-6 and tests 7-8. Then, it is inferred that for rigid frames models where the predicted error is higher than 40 percent, a better approximation would be the Euler-Bernoulli bending beam representation and, that a correction factor can also be derived to account for the combined behaviour where bending deformations are predominant.

5.3 TIMOSHENKO BEAM REPRESENTATION

The use of the Timoshenko beam theory was also tested for several configurations of rigid frames within not only the zone B, but also zone C. The results are shown in Figures 5.9-5.16.

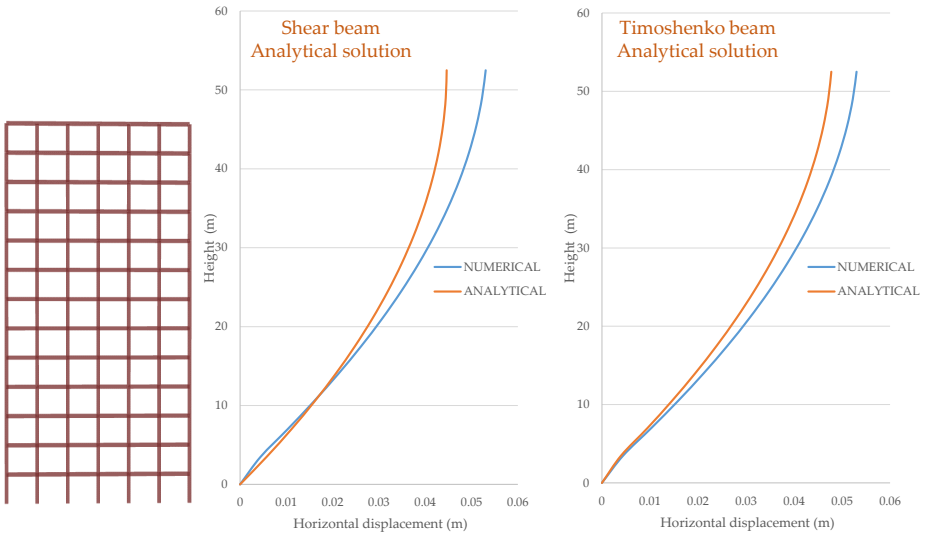

Inertia ratio	1.16	Unitless
Slenderness ratio	2.19	Unitless
Inertia magnitude	75.84	x10-4 m4
Module aspect ratio	1.14	Unitless
Overall size	1260.00	m2
Error of max displacement	-15.83%	
Stiffness unity check	0.76	

Inertia ratio	1.16	Unitless
Slenderness ratio	2.19	Unitless
Inertia magnitude	75.84	x10-4 m4
Module aspect ratio	1.14	Unitless
Overall size	1260.00	m2
Error of max displacement	-9.91%	
Stiffness unity check	0.76	

Figure 5.9: Timoshenko analytical solution - test 9

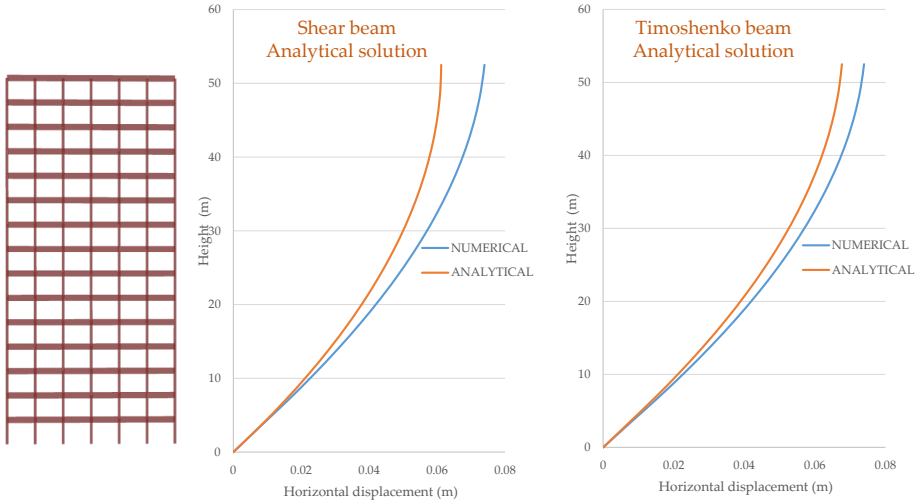

Inertia ratio	12.49	Unitless
Slenderness ratio	2.19	Unitless
Inertia magnitude	177.81	x10-4 m4
Module aspect ratio	1.14	Unitless
Overall size	1260.00	m2
Error of max displacement	-17.21%	
Stiffness unity check	1.06	

Inertia ratio	12.49	Unitless
Slenderness ratio	2.19	Unitless
Inertia magnitude	177.81	x10-4 m4
Module aspect ratio	1.14	Unitless
Overall size	1260.00	m2
Error of max displacement	-0.93%	
Stiffness unity check	1.06	

Figure 5.10: Timoshenko analytical solution - test 10

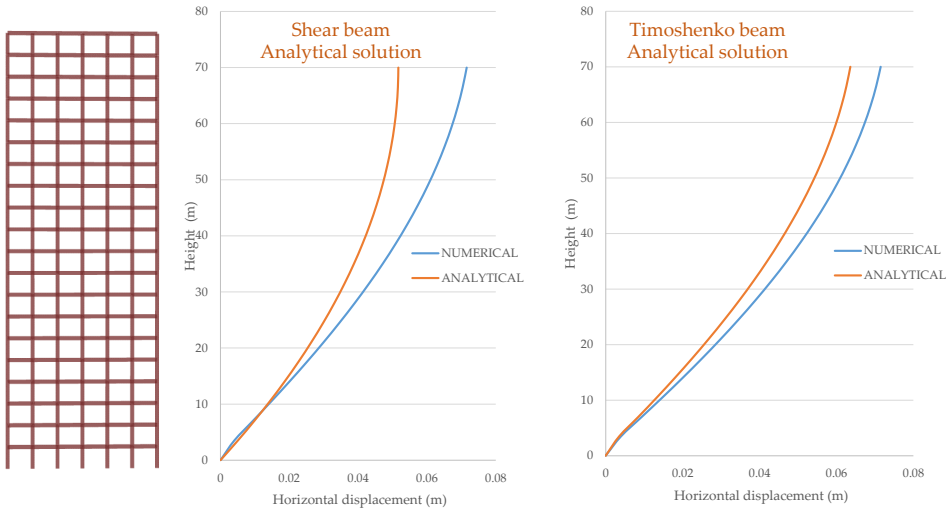

Inertia ratio	1.16	Unitless
Slenderness ratio	2.92	Unitless
Inertia magnitude	116.51	x10-4 m4
Module aspect ratio	1.14	Unitless
Overall size	1680.00	m2
Error of max displacement	-27.74%	
Stiffness unity check	0.77	

Inertia ratio	1.16	Unitless
Slenderness ratio	2.92	Unitless
Inertia magnitude	116.51	x10-4 m4
Module aspect ratio	1.14	Unitless
Overall size	1680.00	m2
Error of max displacement	-11.05%	
Stiffness unity check	0.77	

Figure 5.11: Timoshenko analytical solution - test 11

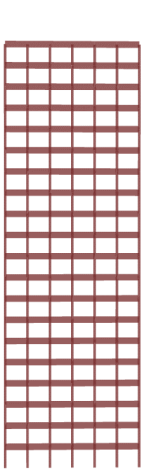

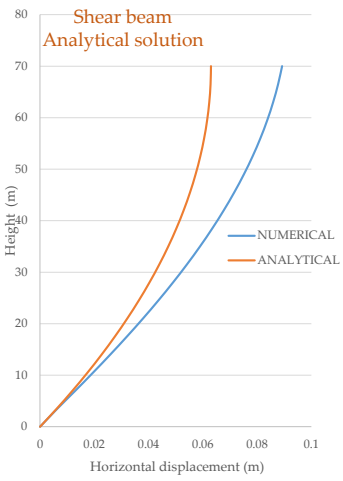

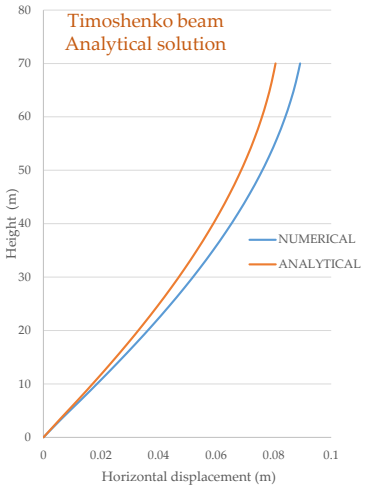

Inertia ratio	12.49	Unitless
Slenderness ratio	2.92	Unitless
Inertia magnitude	307.25	x10-4 m4
Module aspect ratio	1.14	Unitless
Overall size	1680.00	m2
Error of max displacement	-29.38%	
Stiffness unity check	0.96	

Inertia ratio	12.49	Unitless
Slenderness ratio	2.92	Unitless
Inertia magnitude	307.25	x10-4 m4
Module aspect ratio	1.14	Unitless
Overall size	1680.00	m2
Error of max displacement	-9.53%	
Stiffness unity check	0.96	

Figure 5.12: Timoshenko analytical solution - test 12

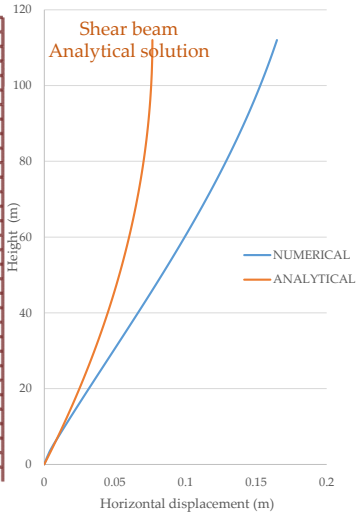

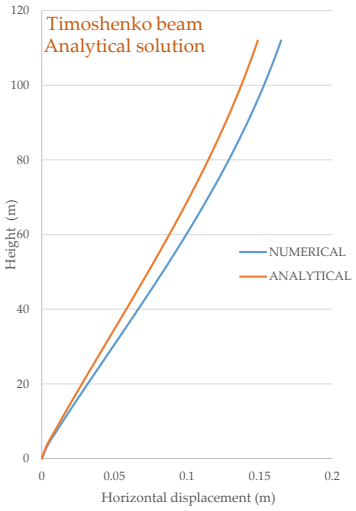

Inertia ratio	1.16	Unitless
Slenderness ratio	4.67	Unitless
Inertia magnitude	201.33	x10-4 m4
Module aspect ratio	1.14	Unitless
Overall size	2688.00	m2
Error of max displacement	-53.54%	
Stiffness unity check	1.10	

Inertia ratio	1.16	Unitless
Slenderness ratio	4.67	Unitless
Inertia magnitude	201.33	x10-4 m4
Module aspect ratio	1.14	Unitless
Overall size	2688.00	m2
Error of max displacement	-9.69%	
Stiffness unity check	1.10	

Figure 5.13: Timoshenko analytical solution - test 13

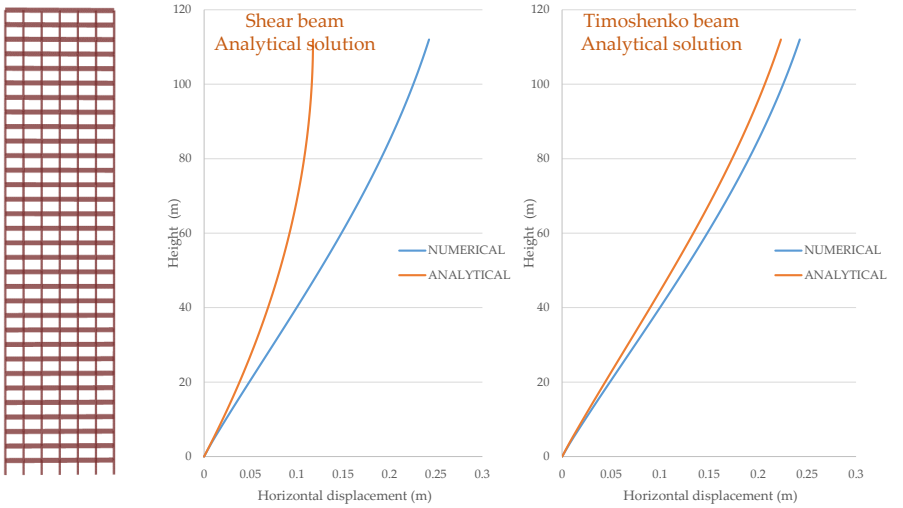

Inertia ratio	12.49	Unitless
Slenderness ratio	4.67	Unitless
Inertia magnitude	421.47	x10-4 m4
Module aspect ratio	1.14	Unitless
Overall size	2688.00	m2
Error of max displacement	-51.53%	
Stiffness unity check	1.62	

Inertia ratio	12.49	Unitless
Slenderness ratio	4.67	Unitless
Inertia magnitude	421.47	x10-4 m4
Module aspect ratio	1.14	Unitless
Overall size	2688.00	m2
Error of max displacement	-7.90%	
Stiffness unity check	1.62	

Figure 5.14: Timoshenko analytical solution - test 14

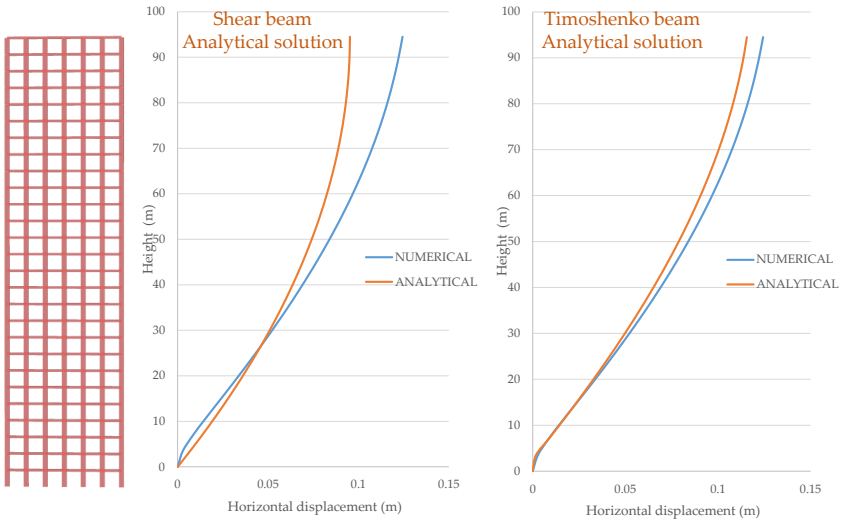

Inertia ratio	0.13	Unitless
Slenderness ratio	3.94	Unitless
Inertia magnitude	325.58	x10-4 m4
Module aspect ratio	1.14	Unitless
Overall size	2268.00	m2
Error of max displacement	-23.42%	
Stiffness unity check	0.99	

Inertia ratio	0.13	Unitless
Slenderness ratio	3.94	Unitless
Inertia magnitude	325.58	x10-4 m4
Module aspect ratio	1.14	Unitless
Overall size	2268.00	m2
Error of max displacement	-7.01%	
Stiffness unity check	0.99	

Figure 5.15: Timoshenko analytical solution - test 15

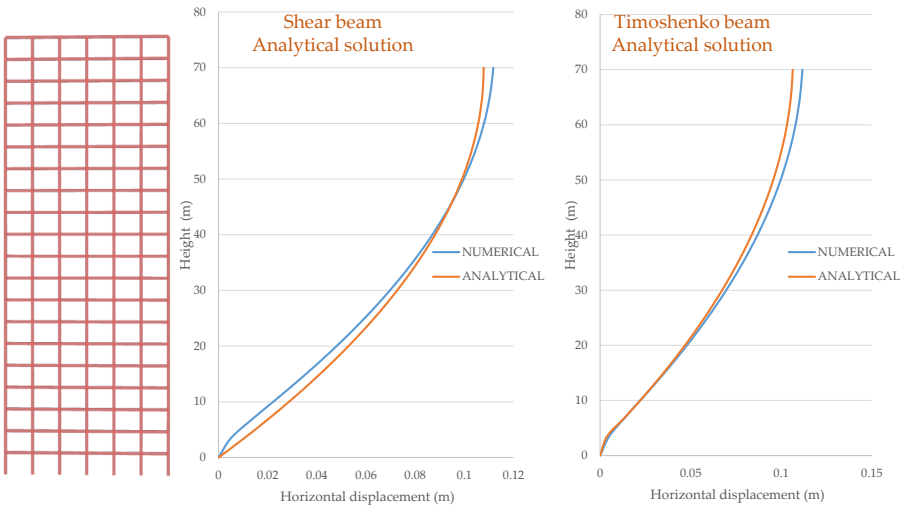

Inertia ratio	0.34	Unitless
Slenderness ratio	1.94	Unitless
Inertia magnitude	110.30	x10-4 m4
Module aspect ratio	1.71	Unitless
Overall size	2520.00	m2
Error of max displacement	-3.48%	
Stiffness unity check	1.20	

Inertia ratio	0.34	Unitless
Slenderness ratio	1.94	Unitless
Inertia magnitude	110.30	x10-4 m4
Module aspect ratio	1.71	Unitless
Overall size	2520.00	m2
Error of max displacement	-4.81%	
Stiffness unity check	1.20	

Figure 5.16: Timoshenko analytical solution - test 16

As explained in the previous chapter, the error of the Timhoshenko analytical representation is mainly because a different shear stiffness for the top floor is not considered. It can also be seen, that the error is greater for the cases where the inertia ratio is larger that one (Large beams cases). This situation coincides with the fact that the contraflexure error on the top floors beams is larger. The contraflexure error is when the flexural moment is not zero at mid-length of the element. This effect can be seen in Figure 3.9 and a close up to the top floors is shown below in Figure 5.17. However, the percent error is less than 10 percent which is a good approximation for the preliminary design.

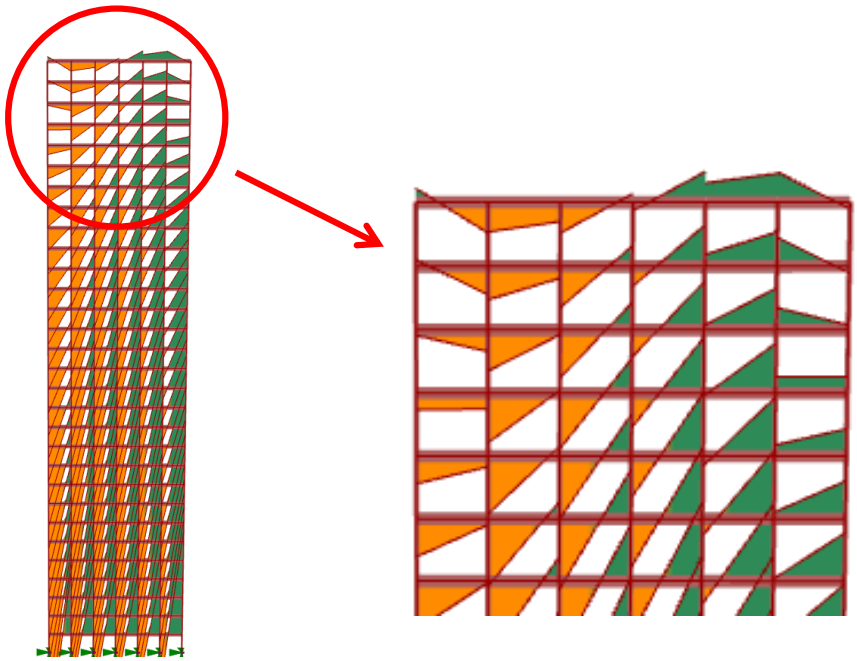

Figure 5.17: Moment diagrams of top floors beams

It also remarkable to notice that in test 16 the percentage error is less for the shear beam representation. This is because this specific configuration of rigid frame can be located in the green area where the bending effects are small. This is represented in Figure 5.18.

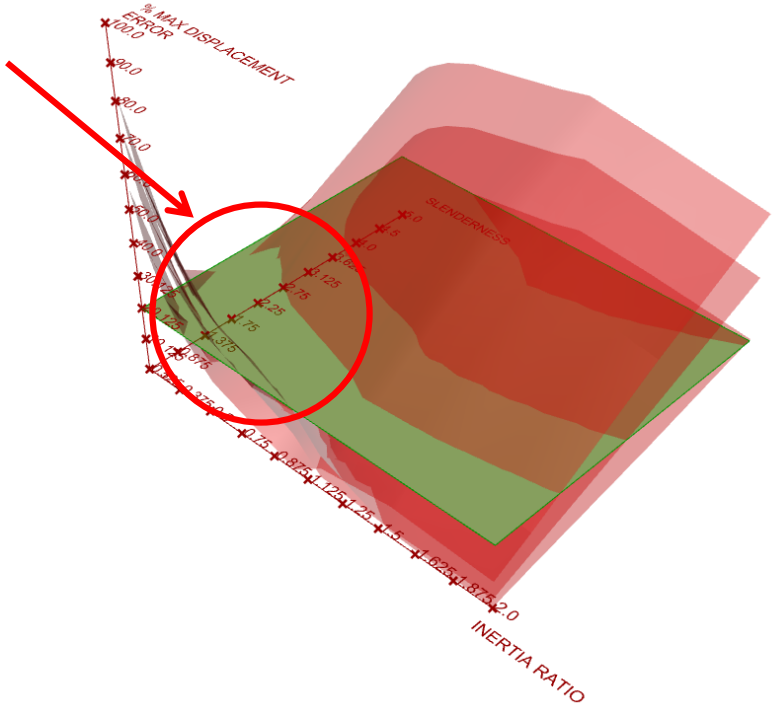

Figure 5.18: Green area with small bending effects

5.4 ANALYTICAL METHOD FOR VERTICAL CONNECTIONS OF COMPONENTS

5.4.1 Correction method for the shear beam representation

The correction method of the shear beam representation was also tested for several types of connections between rigid frames components. Also, the chosen geometries for the model are within the zone B. The results are shown in Figures 5.19-5.23.

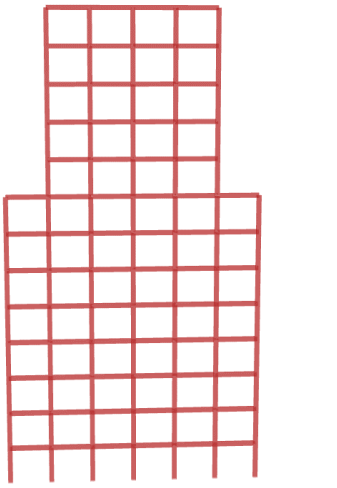

Inertia ratio	1.00	Unitless
Slenderness ratio	1.17	Unitless
Inertia magnitude	45.56	x10-4 m4
Module aspect ratio	1.14	Unitless
Overall size	672.00	m2
Error of max displacement	-3.48%	
Stiffness unity check	0.99	

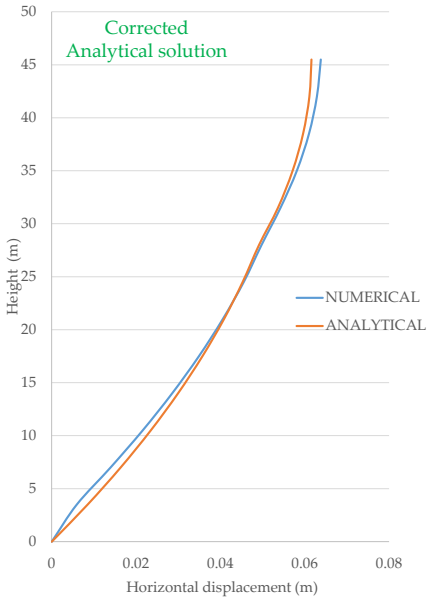

Figure 5.19: Connections - corrected analytical solution - test 17

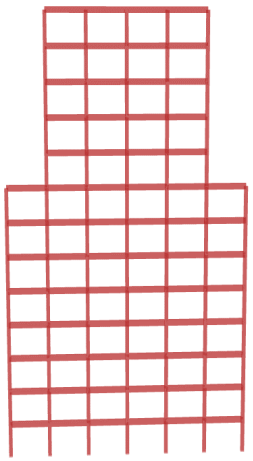

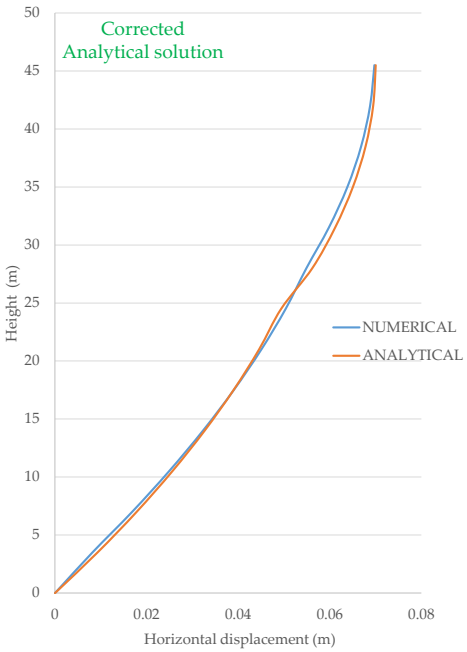

Inertia ratio	5.36	Unitless
Slenderness ratio	1.17	Unitless
Inertia magnitude	74.18	x10-4 m4
Module aspect ratio	1.14	Unitless
Overall size	672.00	m2
Error of max displacement	0.40%	
Stiffness unity check	1.03	

Figure 5.20: Connections - corrected analytical solution - test 18

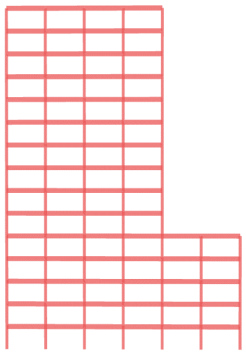

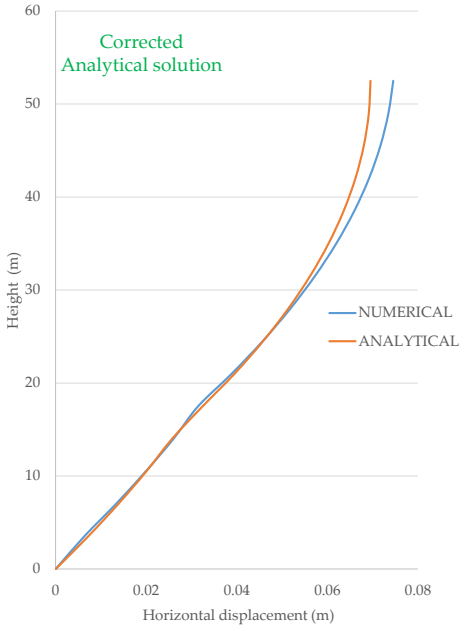

Inertia ratio	5.36	Unitless
Slenderness ratio	0.49	Unitless
Inertia magnitude	117.79	x10-4 m4
Module aspect ratio	1.71	Unitless
Overall size	630.00	m2
Error of max displacement	-6.73%	
Stiffness unity check	0.92	

Figure 5.21: Connections - corrected analytical solution - test 19

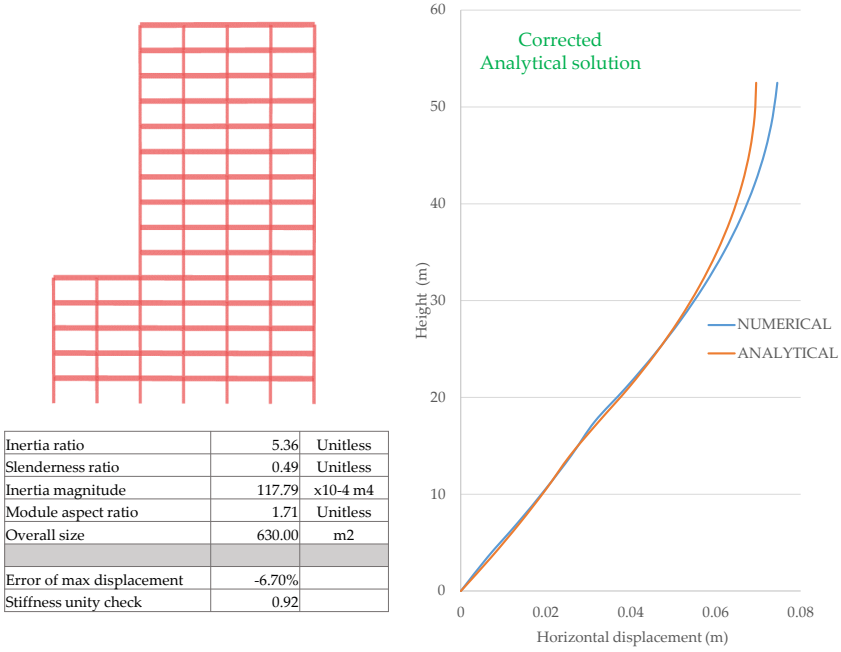

Inertia ratio	5.36	Unitless
Slenderness ratio	0.49	Unitless
Inertia magnitude	117.79	x10-4 m4
Module aspect ratio	1.71	Unitless
Overall size	630.00	m2
Error of max displacement	-6.70%	
Stiffness unity check	0.92	

Figure 5.22: Connections - corrected analytical solution - test 20

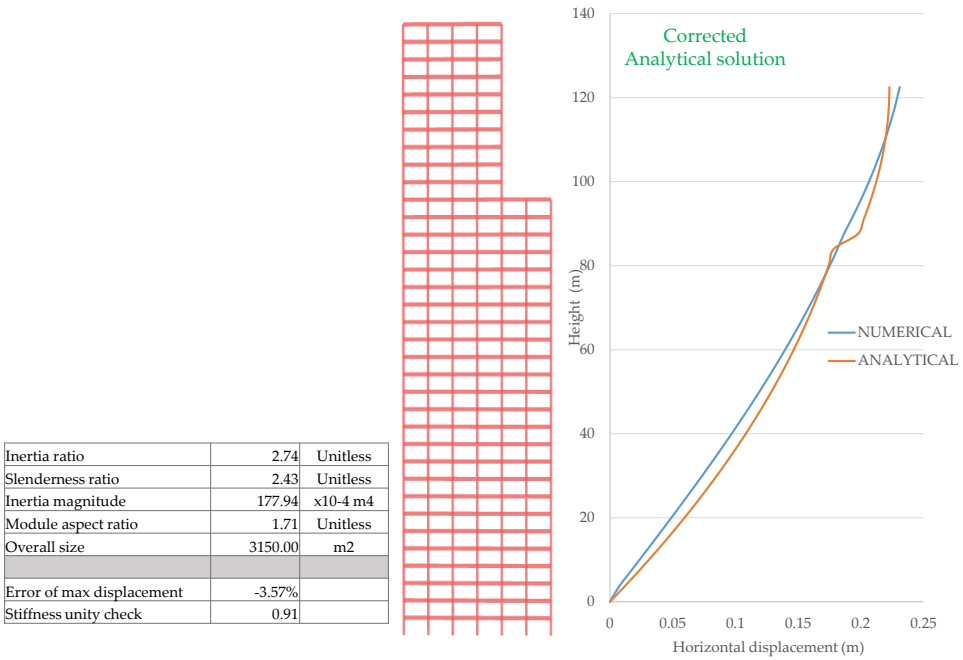

Inertia ratio	2.74	Unitless
Slenderness ratio	2.43	Unitless
Inertia magnitude	177.94	x10-4 m4
Module aspect ratio	1.71	Unitless
Overall size	3150.00	m2
Error of max displacement	-3.57%	
Stiffness unity check	0.91	

Figure 5.23: Connections - corrected analytical solution - test 21

From the figures, it is shown that the error of the different models is less than 10 percent. It is also observed, that the corrected analytical solution is more accurate for the first component, this is due to fact that the correction factor derived comes from models that were assumed clamped a the bottom,

which is not the case for the second block connected at the top of the first one, and because the correction factor for the second block was obtained as the sum of the correction factors of each component.

5.4.2 Timoshenko beam representation

The use of the Timoshenko beam theory was also tested for several types of connections between rigid frames components within not only the zone B but zone C as well. The results are shown in Figures 5.24-5.29.

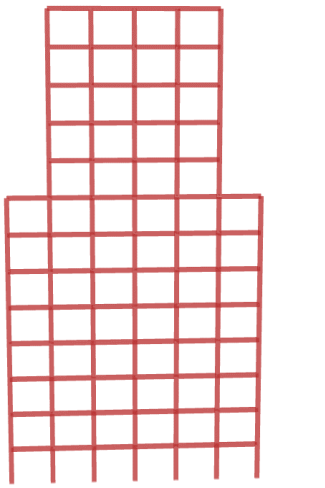

Inertia ratio	1.00	Unitless
Slenderness ratio	1.17	Unitless
Inertia magnitude	45.56	x10-4 m4
Module aspect ratio	1.14	Unitless
Overall size	672.00	m2
Error of max displacement	-5.46%	
Stiffness unity check	0.99	

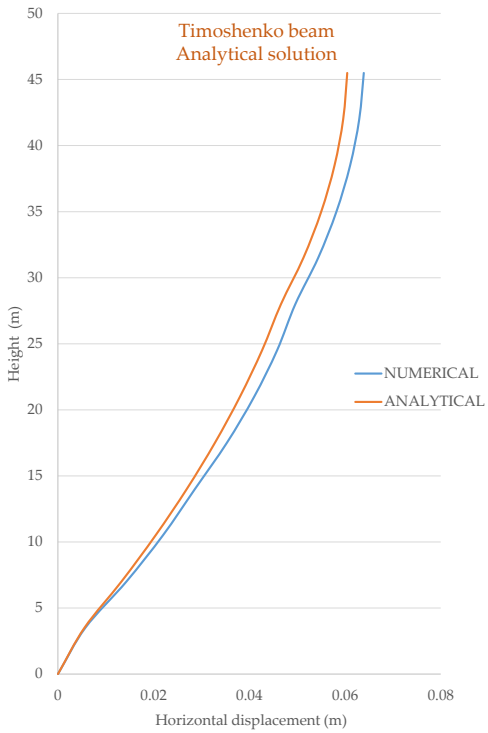

Figure 5.24: Connections - Timoshenko analytical solution - test 22

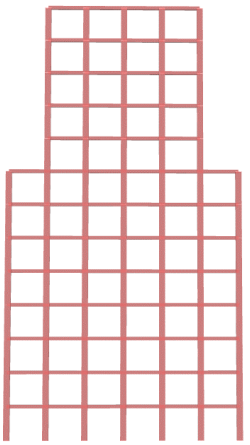

Inertia ratio	0.19	Unitless
Slenderness ratio	1.17	Unitless
Inertia magnitude	74.18	x10-4 m4
Module aspect ratio	1.14	Unitless
Overall size	672.00	m2
Error of max displacement	-0.72%	
Stiffness unity check	0.91	

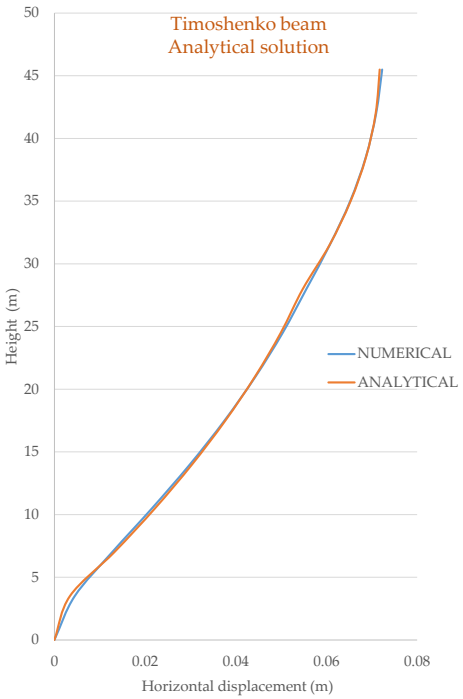

Figure 5.25: Connections - Timoshenko analytical solution - test 23

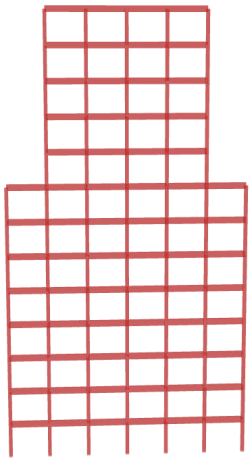

Inertia ratio	5.36	Unitless
Slenderness ratio	1.17	Unitless
Inertia magnitude	74.18	x10-4 m4
Module aspect ratio	1.14	Unitless
Overall size	672.00	m2
Error of max displacement	-6.00%	
Stiffness unity check	0.81	

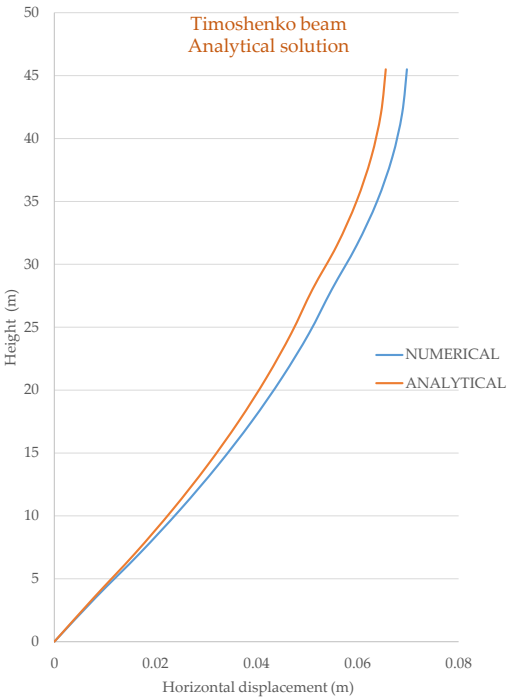

Figure 5.26: Connections - Timoshenko analytical solution - test 24

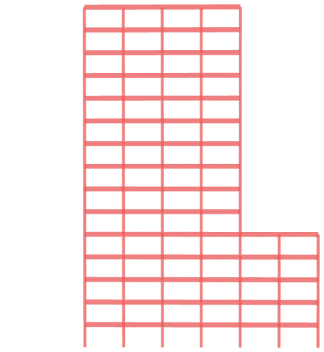

Inertia ratio	5.36	Unitless
Slenderness ratio	0.49	Unitless
Inertia magnitude	117.79	x10-4 m4
Module aspect ratio	1.71	Unitless
Overall size	630.00	m2
Error of max displacement	-10.10%	
Stiffness unity check	0.41	

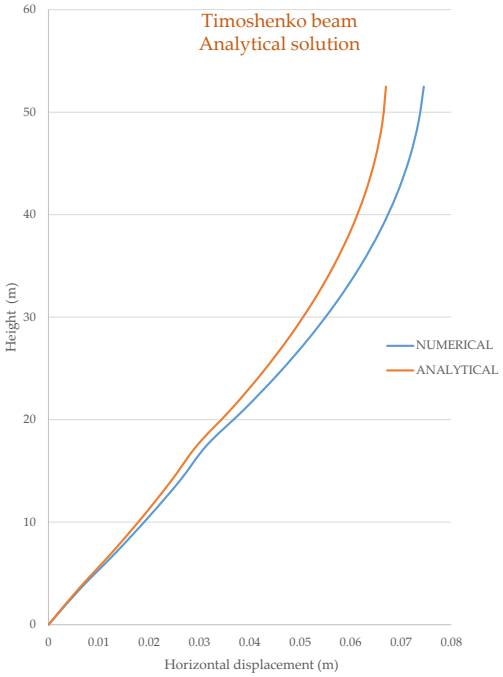

Figure 5.27: Connections - Timoshenko analytical solution - test 25

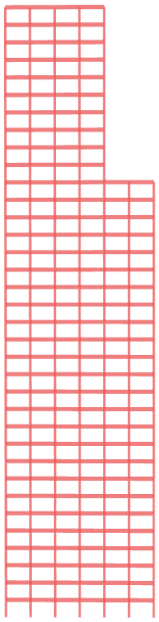

Inertia ratio	2.74	Unitless
Slenderness ratio	2.43	Unitless
Inertia magnitude	177.94	x10-4 m4
Module aspect ratio	1.71	Unitless
Overall size	3150.00	m2
Error of max displacement	-10.36%	
Stiffness unity check	0.91	

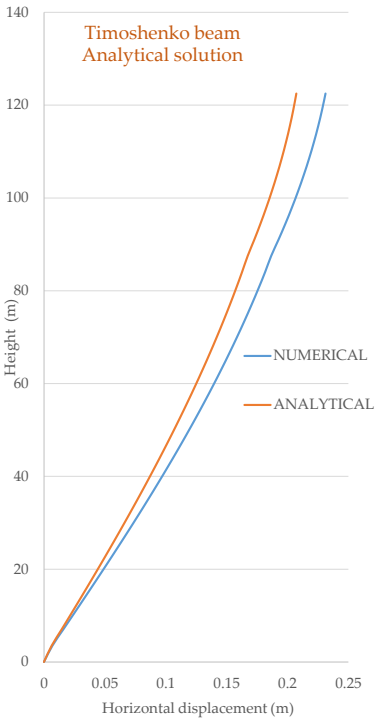

Figure 5.28: Connections - Timoshenko analytical solution - test 26

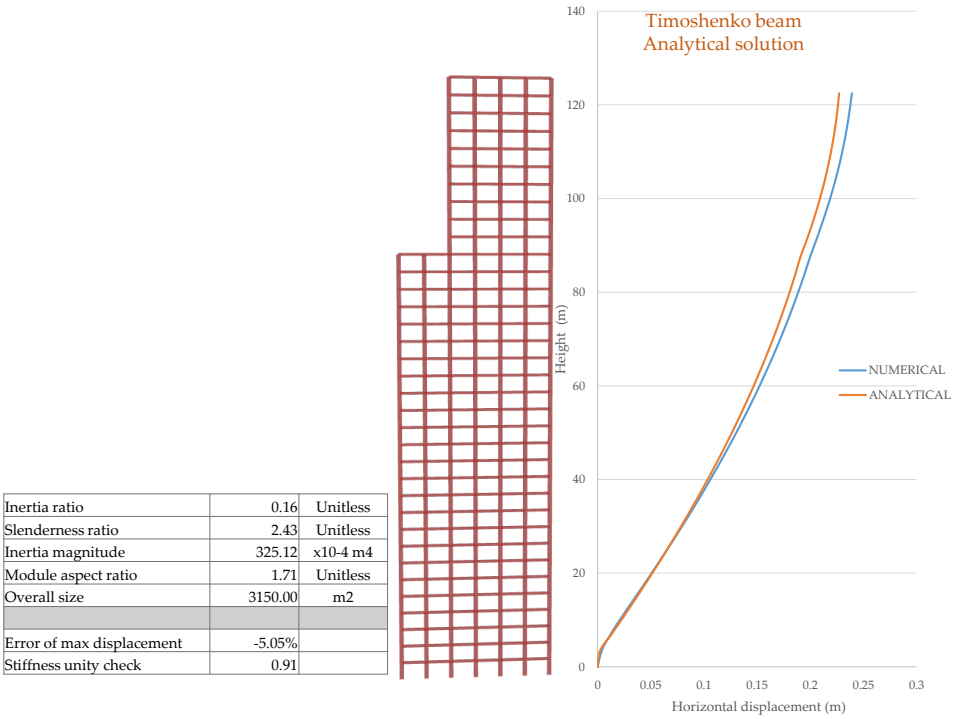

Inertia ratio	0.16	Unitless
Slenderness ratio	2.43	Unitless
Inertia magnitude	325.12	x10-4 m4
Module aspect ratio	1.71	Unitless
Overall size	3150.00	m2
Error of max displacement	-5.05%	
Stiffness unity check	0.91	

Figure 5.29: Connections - Timoshenko analytical solution - test 27

From previous figures it can be seen that also for connections tests, the approximation is better for the cases where the beam-to-column inertia ratio is less than one. The error is maximum at the top, again because of not considering a different shear stiffness at the top floor. Also, it can be seen from test 26, the error is larger because of the eccentricity of the position of the second block and because the second block is taller.

The performed validations showed that both methods, the correction and the implementation of Timoshenko beam theory, yield an error which is considered as allowable for the preliminary design. Also, it was shown that the correction method does not show a good overall fitting approximation when the bending effects are high; while the use of the Timoshenko beam theory shows a better fitting along the height.

6 DISCUSSION

In this chapter, a reflection on computational tools is presented and then the discussion of the achievement and limitations for each of the objectives.

6.1 REFLECTION ON COMPUTATIONAL TOOLS

At the introduction of this research project, several descriptions of current computational tools in the Building Industry were gathered. The data was collected from previous researches of StructuralComponents, from lectures material of courses on computational tools from TU Delft and software developers websites. Tools such as Robot Structural Analysis were included and a comparison with Karamba3D-Parametric engineering was done. Robot and Karamba3D were addressed more deeply due to similarities with some of the general objectives of StucturalComponents such as the collaboration between the architecture and structural engineering disciplines or the parametric and real-time qualities.

Currently, there is a lack of computational tools for the early design, but computation power continues to increase. This tendency can already allow almost a real-time structural performance evaluation by implementing the complete finite element analysis. The increasing computational power can be described by the so-called Moore's law that states that it doubles every two years (Hoogenboom, 2019) . Thus, it is attractive to combine the advantages of StructuralComponents with those of Karamba3D. It may be convenient to develop several pre-programmed building blocks geometries that can be connected to a parametric finite element solver. This would also require some pre-programming on the finite element solver to be able to receive the specific geometry generated by the parametric building blocks. From the finite element analysis, specific additional programming can be done to extract results to show an overall insight of the complete building behaviour and to evaluate the feasibility checks or any other important parameter for the early design. Two reasons to consider this possibility are the geometric flexibility and the accuracy when implementing the finite element analysis. However, if the building model is too big, the analytical representation is still simpler and more adequate for preliminary design stages.

More specific research on computational tools, qualitative and quantitative, should be conducted to reach fair comparisons between tools. The research and comparisons might address at least the following aspects to determine the suitability of the tools for preliminary design purposes.

- Modelling time
- Modelling flexibility
- Results accuracy
- Computational effort
- Speed of real-time results
- Insight on the structural behaviour
- Dynamic effects

6.2 ACHIEVEMENT OF THE OBJECTIVES AND LIMITATIONS

6.2.1 Main objective: Expansion of StructuralComponents by the research on the analytical representation of rigid frames under lateral loads, as well as the development of a parametric real-time computational prototype tool

The main objective of this research project was achieved through the development of a tool prototype that can quickly evaluate the structural feasibility of buildings in which the lateral stability is provided only by concrete rigid frames. The development was based on symbolic analytical expressions instead of the use of the finite element method, such expressions were extracted and derived from the study on rigid frames behaviour.

6.2.2 Objective 1: Investigate rigid frames behaviour and its analytical representation

Achievement of the objectives

The objective was achieved through the research and the parametric study that consisted of 480 rigid frames models each of them evaluated analytically and numerically. Based on this research and study, the following sub-objectives were achieved:

- Range of applicability of the shear beam representation

  By considering the most unfavourable combination of parameters, within the scope of the tests performed, the applicability of the analytical shear beam representation was defined. This was the factor that motivated the development of the correction method and the study of other analytical theories.

- Correction method for the shear beam representation

From the collected data of the parametric study, a procedure was developed based on sequential polynomial interpolations to predict the error of the analytical representation. The correction method was performed based on the predicted error which is dependent on five geometric variables. With the corrected analytical solution, the applicability of the shear beam representation was increased. The validations showed that the error of the maximum displacement using this correction method was less than 5 percent, however, the greater the bending effects the greater is the error for the displacement of the intermediate floors.

- The prediction of the error as a parameter to classify a rigid frame as a flexural or shear type based on the geometric properties.

  It was proposed to classify rigid frames as shear type when the predicted error the analytical shear beam representation is less than 20 percent, and flexural type when the predicted error is greater than 40 percent. The difference of this parameter with the Blume's parameter is the dependency on the five geometric variables defined in this research project.

- Timoshenko beam representation

  It was found that Timoshenko beam theory can represent the combined behaviour of rigid frames. This is because of the analogy of rigid frames to a serial system where the bending and shear deformations are added together. This theory allowed for the use of a differential equation to represent the behaviour of rigid frames in any of the defined four zones. The variable stiffness along the height of the rigid frame was addressed by assigning a different shear stiffness for the ground floor, and by splitting the 1D analytical representation into fields. The validations showed that the error of the maximum displacement using Timoshenko theory was an average of 10 percent, and that the the error reduces for intermediate and ground floors. Also, the error of this theory can be explained for the assumption of the same shear stiffness value for the top floor as for the intermediate floors. However, a 10 percent error can be well justified for the preliminary design.

Limitations

Regarding the correction method, the procedure to predict the error was only developed for the previously defined zone B, where the error can be large and not conservative. Also, the corrected analytical solution always shows a shear beam deformed shape; then, this method fails to give a good approximation for intermediate floors displacements when the bending effects are significant.

In relation to the implementation of the Timoshenko theory derivations, the limitations rely on the accuracy of the approximation. It was explained that the error of this representation is because of the drastic change of stiffness at the ground and top floors. For this research project, a drastic change of stiffness was addressed only for the ground floor, with the calculation of a different shear stiffness for the ground floor.

6.2.3 Objective 2: Implement an analytical method for vertical connections

Achievement of the objectives

The objective was achieved through the derivation and implementation of an analytical method to represent the connection between components. Such a method consisted of the subdivision of the one dimensional representation of a rigid frame, where each division, also called field, is represented with a specific differential equation to account for different stiffness along the height. Then, the analytical solution is calculated for each of the fields with the use of matching conditions.

Limitations

In this research project, the analytical method to perform the vertical connections of components was limited to three fields that allows for only a drastic change in geometry, because two fields are needed for the first component and one field for the second component as shown in Figure 3.39.

Also, the following situations may arise:

- Eccentricity on the analytical representation

  The idea of representing a rigid frame as a 1D element has the restriction of representing symmetric rigid frames. However, when the connection of the components is set to be parametrically adaptable, the possibility of having asymmetric geometries increases. Figure 6.1 shows how the symmetric axis of the components do not coincide. However, it was shown in the validations that for several configurations, were the asymmetry is not prominent, the results of the one-dimensional approximation were sufficiently accurate for the preliminary design.

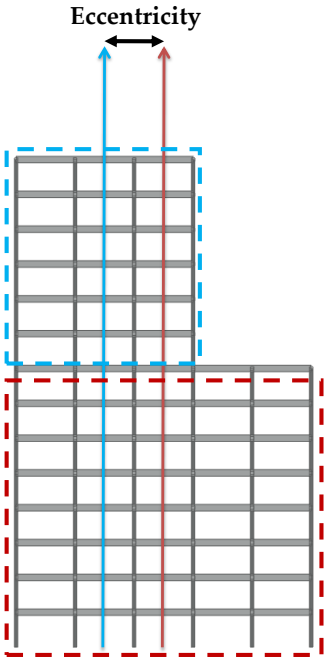

Figure 6.1: Eccentricity between rigid frames geometries

- Concentration of stresses in the corners

  A concentration of stresses in the corners occurs when connecting components as shown in the finite element model of Figure 6.2. Depending on the specific geometry, these concentrated stresses can be relevant for the preliminary design.

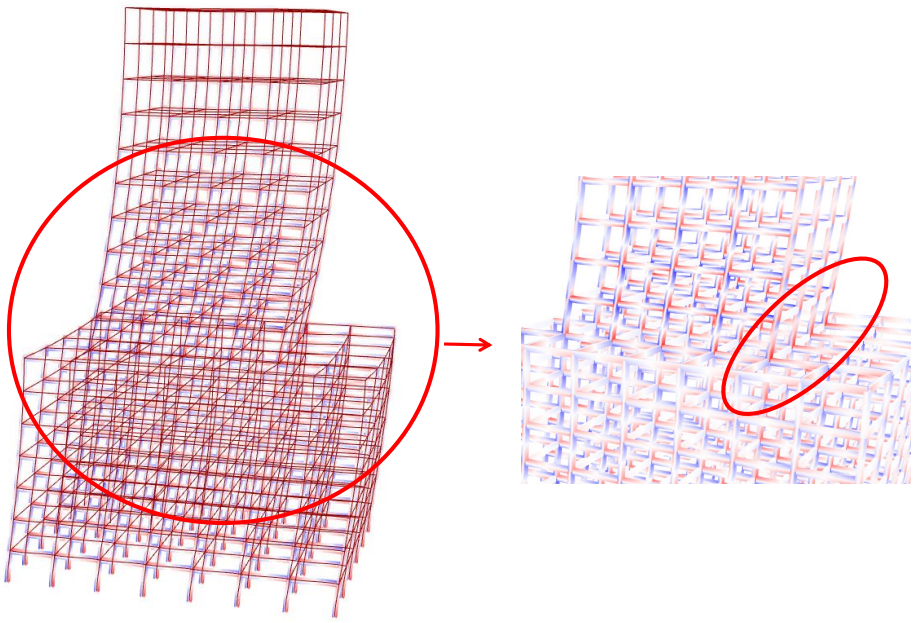

Figure 6.2: Concentration of stresses in the corners (Results from a finite element model)

6.2.4 Objective 3: The development of a real-time tool prototype of rigid frames solved analytically

Achievement of the objectives

The objective was achieved through the development of two rigid frame components called Initial-RFC and Connecting-RFC which are flexible and parametrically adaptable. Inside these components, the structural analysis is performed by symbolic analytical expressions. The tool can also show the displacement, shear and moment plots, and to visually represent the structural feasibility by indicating in red colour the elements that do not comply with the structural requirements for the preliminary design.

Limitations

Regarding the tool prototype, the limitations are mainly due to the time constraints of this research project and are listed below:

- Perpendicular beams and the floor stiffness contribution

  The influence of the perpendicular beams connecting the rigid frames was not taken into account. For the case of regular rigid frame component, the influence of the perpendicular beams is almost zero. For the case of the vertical connection of components, the curved deformation of the perpendicular beams can occur as shown in the finite element model of Figure 6.3. However, if such influence is not considered then

the analytical result is conservative. The influence of the floor stiffness follows a similar pattern. If the perpendicular beam dimensions are increased to simulate a slab, it still does not have a significant influence on the lateral deformation of rigid frames. However, the influence of a concrete slab monolithically joined to the perimeter beams was not considered in this research project.

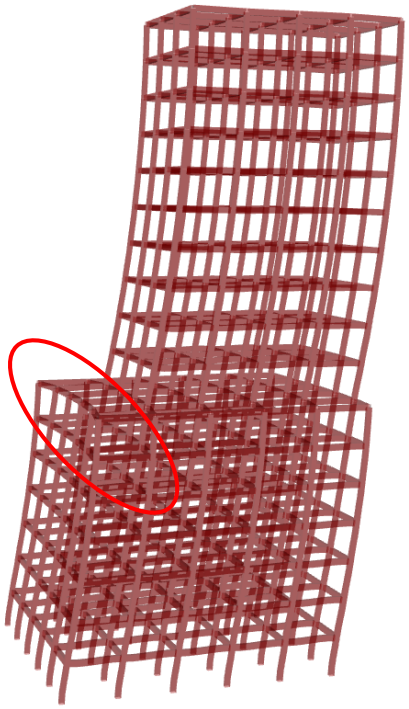

Figure 6.3: Curvature in perpendicular beams (Results from a finite element model)

- The representation of the wind load

  For simplification of the derivation of the analytical solutions, the wind force was represented as a uniformly distributed load along the height of the building. But is known that the wind distribution follows a more closely to a triangular or parabolic distribution.

- Geometric flexibility

  In spite of the number of adjustable parameters enabled for the tool prototype, the assumption of the same cross-sections and length for all columns and beams was made.

- Wind in the other direction

  The wind force was considered for only one perpendicular direction of one of the facades.

- Material

To allow for another material for a rigid frame system, like steel, it is necessary to conduct further research. One of the aspects that need to change for the cases of still rigid frames is the equivalent expressions to calculate the shear stiffness. It might be necessary to include to rotational stiffness as mentioned by Hoenderkamp (2005) . Also, the strength feasibility checks implemented in this research project only apply for reinforced concrete rigid frames.

- Foundation stiffness

  In this tool, the support conditions were defined as fixed. However, in regions where the soil conditions are unfavourable, a foundation stiffness should be calculated and considered in the analysis as mentioned by Hohrath (2018) .

- Dynamic capabilities

  Similar to StructuralComponents5.0, the scope was limited to mid-rise buildings where the dynamic effects can be excluded.

7 CONCLUSIONS AND RECOMMENDATIONS

This chapter contains the specific conclusions and recommendations for each of the defined objectives in this research project. Also, general recommendations for further development are presented.

7.1 CONCLUSIONS

7.1.1 Main objective: Expansion of StructuralComponents by the research on the analytical representation of rigid frames under lateral loads, as well as the development of a parametric real-time computational tool prototype

It can be concluded that during the preliminary design, where an exploration of geometric alternatives is performed, a more appropriate analytical representation for rigid frames is based on the Timoshenko beam theory. And that a parametric real-time tool where components can also be connected in a 'Lego-style' highly contributes to the desired flexibility and to quickly determine the feasibility of a mid-rise building during the early design stages. To support this statement, specific conclusions were drawn for each objective and presented below.

7.1.2 Objective 1: Investigate rigid frames behaviour and its analytical representation

The following conclusions can be made:

- Range of applicability of the shear beam representation

  For parametric purposes, the range of applicability of the shear beam representation of rigid frames can be delimited for geometries that meet both of the following conditionals:

$$\text{Beam-to-column inertia ratio} > 1$$
$$\text{Overall slenderness ratio} < 1$$

- Correction method of the shear beam representation

  - The developed method to predict the error of the shear beam representation can be used as a parameter to classify the behaviour type of a rigid frame as shear, flexural or combined. The larger the error, the larger the bending effects. It can be concluded that for preliminary design purposes an error less than 20 percent indicates a shear type behaviour. Also, from the results of the validations, it can be concluded that if the error is greater than 40 percent, the bending effects are high. The use of the predicted error as a classification parameter is graphically presented in Figure 7.1.

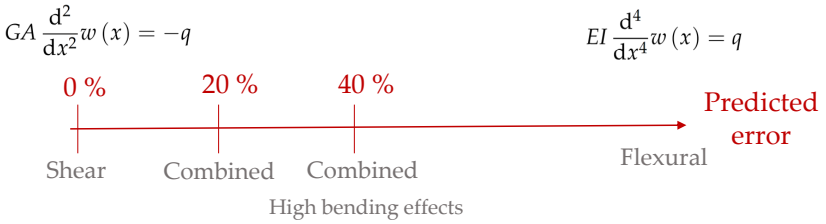

Figure 7.1: Prediction of the error as a behaviour type parameter

  - The correction of the shear beam representation, based on the prediction of the error, gives accurate enough results for the preliminary design when the bending effects are not high, which means less than 40 percent.

- Timoshenko beam theory

  It is more appropriate to represent rigid frames behaviour with the Timoshenko beam theory to account for both bending and shear deformations because the reduced applicability of the shear beam representation for parametric purposes, and because the correction method has the constraint of the necessity of an overall shear deformation shape. Also, the validations showed an error which is less than 15 percent when using Timoshenko theory which is considered as suitable for the preliminary design.

7.1.3 Objective 2: Implement an analytical method for vertical connections

- It can be concluded that with the proposed method to analytically solve the connection between components, the finite element scheme is not essential. Also, because of the validations showed an error which is less than 15 percent this method can be considered as suitable for the preliminary design.

7.1.4 Objective 3: The development of a real-time tool prototype of rigid frames solved analytically

- It can be concluded that Rhino-Grasshopper together with GhPython component comprise a suitable software framework for the tool prototype to use during the preliminary design. This is because of the parametric modelling qualities, the real-time displaying of results, and the possibility to create the modular setup 'Lego-type' for the connections of different rigid frame geometries. Also, it can be said that the consolidating of the modelling, analysis and results stages into one 'Grasshopper cluster', facilitates the use of the tool from the user's perspective. And finally, the amount of adjustable input parameters contributes to the desired flexibility during the preliminary design.

7.2 RECOMMENDATIONS

7.2.1 Objective 1: Investigate rigid frames behaviour and its analytical representation

The recommendations on this objective are listed according to the approaches followed in this research.

- Range of applicability of the shear beam representation

  It is recommended to be aware of the reduced range of applicability of the shear beam representation of rigid frames, even for the preliminary design. This is because during this stage the exploration of different geometric configurations can lead to the cases where the bending effects are relevant, especially if the exploration of alternatives is made in a parametric way.

- Correction method for the shear beam representation

  It is recommended to develop the prediction of the error procedure for the defined zones A and C, so it can also be used as an indicator of rigid frame type (shear, bending or combined) that depends on the five geometric variables defined in this research project.

- Timoshenko beam representation

  It is recommended to analytically represent the behaviour of rigid frames with Timoshenko beam theory, even for preliminary design purposes since it was shown that bending effects can be significant. In spite of the implementation of the Timoshenko beam theory with a different shear stiffness for the ground floor, showed to be suffi-

ciently accurate for preliminary design purposes, it is recommended to increase the accuracy by the derivation of a different shear stiffness expression for the top floor of the rigid frame. Then, to include this change of shear stiffness for the top floor by considering a new field with a specific analytical solution, this is represented in Figure 7.2.

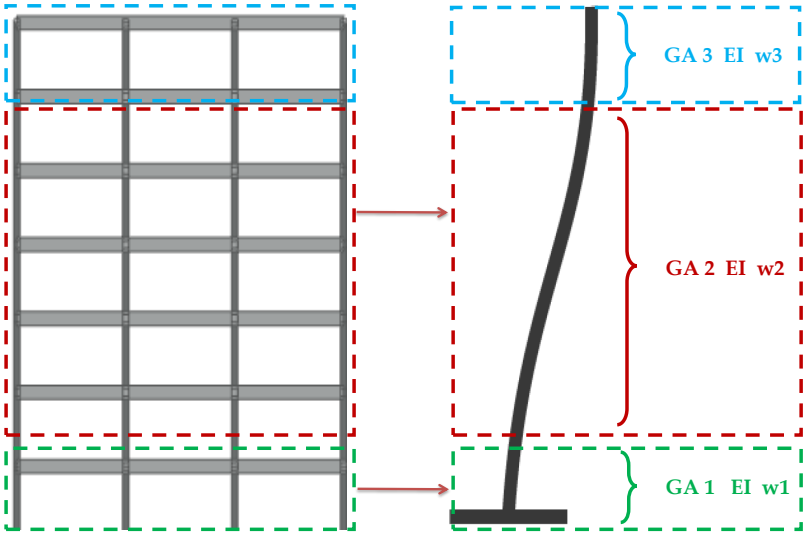

Figure 7.2: Improved Timoshenko beam representation

Also, for this research project, the second-order differential equation to represent a Timoshenko beam was implemented. However, this formulation is only applicable to static determinate cases, such as a cantilever beam. For the generic case, the coupled differential equations to represent a Timoshenko beam can be used; in this way, the Timoshenko theory can also be used for methods where the finite element scheme is followed to account for the boundaries and element's transitions as with the Super Element Method. The coupled differential are presented by Simone (2007) and shown below as Equations 7.1 and 7.2. The process to obtain the analytical solutions for this generic case is presented in Appendix B: Timoshenko beam - one field generic. Moreover, it is also presented in Appendix B the derivations of the analytical solutions for this generic case by also accounting for different fields: Timoshenko beam - three fields - generic. From Appendix B, it can be seen that for the structural scheme of a cantilever beam, both Timsohenko approaches result in the same analytical solution.

$$EI\frac{\mathrm{d}^2}{\mathrm{d}x^2}\phi(x) - GA\left(\frac{\mathrm{d}}{\mathrm{d}x}w(x) + \phi(x)\right) = 0 \tag{7.1}$$

$$GA\left(\frac{\mathrm{d}^2}{\mathrm{d}x^2}w(x) + \frac{\mathrm{d}}{\mathrm{d}x}\phi(x)\right) = -q \tag{7.2}$$

7.2.2 Objective 2: Implement an analytical method for vertical connections

For this research project, the derivation of the analytical solutions for each field was performed manually in Maple, however, it is possible to extend the number of fields from two to any number. This only requires additional programming effort to automate the derivations of the analytical solutions. This automation can be performed as for example with SymPy, which is a library for Python to perform symbolic mathematics. A possible geometry with four fields is shown in Figure 7.3.

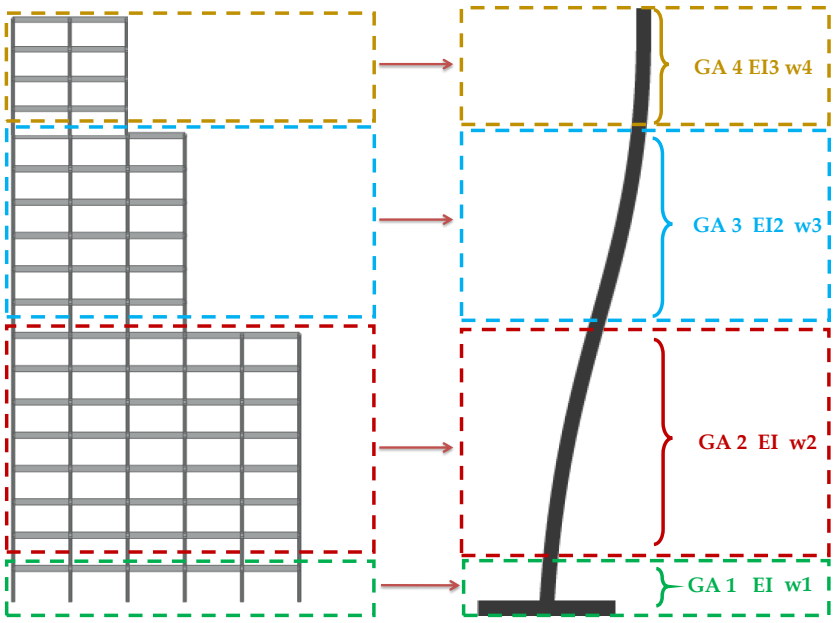

Figure 7.3: Four fields analytical representation

Also, it is recommended to study the eccentricities and concentration of stresses which cannot be taken into account when a rigid frame is analytically idealised as a one-dimensional element. It may be necessary to define a maximum allowed eccentricity and to define a parameter with which it is possible to determine if the concentration of stress in the corners of the connections are significant or not for the preliminary design.

7.2.3 Objective 3: The development of a real-time tool prototype of rigid frames solved analytically

It is recommended to address the programming limitations that can be easily performed by following the same logic as the one already implemented. Priorities, in order to quickly expand the applicability of the prototype, are the following:

- Any number of vertical and horizontal connections. Figure 7.4.

- Wind forces in the other direction, so each rigid frame in the building (in both perpendicular directions) can be simultaneously analysed. Figure 7.5.
- Increase of geometry flexibility.
- To account for steel rigid frames.

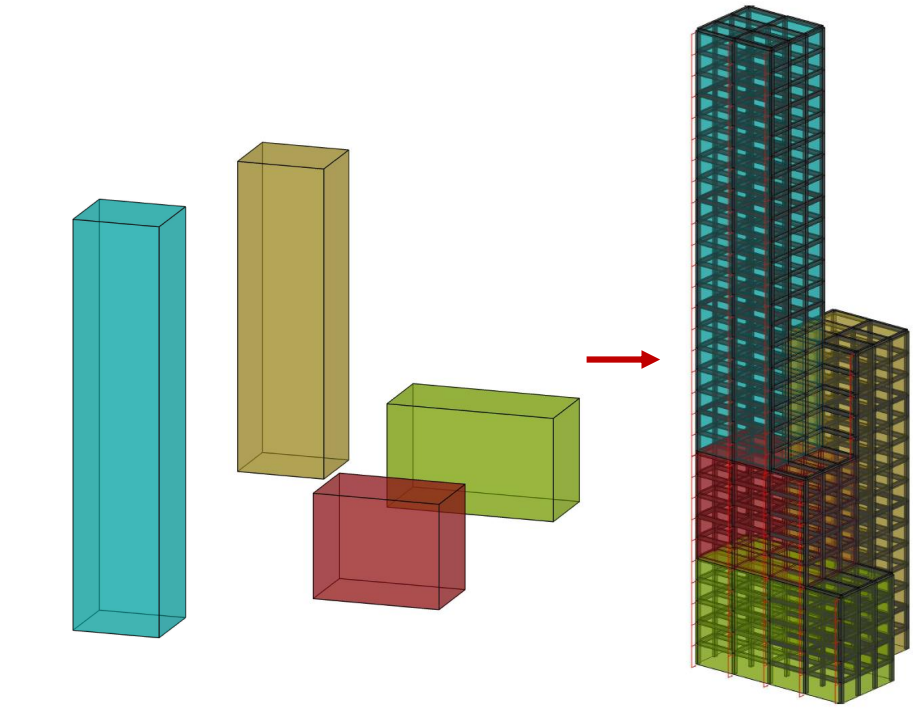

Figure 7.4: Any number of vertical and horizontal connections

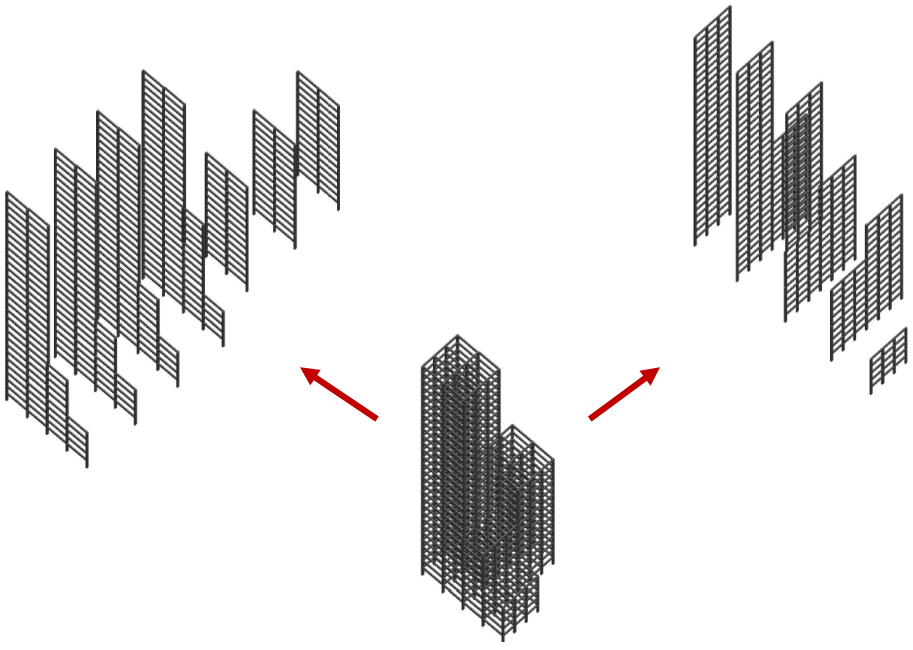

Figure 7.5: Wind forces in both perpendicular directions

It is also recommended to provide the possibility to instantaneously asses the structural feasibility of a complex of buildings. It can be advantageous to have a single file with several building geometries. This idea follows from the impact that surrounding buildings can have on the new project, as the blocking of winds gusts. This is graphically presented in Figures 7.6 and 7.7.

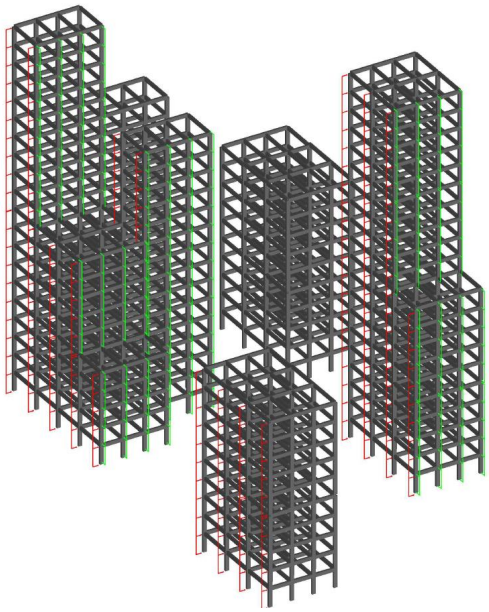

Figure 7.6: A complex of buildings

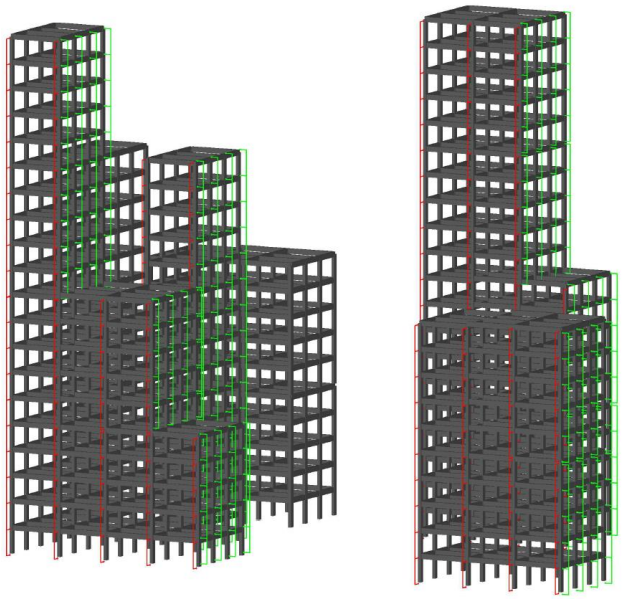

Figure 7.7: A complex of buildings

In this research project, Grasshopper advantage as a graphical algorithm editor was used for the generation of the visualisation scripts. In order to increase the speed of the real-time results for even more complex

and larger geometries, it is recommended to investigate the possibility to integrate the grasshopper visualisation scripts into one single Python code.

7.2.4 General recommendations

- Structural systems

  It is also recommended to expand the tool prototype by including other structural systems where this research on rigid frames can have a potential impact as in the following:

  – Shear walls - rigid frame structure

    In this structural system, which is described as parallel, the assumption that the total bending stiffness is provided by the shear walls is made, as well as the assumption that the total shear stiffness is provided by the rigid frame as shown in Figure 7.8 by Simone (2007) , where k stands for shear stiffness. However, for parametric implementation, it is recommended to determine the impact of the bending effects of the rigid frame. It might be possible to derive a symbolic differential equation to represent this type of system, where the rigid frame contribution is represented with the Timoshenko beam theory as indicated in Figure 7.9. The same recommendation is made for cores - rigid frames systems.

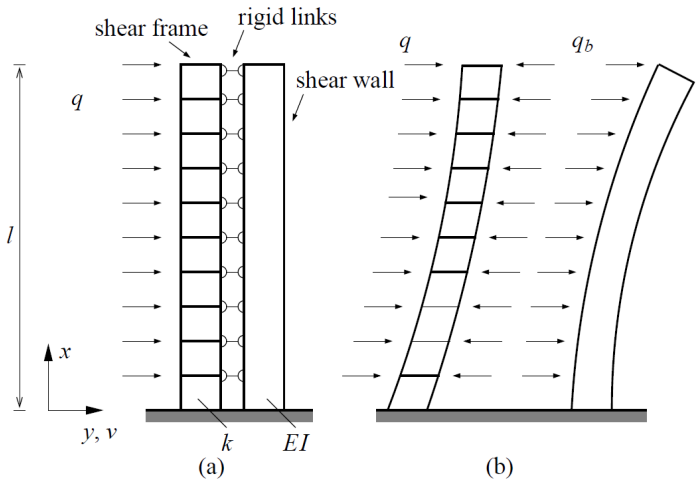

Figure 7.8: Shear wall and rigid frames systems by Simone (2007)

$$EI_{shearwall}\left(\frac{d^4}{dx^4}\,w1(x)\right)\underbrace{-GA_{frame}\left(\frac{d^2}{dx^2}\,w1(x)\right)=q}_{\frac{d^2}{dx^2}\,w(x)=-\frac{q}{GA1_{frame}}-\frac{M}{EI_{frame}}}$$

Timoshenko theory

$$EI_{shearwall}\left(\frac{d^4}{dx^4}\,w2(x)\right)\underbrace{-GA_{frame}\left(\frac{d^2}{dx^2}\,w2(x)\right)=q}_{\frac{d^2}{dx^2}\,w2(x)=-\frac{q}{GA2_{frame}}-\frac{M}{EI_{frame}}}$$

Timoshenko theory

Figure 7.9: Timoshenko beam theory to represent rigid frames in combined systems

- Braced hinged frame
- Outrigger structure
- Mega-frame

Structural systems as the outrigger or the mega-frame are mainly intended for tall buildings, as shown in the classification for structures types related to height by Schueller (1990) . Then, it is highly recommended to integrate dynamic analysis effects on the already developed components. Also, it is recommended to investigate if the change on lateral stiffness for these types of systems can also be addressed with the analytical method for connections proposed in this research project, this idea is graphically represented in Figures 7.10 and 7.11.

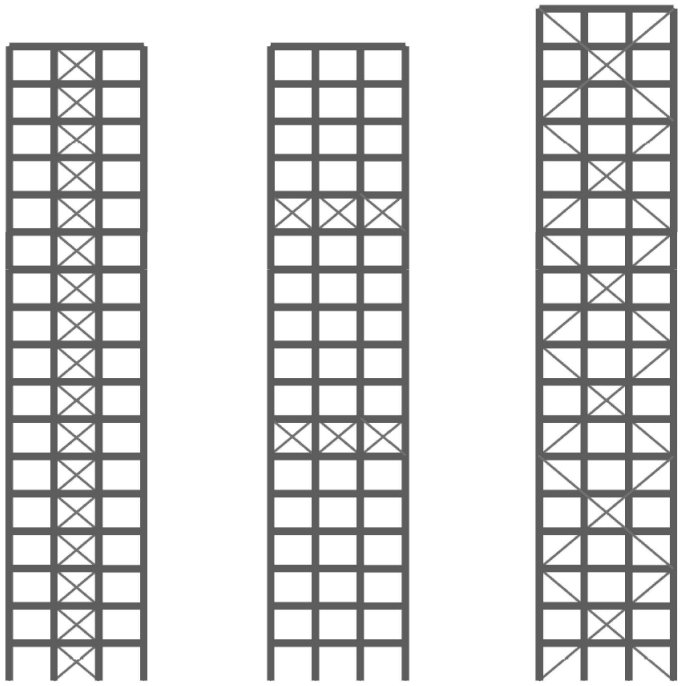

Figure 7.10: Braced rigid frames and/or with outriggers

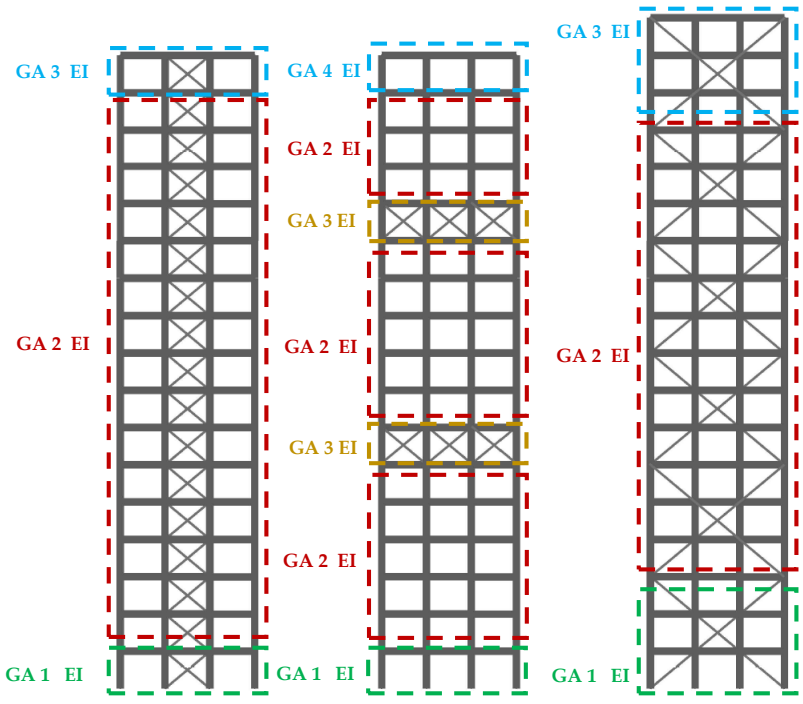

Figure 7.11: Braced rigid frames and/or with outriggers

- Generic differential equation of a basic planar bent

It is presented by Hoenderkamp (2005) the following generic differential equation for a basic planar bent under a uniformly distributed load.

$$EI\,\frac{\mathrm{d}^4}{\mathrm{d}x^4}w1\,(x) - \frac{GA\,\left(\frac{\mathrm{d}^2}{\mathrm{d}x^2}w1\,(x)\right)\left(EAc^2+EI\right)}{EAc^2} = q\left(1-1/2\,\frac{xGA}{EAc^2}\right) \tag{7.3}$$

This differential equation takes into account, bending, shear and axial deformations, so it is recommended to investigate its applicability for different configurations of structural systems. Hoenderkamp also suggests that this generic differential equation can be implemented for asymmetric floor plans. Then, it is attractive to test if this generic differential equation can be used as a general symbolic expression to analytically represent several structural systems as the ones addressed during this research project.

- Feasibility checks

  As mentioned by Hohrath (2018) , addition feasibility checks are needed to have a better structural evaluation of a building during the conceptual or early design. In the same line, it is also recommended in this research project to investigate which feasibility checks are performed in practice by companies which perform the structural engineering of a building.

- StructuralSystems-Boxes

  It is recommended to develop a 'StructuralSystem-Box' where the general prismatic dimensions can be defined as initial inputs; then, to prompt a drop-down list of structural systems that can be appropriate for those initial inputs. This idea is graphically represented in Figures 7.12 and 7.13 where the possibility to use rigid frames, shear walls or cores as principal lateral stability elements is shown.

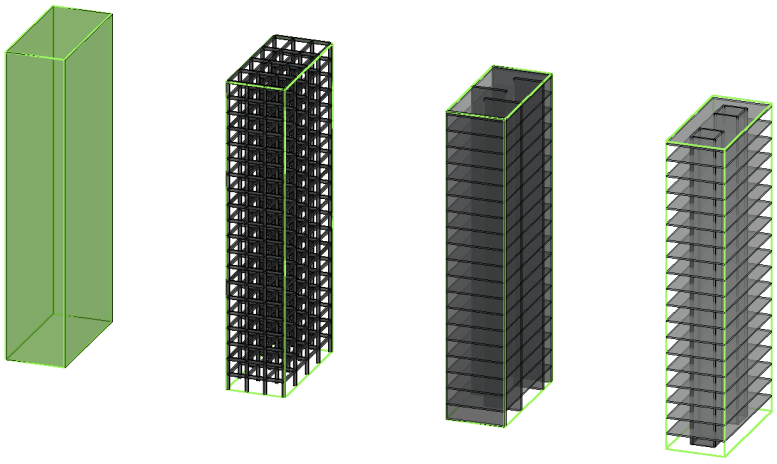

Figure 7.12: StructuralSystems-Box

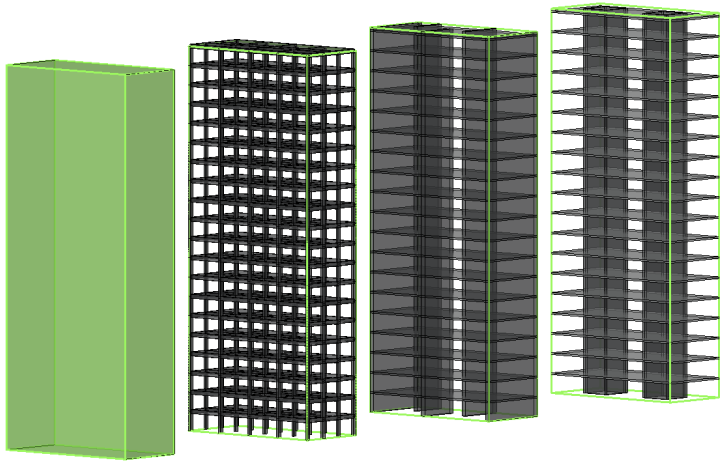

Figure 7.13: StructuralSystems-Box

- StructuralComponents

  It is also recommended to continue with the expansion of StructuralComponents by conducting research on other structural systems, its analytical representation and the applicability of it. Also, by developing new building components that can allow for more flexibility during the preliminary design.

  It is also suggested to explore the possibility to join the already developed components in previous versions of StructuralComponents into one single file or as a plugin for Grasshopper. Finally, it is recommended to additionally provide StructuralComponents with feasibility checks that involve other disciplines (for example architecture, environmental engineering or engineering economics), In so doing, better-

informed decisions can be taken at the preliminary stages during the construction of a building.

LIST OF FIGURES

BIBLIOGRAPHY

Akkar, S., Gülkan, P., and Yazgan, U. (2004). A simple procedure to compute the interstory drift for frame type structures. In *Proceedings of the 13th world conference on earthquake engineering*.

Autodesk (2019). Robot structural analysis. Retrieved from https://www.autodesk.com/products/robot-structural-analysis/overview. Last Accessed 18/10/2019.

Blume, J. A. (1968). Dynamic characteristics of multistory buildings. Technical report, Blume (John A.) and Associates Research Div., San Francisco, Calif.

Bovenberg, A. (2015). Structuralcomponents4.0: Conceptual building models with structural design justification. Master's thesis, Technical University of Delft. Retrieved from http://repository.tudelft.nl.

Bovenberg, A., Rolvink, A., and Coenders, J. (2015). Structuralcomponents 4: Conceptual building models with structural design justification. In *Proceedings of IASS Annual Symposia*, volume 2015, pages 1–10. International Association for Shell and Spatial Structures (IASS).

Breider, J. (2008). Structuralcomponents: Development of parametric associative design tools for the structural design of high-rise buildings. Master's thesis, Technical University of Delft.

Brooker, O. (2006). *Concrete Buildings Scheme Design Manual*. Concrete Information Limited.

BS-EN-1992-1-1 (2004). *Eurocode 2: Design of concrete structures - Part 1-1: General rules and rules for buildings*.

Caterino, N., Cosenza, E., and Azmoodeh, B. (2013). Approximate methods to evaluate storey stiffness and interstory drift of rc buildings in seismic area. *Structural Engineering & Mechanics*, 46(2):245–267.

Coenders, J. (2011). *Networked Design: next generation infrastructure for computational design*. PhD thesis, Technical University of Delft. Retrieved from http://repository.tudelft.nl.

Coenders, J. and Wagemans, L. (2006). Structural design tools: The next step in modelling for structural design. Retrieved from https://www.researchgate.net.

CSI (2019). Sap2000: Integrated software for structural analysis and design. Retrieved from https://www.csiamerica.com/products/sap2000.

Last Accessed 18/10/2019.

Davidson, S. (2019). Grasshopper alorithmic modeling for rhino. Retrieved from https://www.grasshopper3d.com/. Last Accessed 18/10/2019.

Dierker, L. (2019). Structuralcomponents6.0: An early-stage design tool for flexible topologies of mid-rise concrete buildings. Master's thesis, Technical University of Delft. Retrieved from http://repository.tudelft.nl.

Eroğlu, T. and Akkar, S. (2011). Lateral stiffness estimation in frames and its implementation to continuum models for linear and nonlinear static analysis. *Bulletin of Earthquake Engineering*, 9(4):1097–1114.

Ham, P. and Terwel, K. (2017). Structural calculations of high rise structures. Technical University of Delft. Lecture Notes of Building Structures 2.

Heumann, A. (2016). Human ui: A new interface paradigm for grasshopper. Retrieved from https://www.food4rhino.com/app/human-ui. Last Accessed 18/10/2019.

Hoenderkamp, J. (2005). *High-rise Structures: Preliminary Design for Lateral Load*. Technische Universiteit Eindhoven. Department of Architecture, Building and Engineering.

Hohrath, B. (2018). Structuralcomponents5.0: Super element based tool for early design collaboration applied to mid-rise buildings. Master's thesis, Technical University of Delft. Retrieved from http://repository.tudelft.nl.

Hohrath, B., Coenders, J., Rolvink, A., Turrin, M., and Steenbergen, R. (2018). Structural components 5.0: Collaborative conceptual design tool for structural and architectural feasibility using super elements. In *Proceedings of IASS Annual Symposia*, volume 2018, pages 1–8. International Association for Shell and Spatial Structures (IASS).

Hoogenboom, P. (2019). Shell analysis, theory and application. Technical University of Delft. Lecture Notes of Building Structures 2.

MacLeamy, P. (2004). Macleamy curve. *Collaboration, Integrated Information, and the Project Lifecycle in Building Design and Construction and Operation (WP-1202)*.

Maplesoft, a. d. o. W. M. I. (2019). Maplesoft^{TM}, a subsidiary of cybernet systems co. ltd. Retrieved from https://www.maplesoft.com. Last Accessed 04/11/2019.

MathWorks (2019). Fit curves and surfaces to data using regression, interpolation, and smoothing. Retrieved from https://nl.mathworks.com/products/curvefitting.html. Last Accessed 04/11/2019.

McNeel (2019). Ghpython. Retrieved from https://www.food4rhino.com/app/ghpython. Last Accessed 04/11/2019.

Muto, K. (1965). *Seismic analysis of reinforced concrete buildings*. Shokoku-sha.

NBBJ (2019). Telepathy plug-in. Retrieved from https://www.food4rhino.com/app/telepathy. Last Accessed 04/11/2019.

NEN-EN-1991-1-4 (2005). *Eurocode 1: Actions on structures - Part 1-4: General actions - Wind actions*.

Olowokere, D., Aktan, H., and Akanni, A. (1991). Towards an exact value for the flexural stiffness of tall rigid frames. *Computers & Structures*, 39(1-2):57–62.

Preisinger, C. (2019). Karamba3d-parametric engineering. Retrieved from https://www.karamba3d.com. Last Accessed 18/10/2019.

Rolvink, A. (2010). Structuralcomponents2.0: A parametric and associative toolbox for conceptual design of tall building structures. Master's thesis, Technical University of Delft. Retrieved from http://repository.tudelft.nl.

Rolvink, A., BREIDER, J., and COENDERS, J. (2010a). Structural components-a parametric associative design toolbox for conceptual structural design. In *Symposium of the International Association for Shell and Spatial Structures (50th. 2009. Valencia)*. Editorial Universitat Politècnica de València.

Rolvink, A., Breider, J., and Coenders, J. (2010b). Structuralcomponents–a toolbox for conceptual structural design. In *IABSE Symposium Report*, volume 97, pages 32–39. International Association for Bridge and Structural Engineering.

Rutten, D. (2019). Galapagos. Retrieved from https://www.grasshopper3d.com/group/galapagos. Last Accessed 04/11/2019.

Schueller, W. (1990). *The vertical building structure*. Van Nostrand Reinhold.

Simone, A. (2007). An introduction to the analysis of slender structures.

Stafford Smith, B. and Coull, A. (1991). Tall building structures: analysis and design.

Steenbergen, R. (2007). *Super elements in high-rise buildings under stochastic wind load*. PhD thesis, Technical University of Delft, The Netherlands. Retrieved from http://repository.tudelft.nl.

Vanderlinden, L., Crielaard, R., Andrejevic, A., Riedijk, W., Torpiano, G., Spiegeler, J., Beekman, M., Winter, R., and Titulaer, R. (2018). Parametric engineering version 1.0. Technical University of Delft. Lecture Notes of Parametric Engineering.

VandeWeerd, B. (2013). Structuralcomponents3.0: A client-server software architecture for fem-based structural design exploration. Master's thesis, Technical University of Delft. Retrieved from http://repository.tudelft.nl.

Welleman, H. (2017). Analysis of slender structures. Technical University of Delft. Lectures material. Retrieved from http://icozct.tudelft.nl/TUD$_C$T/.

Wells, G. (2006). The finite element method: An introduction. University of Cambridge and Technical University of Delft.

Appendices

A APPENDIX A

PARAMETRIC STUDY OF RIGID FRAMES AND PREDICTION OF THE ERROR

To study the behaviour of rigid frames and to predict the error of the shear beam representation, 480 models were developed with different geometric configurations. For each model, the analytical solution (representing a rigid frame as a shear beam) was compared to the numerical solution to obtain the percentage error, which was defined as one point for the data in this study. With the models, different patterns were found, the polynomial interpolations were derived and a procedure was developed to predict the error of the analytical representation. The procedure is illustrated in Figures A.1 and A.2. The surface polynomial interpolations were obtained with the MatLab curve fitting tool, as shown in Figure A.3, and polynomial interpolation 2 was generated with the concept of Lagrange polynomials as shown in Figure A.4. The last two polynomials were obtained with the tendency line tool of Excel. The resulting polynomial equations are shown below.

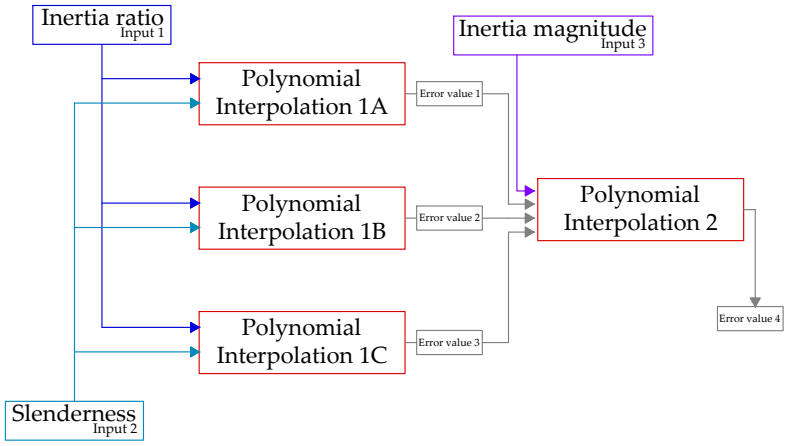

Figure A.1: Prediction of the error procedure: Stage 1

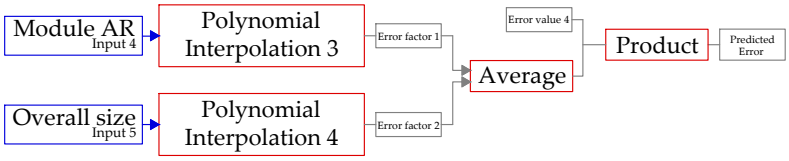

Figure A.2: Prediction of the error procedure: Stage 2

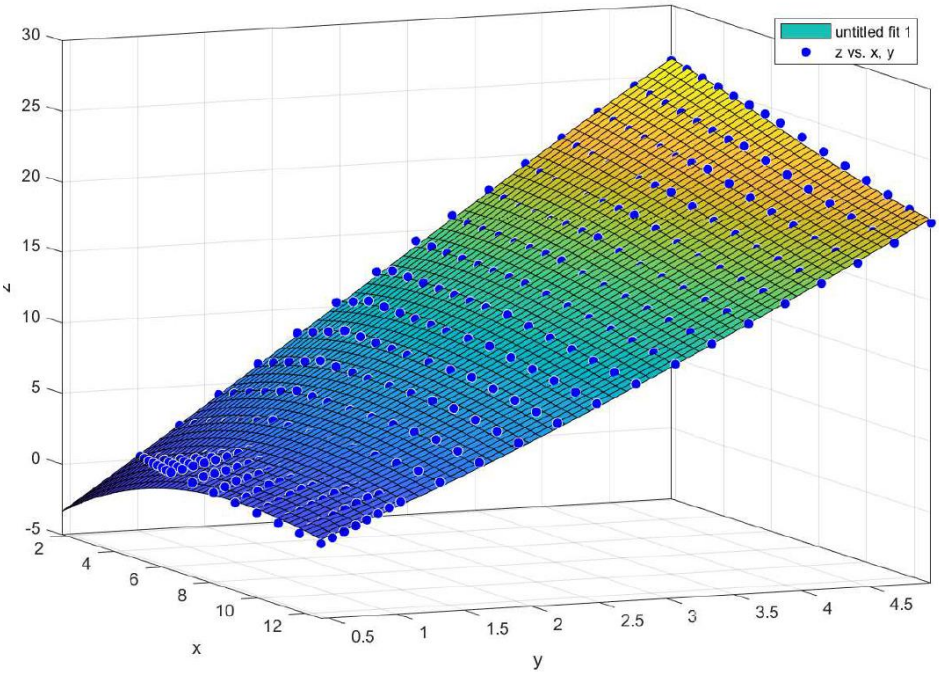

$$Ip1 = p03\,y^3 + p12\,xy^2 + p21\,x^2y + p30\,x^3 + p02\,y^2 + p11\,xy + p20\,x^2 + p01\,y + p10\,x + p00$$

Figure A.3: MATLAB curve fitting tool

$$\begin{aligned} L_2(x) &= f(x_1)\frac{x-x_2}{x_1-x_2}\cdot\frac{x-x_3}{x_1-x_3} \\ &+ f(x_2)\frac{x-x_1}{x_2-x_1}\cdot\frac{x-x_3}{x_2-x_3} \\ &+ f(x_3)\frac{x-x_1}{x_3-x_1}\cdot\frac{x-x_2}{x_3-x_2} \end{aligned}$$

Figure A.4: Lagrange polynomial

STAGE 1

Polynomial interpolation 1A

$$\begin{aligned} Error1 = 0.002707403\,x^3 + 0.020317282\,x^2y + 0.017878956\,xy^2 \\ -0.027332308\,y^3 - 0.150394736\,x^2 - 0.583162038\,xy + 0.168701688\,y^2 \\ +2.167768044\,x + 7.186744546\,y - 9.596476497 \end{aligned}$$

Polynomial interpolation 1B

$$\begin{aligned} Error2 = 0.000330326\,x^3 + 0.01640824\,x^2y + 0.073811799\,xy^2 \\ +0.056368706\,y^3 - 0.076429036\,x^2 - 0.862199731\,xy - 1.282740736\,y^2 \\ +1.547532102\,x + 18.49469127\,y - 7.012759178 \end{aligned}$$

Polynomial interpolation 1C

$$\begin{aligned} Error3 = 0.00196134\,x^3 + 0.012187869\,x^2y + 0.083997985\,xy^2 \\ -0.055107291\,y^3 - 0.091217811\,x^2 - 0.794222218\,xy - 0.627013409\,y^2 \\ +1.246846103\,x + 18.25178536\,y - 1.055955548 \end{aligned}$$

Polynomial interpolation 2

$$\begin{aligned} Error4 = \frac{(x-x2)\,(x-x3)\,Error1}{(x1-x2)\,(x1-x3)} + \frac{(x-x1)\,(x-x3)\,Error2}{(x2-x1)\,(x2-x3)} \\ + \frac{(x-x1)\,(x-x2)\,Error3}{(x3-x1)\,(x3-x2)} \end{aligned}$$

STAGE 2

Polynomial interpolation 3

$$ErrorFactor1 = 0.09113\,x^2 - 0.238\,x + 1$$

Polynomial interpolation 4

$$ErrorFactor2 = -0.00000001\,x2 + 0.0001\,x + 1$$

Table A.1: Amount of different values per variable

Variable	Amount of different values
Inertia ratio (IR)	10
Slenderness (S)	4
Inertia magnitude (IM)	3
Module aspect ratio (AR)	3
Overall size (A)	3

The geometric configurations for the models come from combinations of different values for each of the defined five variables. Table A.1 shows the amount of different values for each variable.

For each of the four slenderness values, 10 different inertia ratios were considered, this is graphically shown in Figure A.5. Then, 40 points are generated. Each point represents the error of the shear beam representation. From these 40 points, an interpolated surface was generated, this process is graphically explained in Figure 3.15. For each slenderness value, 3 different inertia magnitudes values were considered, this is graphically shown in Figure A.6. Then, 80 more points were generated. This can also be visualised as extrapolations of the interpolated surface as shown in Figure 3.21. For each inertia magnitude, 3 different module aspect ratios were considered, this is graphically shown in Figure A.7. Then, 240 more points were generated. This also means the generation of 6 more interpolated surfaces. Finally, to find the pattern of the error due to the overall size variable, 120 more models were generated for three different overall sizes. This is shown in figure A.8.

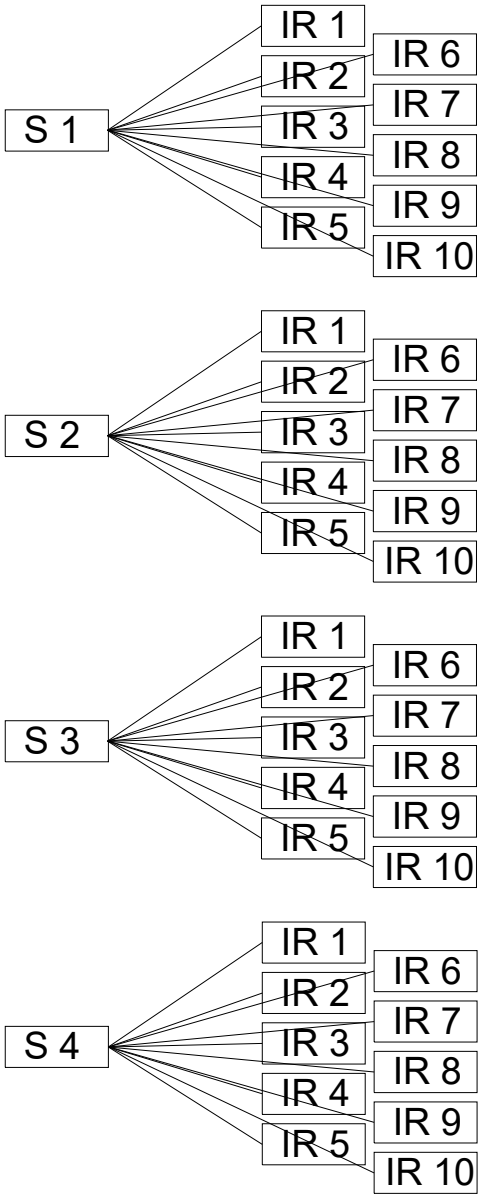

Figure A.5: Different inertia ratio values

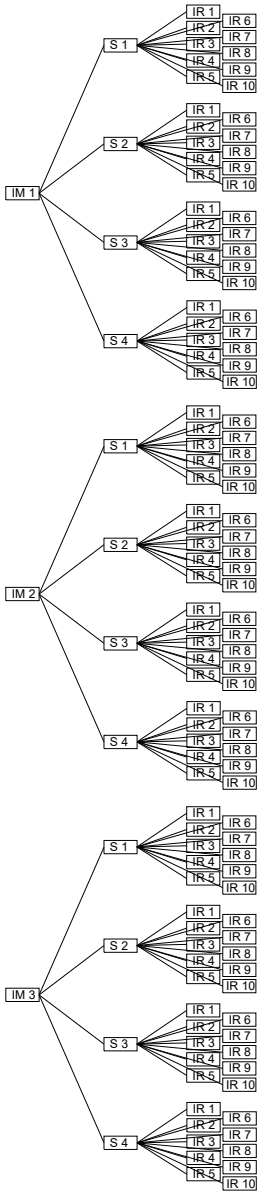

Figure A.6: Different inertia magnitude values

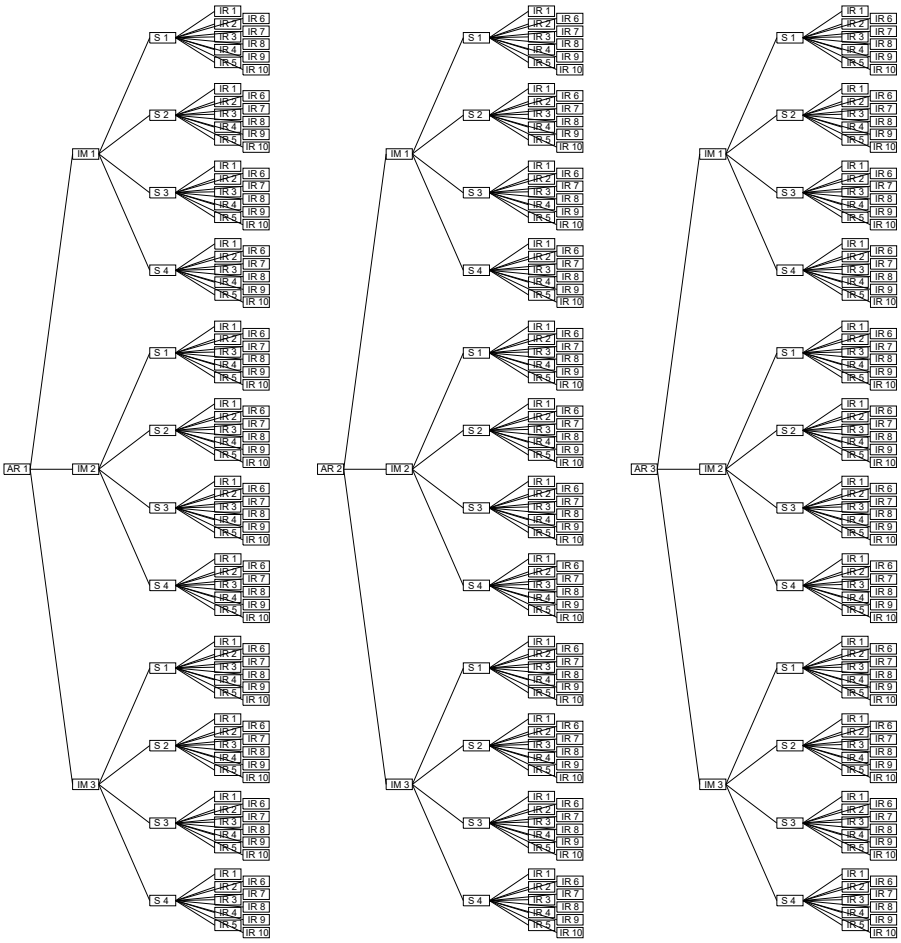

Figure A.7: Different module aspect ratio values

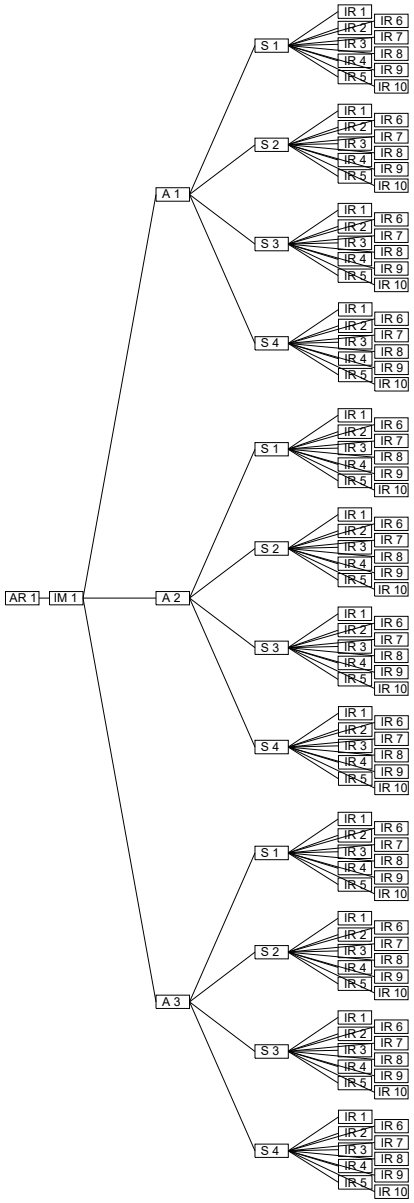

Figure A.8: Different overall area values

In total 12 surfaces, each of them generated with 40 different models, were developed for this parametric study. For each surface, a Grasshopper script is developed as the one shown in figure A.9.

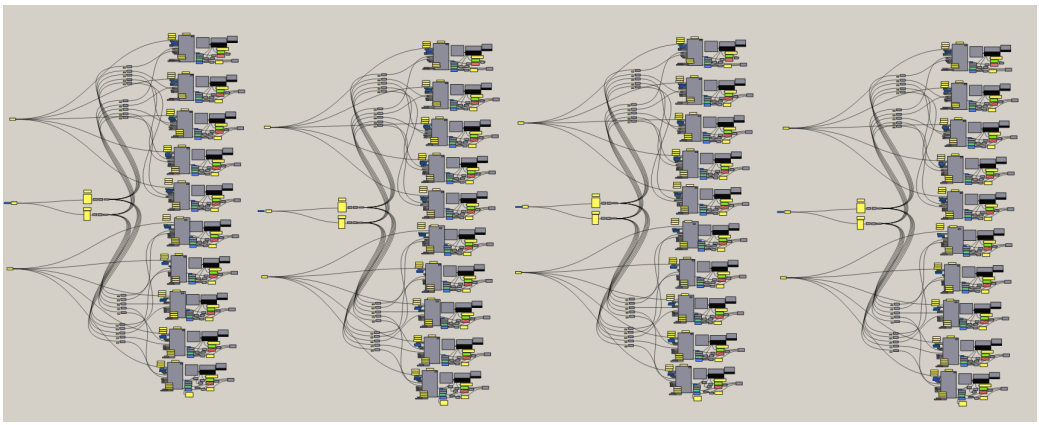

Figure A.9: Script for each surface

The figures below show the geometric properties for the 480 models within this parametric study.

Beams cross-section		Columns cross-section		Floor height	Floors	Bays width	Bays	Inertia ratio	Slender-ness	Inertia magni-tude	Module aspect ratio	Overall size
h (m)	w(m)	h (m)	w(m)	hf (m)	Amount	bw (m)	Amount	IR	S	IM (x10-4 m4)	AR	A (m2)
0.21	0.30	0.49	0.30	3.5	3	4	6	0.08	0.44	31.73	1.14	252
0.25	0.30	0.46	0.30	3.5	3	4	6	0.16	0.44	27.23	1.14	252
0.26	0.30	0.44	0.30	3.5	3	4	6	0.22	0.44	25.46	1.14	252
0.28	0.30	0.42	0.30	3.5	3	4	6	0.30	0.44	24.01	1.14	252
0.30	0.30	0.40	0.30	3.5	3	4	6	0.40	0.44	22.88	1.14	252
0.32	0.30	0.39	0.30	3.5	3	4	6	0.55	0.44	22.08	1.14	252
0.35	0.30	0.35	0.30	3.5	3	4	6	1.00	0.44	21.44	1.14	252
0.39	0.30	0.32	0.30	3.5	3	4	6	1.83	0.44	22.08	1.14	252
0.46	0.30	0.25	0.30	3.5	3	4	6	6.41	0.44	27.23	1.14	252
0.49	0.30	0.21	0.30	3.5	3	4	6	12.70	0.44	31.73	1.14	252
0.21	0.30	0.49	0.30	3.5	7	4	6	0.08	1.02	31.73	1.14	588
0.25	0.30	0.46	0.30	3.5	7	4	6	0.16	1.02	27.23	1.14	588
0.26	0.30	0.44	0.30	3.5	7	4	6	0.22	1.02	25.46	1.14	588
0.28	0.30	0.42	0.30	3.5	7	4	6	0.30	1.02	24.01	1.14	588
0.30	0.30	0.40	0.30	3.5	7	4	6	0.40	1.02	22.88	1.14	588
0.32	0.30	0.39	0.30	3.5	7	4	6	0.55	1.02	22.08	1.14	588
0.35	0.30	0.35	0.30	3.5	7	4	6	1.00	1.02	21.44	1.14	588
0.39	0.30	0.32	0.30	3.5	7	4	6	1.83	1.02	22.08	1.14	588
0.46	0.30	0.25	0.30	3.5	7	4	6	6.41	1.02	27.23	1.14	588
0.49	0.30	0.21	0.30	3.5	7	4	6	12.70	1.02	31.73	1.14	588
0.21	0.30	0.49	0.30	3.5	21	4	6	0.08	3.06	31.73	1.14	1764
0.25	0.30	0.46	0.30	3.5	21	4	6	0.16	3.06	27.23	1.14	1764
0.26	0.30	0.44	0.30	3.5	21	4	6	0.22	3.06	25.46	1.14	1764
0.28	0.30	0.42	0.30	3.5	21	4	6	0.30	3.06	24.01	1.14	1764
0.30	0.30	0.40	0.30	3.5	21	4	6	0.40	3.06	22.88	1.14	1764
0.32	0.30	0.39	0.30	3.5	21	4	6	0.55	3.06	22.08	1.14	1764
0.35	0.30	0.35	0.30	3.5	21	4	6	1.00	3.06	21.44	1.14	1764
0.39	0.30	0.32	0.30	3.5	21	4	6	1.83	3.06	22.08	1.14	1764
0.46	0.30	0.25	0.30	3.5	21	4	6	6.41	3.06	27.23	1.14	1764
0.49	0.30	0.21	0.30	3.5	21	4	6	12.70	3.06	31.73	1.14	1764
0.21	0.30	0.49	0.30	3.5	34	4	6	0.08	4.95	31.73	1.14	2856
0.25	0.30	0.46	0.30	3.5	34	4	6	0.16	4.95	27.23	1.14	2856
0.26	0.30	0.44	0.30	3.5	34	4	6	0.22	4.95	25.46	1.14	2856
0.28	0.30	0.42	0.30	3.5	34	4	6	0.30	4.95	24.01	1.14	2856
0.30	0.30	0.40	0.30	3.5	34	4	6	0.40	4.95	22.88	1.14	2856
0.32	0.30	0.39	0.30	3.5	34	4	6	0.55	4.95	22.08	1.14	2856
0.35	0.30	0.35	0.30	3.5	34	4	6	1.00	4.95	21.44	1.14	2856
0.39	0.30	0.32	0.30	3.5	34	4	6	1.83	4.95	22.08	1.14	2856
0.46	0.30	0.25	0.30	3.5	34	4	6	6.41	4.95	27.23	1.14	2856
0.49	0.30	0.21	0.30	3.5	34	4	6	12.70	4.95	31.73	1.14	2856
0.45	0.30	1.05	0.30	3.5	3	4	6	0.08	0.44	312.19	1.14	252
0.53	0.30	0.98	0.30	3.5	3	4	6	0.16	0.44	267.89	1.14	252
0.56	0.30	0.94	0.30	3.5	3	4	6	0.22	0.44	250.49	1.14	252
0.60	0.30	0.90	0.30	3.5	3	4	6	0.30	0.44	236.25	1.14	252
0.64	0.30	0.86	0.30	3.5	3	4	6	0.40	0.44	225.18	1.14	252

Figure A.10: Geometric properties of each model

0.68	0.30	0.83	0.30	3.5	3	4	6	0.55	0.44	217.27	1.14	252
0.75	0.30	0.75	0.30	3.5	3	4	6	1.00	0.44	210.94	1.14	252
0.83	0.30	0.68	0.30	3.5	3	4	6	1.83	0.44	217.27	1.14	252
0.98	0.30	0.53	0.30	3.5	3	4	6	6.41	0.44	267.89	1.14	252
1.05	0.30	0.45	0.30	3.5	3	4	6	12.70	0.44	312.19	1.14	252
0.45	0.30	1.05	0.30	3.5	7	4	6	0.08	1.02	312.19	1.14	588
0.53	0.30	0.98	0.30	3.5	7	4	6	0.16	1.02	267.89	1.14	588
0.56	0.30	0.94	0.30	3.5	7	4	6	0.22	1.02	250.49	1.14	588
0.60	0.30	0.90	0.30	3.5	7	4	6	0.30	1.02	236.25	1.14	588
0.64	0.30	0.86	0.30	3.5	7	4	6	0.40	1.02	225.18	1.14	588
0.68	0.30	0.83	0.30	3.5	7	4	6	0.55	1.02	217.27	1.14	588
0.75	0.30	0.75	0.30	3.5	7	4	6	1.00	1.02	210.94	1.14	588
0.83	0.30	0.68	0.30	3.5	7	4	6	1.83	1.02	217.27	1.14	588
0.98	0.30	0.53	0.30	3.5	7	4	6	6.41	1.02	267.89	1.14	588
1.05	0.30	0.45	0.30	3.5	7	4	6	12.70	1.02	312.19	1.14	588
0.45	0.30	1.05	0.30	3.5	21	4	6	0.08	3.06	312.19	1.14	1764
0.53	0.30	0.98	0.30	3.5	21	4	6	0.16	3.06	267.89	1.14	1764
0.56	0.30	0.94	0.30	3.5	21	4	6	0.22	3.06	250.49	1.14	1764
0.60	0.30	0.90	0.30	3.5	21	4	6	0.30	3.06	236.25	1.14	1764
0.64	0.30	0.86	0.30	3.5	21	4	6	0.40	3.06	225.18	1.14	1764
0.68	0.30	0.83	0.30	3.5	21	4	6	0.55	3.06	217.27	1.14	1764
0.75	0.30	0.75	0.30	3.5	21	4	6	1.00	3.06	210.94	1.14	1764
0.83	0.30	0.68	0.30	3.5	21	4	6	1.83	3.06	217.27	1.14	1764
0.98	0.30	0.53	0.30	3.5	21	4	6	6.41	3.06	267.89	1.14	1764
1.05	0.30	0.45	0.30	3.5	21	4	6	12.70	3.06	312.19	1.14	1764
0.45	0.30	1.05	0.30	3.5	34	4	6	0.08	4.95	312.19	1.14	2856
0.53	0.30	0.98	0.30	3.5	34	4	6	0.16	4.95	267.89	1.14	2856
0.56	0.30	0.94	0.30	3.5	34	4	6	0.22	4.95	250.49	1.14	2856
0.60	0.30	0.90	0.30	3.5	34	4	6	0.30	4.95	236.25	1.14	2856
0.64	0.30	0.86	0.30	3.5	34	4	6	0.40	4.95	225.18	1.14	2856
0.68	0.30	0.83	0.30	3.5	34	4	6	0.55	4.95	217.27	1.14	2856
0.75	0.30	0.75	0.30	3.5	34	4	6	1.00	4.95	210.94	1.14	2856
0.83	0.30	0.68	0.30	3.5	34	4	6	1.83	4.95	217.27	1.14	2856
0.98	0.30	0.53	0.30	3.5	34	4	6	6.41	4.95	267.89	1.14	2856
1.05	0.30	0.45	0.30	3.5	34	4	6	12.70	4.95	312.19	1.14	2856
0.54	0.30	1.26	0.30	3.5	3	4	6	0.08	0.44	539.46	1.14	252
0.63	0.30	1.17	0.30	3.5	3	4	6	0.16	0.44	462.92	1.14	252
0.68	0.30	1.13	0.30	3.5	3	4	6	0.22	0.44	432.84	1.14	252
0.72	0.30	1.08	0.30	3.5	3	4	6	0.30	0.44	408.24	1.14	252
0.77	0.30	1.04	0.30	3.5	3	4	6	0.40	0.44	389.10	1.14	252
0.81	0.30	0.99	0.30	3.5	3	4	6	0.55	0.44	375.44	1.14	252
0.90	0.30	0.90	0.30	3.5	3	4	6	1.00	0.44	364.50	1.14	252
0.99	0.30	0.81	0.30	3.5	3	4	6	1.83	0.44	375.44	1.14	252
1.17	0.30	0.63	0.30	3.5	3	4	6	6.41	0.44	462.92	1.14	252
1.26	0.30	0.54	0.30	3.5	3	4	6	12.70	0.44	539.46	1.14	252
0.54	0.30	1.26	0.30	3.5	7	4	6	0.08	1.02	539.46	1.14	588
0.63	0.30	1.17	0.30	3.5	7	4	6	0.16	1.02	462.92	1.14	588
0.68	0.30	1.13	0.30	3.5	7	4	6	0.22	1.02	432.84	1.14	588
0.72	0.30	1.08	0.30	3.5	7	4	6	0.30	1.02	408.24	1.14	588

Figure A.11: Geometric properties of each model

	0.77	0.30	1.04	0.30	3.5	7	4	6	0.40	1.02	389.10	1.14	588
	0.81	0.30	0.99	0.30	3.5	7	4	6	0.55	1.02	375.44	1.14	588
	0.90	0.30	0.90	0.30	3.5	7	4	6	1.00	1.02	364.50	1.14	588
	0.99	0.30	0.81	0.30	3.5	7	4	6	1.83	1.02	375.44	1.14	588
	1.17	0.30	0.63	0.30	3.5	7	4	6	6.41	1.02	462.92	1.14	588
	1.26	0.30	0.54	0.30	3.5	7	4	6	12.70	1.02	539.46	1.14	588
	0.54	0.30	1.26	0.30	3.5	21	4	6	0.08	3.06	539.46	1.14	1764
	0.63	0.30	1.17	0.30	3.5	21	4	6	0.16	3.06	462.92	1.14	1764
	0.68	0.30	1.13	0.30	3.5	21	4	6	0.22	3.06	432.84	1.14	1764
	0.72	0.30	1.08	0.30	3.5	21	4	6	0.30	3.06	408.24	1.14	1764
	0.77	0.30	1.04	0.30	3.5	21	4	6	0.40	3.06	389.10	1.14	1764
	0.81	0.30	0.99	0.30	3.5	21	4	6	0.55	3.06	375.44	1.14	1764
	0.90	0.30	0.90	0.30	3.5	21	4	6	1.00	3.06	364.50	1.14	1764
	0.99	0.30	0.81	0.30	3.5	21	4	6	1.83	3.06	375.44	1.14	1764
	1.17	0.30	0.63	0.30	3.5	21	4	6	6.41	3.06	462.92	1.14	1764
	1.26	0.30	0.54	0.30	3.5	21	4	6	12.70	3.06	539.46	1.14	1764
	0.54	0.30	1.26	0.30	3.5	34	4	6	0.08	4.95	539.46	1.14	2856
	0.63	0.30	1.17	0.30	3.5	34	4	6	0.16	4.95	462.92	1.14	2856
	0.68	0.30	1.13	0.30	3.5	34	4	6	0.22	4.95	432.84	1.14	2856
	0.72	0.30	1.08	0.30	3.5	34	4	6	0.30	4.95	408.24	1.14	2856
	0.77	0.30	1.04	0.30	3.5	34	4	6	0.40	4.95	389.10	1.14	2856
	0.81	0.30	0.99	0.30	3.5	34	4	6	0.55	4.95	375.44	1.14	2856
	0.90	0.30	0.90	0.30	3.5	34	4	6	1.00	4.95	364.50	1.14	2856
	0.99	0.30	0.81	0.30	3.5	34	4	6	1.83	4.95	375.44	1.14	2856
	1.17	0.30	0.63	0.30	3.5	34	4	6	6.41	4.95	462.92	1.14	2856
	1.26	0.30	0.54	0.30	3.5	34	4	6	12.70	4.95	539.46	1.14	2856

Figure A.12: Geometric properties of each model

Beams cross-section		Columns cross-section		Floor height	Floors	Bays width	Bays	Inertia ratio	Slender-ness	Inertia magni-tude	Module aspect ratio	Overall size
h (m)	w(m)	h (m)	w(m)	hf (m)	Amount	bw (m)	Amount	IR	S	IM (x10-4 m4)	AR	A (m2)
0.21	0.30	0.49	0.30	3.5	3	6	6	0.08	0.44	31.73	1.71	378
0.25	0.30	0.46	0.30	3.5	3	6	6	0.16	0.44	27.23	1.71	378
0.26	0.30	0.44	0.30	3.5	3	6	6	0.22	0.44	25.46	1.71	378
0.28	0.30	0.42	0.30	3.5	3	6	6	0.30	0.44	24.01	1.71	378
0.30	0.30	0.40	0.30	3.5	3	6	6	0.40	0.44	22.88	1.71	378
0.32	0.30	0.39	0.30	3.5	3	6	6	0.55	0.44	22.08	1.71	378
0.35	0.30	0.35	0.30	3.5	3	6	6	1.00	0.44	21.44	1.71	378
0.39	0.30	0.32	0.30	3.5	3	6	6	1.83	0.44	22.08	1.71	378
0.46	0.30	0.25	0.30	3.5	3	6	6	6.41	0.44	27.23	1.71	378
0.49	0.30	0.21	0.30	3.5	3	6	6	12.70	0.44	31.73	1.71	378
0.21	0.30	0.49	0.30	3.5	7	6	6	0.08	1.02	31.73	1.71	882
0.25	0.30	0.46	0.30	3.5	7	6	6	0.16	1.02	27.23	1.71	882
0.26	0.30	0.44	0.30	3.5	7	6	6	0.22	1.02	25.46	1.71	882
0.28	0.30	0.42	0.30	3.5	7	6	6	0.30	1.02	24.01	1.71	882
0.30	0.30	0.40	0.30	3.5	7	6	6	0.40	1.02	22.88	1.71	882
0.32	0.30	0.39	0.30	3.5	7	6	6	0.55	1.02	22.08	1.71	882
0.35	0.30	0.35	0.30	3.5	7	6	6	1.00	1.02	21.44	1.71	882
0.39	0.30	0.32	0.30	3.5	7	6	6	1.83	1.02	22.08	1.71	882
0.46	0.30	0.25	0.30	3.5	7	6	6	6.41	1.02	27.23	1.71	882
0.49	0.30	0.21	0.30	3.5	7	6	6	12.70	1.02	31.73	1.71	882
0.21	0.30	0.49	0.30	3.5	21	6	6	0.08	3.06	31.73	1.71	2646
0.25	0.30	0.46	0.30	3.5	21	6	6	0.16	3.06	27.23	1.71	2646
0.26	0.30	0.44	0.30	3.5	21	6	6	0.22	3.06	25.46	1.71	2646
0.28	0.30	0.42	0.30	3.5	21	6	6	0.30	3.06	24.01	1.71	2646
0.30	0.30	0.40	0.30	3.5	21	6	6	0.40	3.06	22.88	1.71	2646
0.32	0.30	0.39	0.30	3.5	21	6	6	0.55	3.06	22.08	1.71	2646
0.35	0.30	0.35	0.30	3.5	21	6	6	1.00	3.06	21.44	1.71	2646
0.39	0.30	0.32	0.30	3.5	21	6	6	1.83	3.06	22.08	1.71	2646
0.46	0.30	0.25	0.30	3.5	21	6	6	6.41	3.06	27.23	1.71	2646
0.49	0.30	0.21	0.30	3.5	21	6	6	12.70	3.06	31.73	1.71	2646
0.21	0.30	0.49	0.30	3.5	34	6	6	0.08	4.95	31.73	1.71	4284
0.25	0.30	0.46	0.30	3.5	34	6	6	0.16	4.95	27.23	1.71	4284
0.26	0.30	0.44	0.30	3.5	34	6	6	0.22	4.95	25.46	1.71	4284
0.28	0.30	0.42	0.30	3.5	34	6	6	0.30	4.95	24.01	1.71	4284
0.30	0.30	0.40	0.30	3.5	34	6	6	0.40	4.95	22.88	1.71	4284
0.32	0.30	0.39	0.30	3.5	34	6	6	0.55	4.95	22.08	1.71	4284
0.35	0.30	0.35	0.30	3.5	34	6	6	1.00	4.95	21.44	1.71	4284
0.39	0.30	0.32	0.30	3.5	34	6	6	1.83	4.95	22.08	1.71	4284
0.46	0.30	0.25	0.30	3.5	34	6	6	6.41	4.95	27.23	1.71	4284
0.49	0.30	0.21	0.30	3.5	34	6	6	12.70	4.95	31.73	1.71	4284
		0.70						IR	S			
0.45	0.30	1.05	0.30	3.5	3	6	6	0.08	0.44	312.19	1.71	378
0.53	0.30	0.98	0.30	3.5	3	6	6	0.16	0.44	267.89	1.71	378
0.56	0.30	0.94	0.30	3.5	3	6	6	0.22	0.44	250.49	1.71	378
0.60	0.30	0.90	0.30	3.5	3	6	6	0.30	0.44	236.25	1.71	378
0.64	0.30	0.86	0.30	3.5	3	6	6	0.40	0.44	225.18	1.71	378
0.68	0.30	0.83	0.30	3.5	3	6	6	0.55	0.44	217.27	1.71	378
0.75	0.30	0.75	0.30	3.5	3	6	6	1.00	0.44	210.94	1.71	378
0.83	0.30	0.68	0.30	3.5	3	6	6	1.83	0.44	217.27	1.71	378

Figure A.13: Geometric properties of each model

	0.98	0.30	0.53	0.30	3.5	3	6	6	6.41	0.44	267.89	1.71	378
	1.05	0.30	0.45	0.30	3.5	3	6	6	12.70	0.44	312.19	1.71	378
	0.45	0.30	1.05	0.30	3.5	7	6	6	0.08	1.02	312.19	1.71	882
	0.53	0.30	0.98	0.30	3.5	7	6	6	0.16	1.02	267.89	1.71	882
	0.56	0.30	0.94	0.30	3.5	7	6	6	0.22	1.02	250.49	1.71	882
	0.60	0.30	0.90	0.30	3.5	7	6	6	0.30	1.02	236.25	1.71	882
	0.64	0.30	0.86	0.30	3.5	7	6	6	0.40	1.02	225.18	1.71	882
	0.68	0.30	0.83	0.30	3.5	7	6	6	0.55	1.02	217.27	1.71	882
	0.75	0.30	0.75	0.30	3.5	7	6	6	1.00	1.02	210.94	1.71	882
	0.83	0.30	0.68	0.30	3.5	7	6	6	1.83	1.02	217.27	1.71	882
	0.98	0.30	0.53	0.30	3.5	7	6	6	6.41	1.02	267.89	1.71	882
	1.05	0.30	0.45	0.30	3.5	7	6	6	12.70	1.02	312.19	1.71	882
	0.45	0.30	1.05	0.30	3.5	21	6	6	0.08	3.06	312.19	1.71	2646
	0.53	0.30	0.98	0.30	3.5	21	6	6	0.16	3.06	267.89	1.71	2646
	0.56	0.30	0.94	0.30	3.5	21	6	6	0.22	3.06	250.49	1.71	2646
	0.60	0.30	0.90	0.30	3.5	21	6	6	0.30	3.06	236.25	1.71	2646
	0.64	0.30	0.86	0.30	3.5	21	6	6	0.40	3.06	225.18	1.71	2646
	0.68	0.30	0.83	0.30	3.5	21	6	6	0.55	3.06	217.27	1.71	2646
	0.75	0.30	0.75	0.30	3.5	21	6	6	1.00	3.06	210.94	1.71	2646
	0.83	0.30	0.68	0.30	3.5	21	6	6	1.83	3.06	217.27	1.71	2646
	0.98	0.30	0.53	0.30	3.5	21	6	6	6.41	3.06	267.89	1.71	2646
	1.05	0.30	0.45	0.30	3.5	21	6	6	12.70	3.06	312.19	1.71	2646
	0.45	0.30	1.05	0.30	3.5	34	6	6	0.08	4.95	312.19	1.71	4284
	0.53	0.30	0.98	0.30	3.5	34	6	6	0.16	4.95	267.89	1.71	4284
	0.56	0.30	0.94	0.30	3.5	34	6	6	0.22	4.95	250.49	1.71	4284
	0.60	0.30	0.90	0.30	3.5	34	6	6	0.30	4.95	236.25	1.71	4284
	0.64	0.30	0.86	0.30	3.5	34	6	6	0.40	4.95	225.18	1.71	4284
	0.68	0.30	0.83	0.30	3.5	34	6	6	0.55	4.95	217.27	1.71	4284
	0.75	0.30	0.75	0.30	3.5	34	6	6	1.00	4.95	210.94	1.71	4284
	0.83	0.30	0.68	0.30	3.5	34	6	6	1.83	4.95	217.27	1.71	4284
	0.98	0.30	0.53	0.30	3.5	34	6	6	6.41	4.95	267.89	1.71	4284
	1.05	0.30	0.45	0.30	3.5	34	6	6	12.70	4.95	312.19	1.71	4284
	0.54	0.30	1.26	0.30	3.5	3	6	6	0.08	0.44	539.46	1.71	378
	0.63	0.30	1.17	0.30	3.5	3	6	6	0.16	0.44	462.92	1.71	378
	0.68	0.30	1.13	0.30	3.5	3	6	6	0.22	0.44	432.84	1.71	378
	0.72	0.30	1.08	0.30	3.5	3	6	6	0.30	0.44	408.24	1.71	378
	0.77	0.30	1.04	0.30	3.5	3	6	6	0.40	0.44	389.10	1.71	378
	0.81	0.30	0.99	0.30	3.5	3	6	6	0.55	0.44	375.44	1.71	378
	0.90	0.30	0.90	0.30	3.5	3	6	6	1.00	0.44	364.50	1.71	378
	0.99	0.30	0.81	0.30	3.5	3	6	6	1.83	0.44	375.44	1.71	378
	1.17	0.30	0.63	0.30	3.5	3	6	6	6.41	0.44	462.92	1.71	378
	1.26	0.30	0.54	0.30	3.5	3	6	6	12.70	0.44	539.46	1.71	378
	0.54	0.30	1.26	0.30	3.5	7	6	6	0.08	1.02	539.46	1.71	882
	0.63	0.30	1.17	0.30	3.5	7	6	6	0.16	1.02	462.92	1.71	882
	0.68	0.30	1.13	0.30	3.5	7	6	6	0.22	1.02	432.84	1.71	882
	0.72	0.30	1.08	0.30	3.5	7	6	6	0.30	1.02	408.24	1.71	882
	0.77	0.30	1.04	0.30	3.5	7	6	6	0.40	1.02	389.10	1.71	882
	0.81	0.30	0.99	0.30	3.5	7	6	6	0.55	1.02	375.44	1.71	882
	0.90	0.30	0.90	0.30	3.5	7	6	6	1.00	1.02	364.50	1.71	882
	0.99	0.30	0.81	0.30	3.5	7	6	6	1.83	1.02	375.44	1.71	882
	1.17	0.30	0.63	0.30	3.5	7	6	6	6.41	1.02	462.92	1.71	882
	1.26	0.30	0.54	0.30	3.5	7	6	6	12.70	1.02	539.46	1.71	882

Figure A.14: Geometric properties of each model

0.54	0.30	1.26	0.30	3.5	21	6	6	0.08	3.06	539.46	1.71	2646
0.63	0.30	1.17	0.30	3.5	21	6	6	0.16	3.06	462.92	1.71	2646
0.68	0.30	1.13	0.30	3.5	21	6	6	0.22	3.06	432.84	1.71	2646
0.72	0.30	1.08	0.30	3.5	21	6	6	0.30	3.06	408.24	1.71	2646
0.77	0.30	1.04	0.30	3.5	21	6	6	0.40	3.06	389.10	1.71	2646
0.81	0.30	0.99	0.30	3.5	21	6	6	0.55	3.06	375.44	1.71	2646
0.90	0.30	0.90	0.30	3.5	21	6	6	1.00	3.06	364.50	1.71	2646
0.99	0.30	0.81	0.30	3.5	21	6	6	1.83	3.06	375.44	1.71	2646
1.17	0.30	0.63	0.30	3.5	21	6	6	6.41	3.06	462.92	1.71	2646
1.26	0.30	0.54	0.30	3.5	21	6	6	12.70	3.06	539.46	1.71	2646
0.54	0.30	1.26	0.30	3.5	34	6	6	0.08	4.95	539.46	1.71	4284
0.63	0.30	1.17	0.30	3.5	34	6	6	0.16	4.95	462.92	1.71	4284
0.68	0.30	1.13	0.30	3.5	34	6	6	0.22	4.95	432.84	1.71	4284
0.72	0.30	1.08	0.30	3.5	34	6	6	0.30	4.95	408.24	1.71	4284
0.77	0.30	1.04	0.30	3.5	34	6	6	0.40	4.95	389.10	1.71	4284
0.81	0.30	0.99	0.30	3.5	34	6	6	0.55	4.95	375.44	1.71	4284
0.90	0.30	0.90	0.30	3.5	34	6	6	1.00	4.95	364.50	1.71	4284
0.99	0.30	0.81	0.30	3.5	34	6	6	1.83	4.95	375.44	1.71	4284
1.17	0.30	0.63	0.30	3.5	34	6	6	6.41	4.95	462.92	1.71	4284
1.26	0.30	0.54	0.30	3.5	34	6	6	12.70	4.95	539.46	1.71	4284

Figure A.15: Geometric properties of each model

Beams cross-section		Columns cross-section		Floor height	Floors	Bays width	Bays	Inertia ratio	Slender-ness	Inertia magni-tude	Module aspect ratio	Overall size
h (m)	w(m)	h (m)	w(m)	hf (m)	Amount	bw (m)	Amount	IR	S	IM (x10-4 m4)	AR	A (m2)
0.21	0.30	0.49	0.30	3.5	3	8	6	0.08	0.44	31.73	2.29	504
0.25	0.30	0.46	0.30	3.5	3	8	6	0.16	0.44	27.23	2.29	504
0.26	0.30	0.44	0.30	3.5	3	8	6	0.22	0.44	25.46	2.29	504
0.28	0.30	0.42	0.30	3.5	3	8	6	0.30	0.44	24.01	2.29	504
0.30	0.30	0.40	0.30	3.5	3	8	6	0.40	0.44	22.88	2.29	504
0.32	0.30	0.39	0.30	3.5	3	8	6	0.55	0.44	22.08	2.29	504
0.35	0.30	0.35	0.30	3.5	3	8	6	1.00	0.44	21.44	2.29	504
0.39	0.30	0.32	0.30	3.5	3	8	6	1.83	0.44	22.08	2.29	504
0.46	0.30	0.25	0.30	3.5	3	8	6	6.41	0.44	27.23	2.29	504
0.49	0.30	0.21	0.30	3.5	3	8	6	12.70	0.44	31.73	2.29	504
0.21	0.30	0.49	0.30	3.5	7	8	6	0.08	1.02	31.73	2.29	1176
0.25	0.30	0.46	0.30	3.5	7	8	6	0.16	1.02	27.23	2.29	1176
0.26	0.30	0.44	0.30	3.5	7	8	6	0.22	1.02	25.46	2.29	1176
0.28	0.30	0.42	0.30	3.5	7	8	6	0.30	1.02	24.01	2.29	1176
0.30	0.30	0.40	0.30	3.5	7	8	6	0.40	1.02	22.88	2.29	1176
0.32	0.30	0.39	0.30	3.5	7	8	6	0.55	1.02	22.08	2.29	1176
0.35	0.30	0.35	0.30	3.5	7	8	6	1.00	1.02	21.44	2.29	1176
0.39	0.30	0.32	0.30	3.5	7	8	6	1.83	1.02	22.08	2.29	1176
0.46	0.30	0.25	0.30	3.5	7	8	6	6.41	1.02	27.23	2.29	1176
0.49	0.30	0.21	0.30	3.5	7	8	6	12.70	1.02	31.73	2.29	1176
0.21	0.30	0.49	0.30	3.5	21	8	6	0.08	3.06	31.73	2.29	3528
0.25	0.30	0.46	0.30	3.5	21	8	6	0.16	3.06	27.23	2.29	3528
0.26	0.30	0.44	0.30	3.5	21	8	6	0.22	3.06	25.46	2.29	3528
0.28	0.30	0.42	0.30	3.5	21	8	6	0.30	3.06	24.01	2.29	3528
0.30	0.30	0.40	0.30	3.5	21	8	6	0.40	3.06	22.88	2.29	3528
0.32	0.30	0.39	0.30	3.5	21	8	6	0.55	3.06	22.08	2.29	3528
0.35	0.30	0.35	0.30	3.5	21	8	6	1.00	3.06	21.44	2.29	3528
0.39	0.30	0.32	0.30	3.5	21	8	6	1.83	3.06	22.08	2.29	3528
0.46	0.30	0.25	0.30	3.5	21	8	6	6.41	3.06	27.23	2.29	3528
0.49	0.30	0.21	0.30	3.5	21	8	6	12.70	3.06	31.73	2.29	3528
0.21	0.30	0.49	0.30	3.5	34	8	6	0.08	4.95	31.73	2.29	5712
0.25	0.30	0.46	0.30	3.5	34	8	6	0.16	4.95	27.23	2.29	5712
0.26	0.30	0.44	0.30	3.5	34	8	6	0.22	4.95	25.46	2.29	5712
0.28	0.30	0.42	0.30	3.5	34	8	6	0.30	4.95	24.01	2.29	5712
0.30	0.30	0.40	0.30	3.5	34	8	6	0.40	4.95	22.88	2.29	5712
0.32	0.30	0.39	0.30	3.5	34	8	6	0.55	4.95	22.08	2.29	5712
0.35	0.30	0.35	0.30	3.5	34	8	6	1.00	4.95	21.44	2.29	5712
0.39	0.30	0.32	0.30	3.5	34	8	6	1.83	4.95	22.08	2.29	5712
0.46	0.30	0.25	0.30	3.5	34	8	6	6.41	4.95	27.23	2.29	5712
0.49	0.30	0.21	0.30	3.5	34	8	6	12.70	4.95	31.73	2.29	5712
		0.70						IR	S			
0.45	0.30	1.05	0.30	3.5	3	8	6	0.08	0.44	312.19	2.29	504
0.53	0.30	0.98	0.30	3.5	3	8	6	0.16	0.44	267.89	2.29	504
0.56	0.30	0.94	0.30	3.5	3	8	6	0.22	0.44	250.49	2.29	504
0.60	0.30	0.90	0.30	3.5	3	8	6	0.30	0.44	236.25	2.29	504
0.64	0.30	0.86	0.30	3.5	3	8	6	0.40	0.44	225.18	2.29	504
0.68	0.30	0.83	0.30	3.5	3	8	6	0.55	0.44	217.27	2.29	504
0.75	0.30	0.75	0.30	3.5	3	8	6	1.00	0.44	210.94	2.29	504
0.83	0.30	0.68	0.30	3.5	3	8	6	1.83	0.44	217.27	2.29	504
0.98	0.30	0.53	0.30	3.5	3	8	6	6.41	0.44	267.89	2.29	504
1.05	0.30	0.45	0.30	3.5	3	8	6	12.70	0.44	312.19	2.29	504

Figure A.16: Geometric properties of each model

0.45	0.30	1.05	0.30	3.5	7	8	6	0.08	1.02	312.19	2.29	1176
0.53	0.30	0.98	0.30	3.5	7	8	6	0.16	1.02	267.89	2.29	1176
0.56	0.30	0.94	0.30	3.5	7	8	6	0.22	1.02	250.49	2.29	1176
0.60	0.30	0.90	0.30	3.5	7	8	6	0.30	1.02	236.25	2.29	1176
0.64	0.30	0.86	0.30	3.5	7	8	6	0.40	1.02	225.18	2.29	1176
0.68	0.30	0.83	0.30	3.5	7	8	6	0.55	1.02	217.27	2.29	1176
0.75	0.30	0.75	0.30	3.5	7	8	6	1.00	1.02	210.94	2.29	1176
0.83	0.30	0.68	0.30	3.5	7	8	6	1.83	1.02	217.27	2.29	1176
0.98	0.30	0.53	0.30	3.5	7	8	6	6.41	1.02	267.89	2.29	1176
1.05	0.30	0.45	0.30	3.5	7	8	6	12.70	1.02	312.19	2.29	1176
0.45	0.30	1.05	0.30	3.5	21	8	6	0.08	3.06	312.19	2.29	3528
0.53	0.30	0.98	0.30	3.5	21	8	6	0.16	3.06	267.89	2.29	3528
0.56	0.30	0.94	0.30	3.5	21	8	6	0.22	3.06	250.49	2.29	3528
0.60	0.30	0.90	0.30	3.5	21	8	6	0.30	3.06	236.25	2.29	3528
0.64	0.30	0.86	0.30	3.5	21	8	6	0.40	3.06	225.18	2.29	3528
0.68	0.30	0.83	0.30	3.5	21	8	6	0.55	3.06	217.27	2.29	3528
0.75	0.30	0.75	0.30	3.5	21	8	6	1.00	3.06	210.94	2.29	3528
0.83	0.30	0.68	0.30	3.5	21	8	6	1.83	3.06	217.27	2.29	3528
0.98	0.30	0.53	0.30	3.5	21	8	6	6.41	3.06	267.89	2.29	3528
1.05	0.30	0.45	0.30	3.5	21	8	6	12.70	3.06	312.19	2.29	3528
0.45	0.30	1.05	0.30	3.5	34	8	6	0.08	4.95	312.19	2.29	5712
0.53	0.30	0.98	0.30	3.5	34	8	6	0.16	4.95	267.89	2.29	5712
0.56	0.30	0.94	0.30	3.5	34	8	6	0.22	4.95	250.49	2.29	5712
0.60	0.30	0.90	0.30	3.5	34	8	6	0.30	4.95	236.25	2.29	5712
0.64	0.30	0.86	0.30	3.5	34	8	6	0.40	4.95	225.18	2.29	5712
0.68	0.30	0.83	0.30	3.5	34	8	6	0.55	4.95	217.27	2.29	5712
0.75	0.30	0.75	0.30	3.5	34	8	6	1.00	4.95	210.94	2.29	5712
0.83	0.30	0.68	0.30	3.5	34	8	6	1.83	4.95	217.27	2.29	5712
0.98	0.30	0.53	0.30	3.5	34	8	6	6.41	4.95	267.89	2.29	5712
1.05	0.30	0.45	0.30	3.5	34	8	6	12.70	4.95	312.19	2.29	5712
0.54	0.30	1.26	0.30	3.5	3	8	6	0.08	0.44	539.46	2.29	504
0.63	0.30	1.17	0.30	3.5	3	8	6	0.16	0.44	462.92	2.29	504
0.68	0.30	1.13	0.30	3.5	3	8	6	0.22	0.44	432.84	2.29	504
0.72	0.30	1.08	0.30	3.5	3	8	6	0.30	0.44	408.24	2.29	504
0.77	0.30	1.04	0.30	3.5	3	8	6	0.40	0.44	389.10	2.29	504
0.81	0.30	0.99	0.30	3.5	3	8	6	0.55	0.44	375.44	2.29	504
0.90	0.30	0.90	0.30	3.5	3	8	6	1.00	0.44	364.50	2.29	504
0.99	0.30	0.81	0.30	3.5	3	8	6	1.83	0.44	375.44	2.29	504
1.17	0.30	0.63	0.30	3.5	3	8	6	6.41	0.44	462.92	2.29	504
1.26	0.30	0.54	0.30	3.5	3	8	6	12.70	0.44	539.46	2.29	504
0.54	0.30	1.26	0.30	3.5	7	8	6	0.08	1.02	539.46	2.29	1176
0.63	0.30	1.17	0.30	3.5	7	8	6	0.16	1.02	462.92	2.29	1176
0.68	0.30	1.13	0.30	3.5	7	8	6	0.22	1.02	432.84	2.29	1176
0.72	0.30	1.08	0.30	3.5	7	8	6	0.30	1.02	408.24	2.29	1176
0.77	0.30	1.04	0.30	3.5	7	8	6	0.40	1.02	389.10	2.29	1176
0.81	0.30	0.99	0.30	3.5	7	8	6	0.55	1.02	375.44	2.29	1176
0.90	0.30	0.90	0.30	3.5	7	8	6	1.00	1.02	364.50	2.29	1176
0.99	0.30	0.81	0.30	3.5	7	8	6	1.83	1.02	375.44	2.29	1176
1.17	0.30	0.63	0.30	3.5	7	8	6	6.41	1.02	462.92	2.29	1176
1.26	0.30	0.54	0.30	3.5	7	8	6	12.70	1.02	539.46	2.29	1176
0.54	0.30	1.26	0.30	3.5	21	8	6	0.08	3.06	539.46	2.29	3528
0.63	0.30	1.17	0.30	3.5	21	8	6	0.16	3.06	462.92	2.29	3528
0.68	0.30	1.13	0.30	3.5	21	8	6	0.22	3.06	432.84	2.29	3528
0.72	0.30	1.08	0.30	3.5	21	8	6	0.30	3.06	408.24	2.29	3528
0.77	0.30	1.04	0.30	3.5	21	8	6	0.40	3.06	389.10	2.29	3528

Figure A.17: Geometric properties of each model

	0.81	0.30	0.99	0.30	3.5	21	8	6	0.55	3.06	375.44	2.29	3528
	0.90	0.30	0.90	0.30	3.5	21	8	6	1.00	3.06	364.50	2.29	3528
	0.99	0.30	0.81	0.30	3.5	21	8	6	1.83	3.06	375.44	2.29	3528
	1.17	0.30	0.63	0.30	3.5	21	8	6	6.41	3.06	462.92	2.29	3528
	1.26	0.30	0.54	0.30	3.5	21	8	6	12.70	3.06	539.46	2.29	3528
	0.54	0.30	1.26	0.30	3.5	34	8	6	0.08	4.95	539.46	2.29	5712
	0.63	0.30	1.17	0.30	3.5	34	8	6	0.16	4.95	462.92	2.29	5712
	0.68	0.30	1.13	0.30	3.5	34	8	6	0.22	4.95	432.84	2.29	5712
	0.72	0.30	1.08	0.30	3.5	34	8	6	0.30	4.95	408.24	2.29	5712
	0.77	0.30	1.04	0.30	3.5	34	8	6	0.40	4.95	389.10	2.29	5712
	0.81	0.30	0.99	0.30	3.5	34	8	6	0.55	4.95	375.44	2.29	5712
	0.90	0.30	0.90	0.30	3.5	34	8	6	1.00	4.95	364.50	2.29	5712
	0.99	0.30	0.81	0.30	3.5	34	8	6	1.83	4.95	375.44	2.29	5712
	1.17	0.30	0.63	0.30	3.5	34	8	6	6.41	4.95	462.92	2.29	5712
	1.26	0.30	0.54	0.30	3.5	34	8	6	12.70	4.95	539.46	2.29	5712

Figure A.18: Geometric properties of each model

Beams cross-section		Columns cross-section		Floor height	Floors	Bays width	Bays	Inertia ratio	Slender-ness	Inertia magni-tude	Module aspect ratio	Overall size
h (m)	w(m)	h (m)	w(m)	hf (m)	Amount	bw (m)	Amount	IR	S	IM (x10-4 m4)	AR	A (m2)
0.54	0.30	1.26	0.30	3.5	3	4	6	0.08	0.44	539.46	1.14	252
0.63	0.30	1.17	0.30	3.5	3	4	6	0.16	0.44	462.92	1.14	252
0.68	0.30	1.13	0.30	3.5	3	4	6	0.22	0.44	432.84	1.14	252
0.72	0.30	1.08	0.30	3.5	3	4	6	0.30	0.44	408.24	1.14	252
0.77	0.30	1.04	0.30	3.5	3	4	6	0.40	0.44	389.10	1.14	252
0.81	0.30	0.99	0.30	3.5	3	4	6	0.55	0.44	375.44	1.14	252
0.90	0.30	0.90	0.30	3.5	3	4	6	1.00	0.44	364.50	1.14	252
0.99	0.30	0.81	0.30	3.5	3	4	6	1.83	0.44	375.44	1.14	252
1.17	0.30	0.63	0.30	3.5	3	4	6	6.41	0.44	462.92	1.14	252
1.26	0.30	0.54	0.30	3.5	3	4	6	12.70	0.44	539.46	1.14	252
0.54	0.30	1.26	0.30	3.5	7	4	6	0.08	1.02	539.46	1.14	588
0.63	0.30	1.17	0.30	3.5	7	4	6	0.16	1.02	462.92	1.14	588
0.68	0.30	1.13	0.30	3.5	7	4	6	0.22	1.02	432.84	1.14	588
0.72	0.30	1.08	0.30	3.5	7	4	6	0.30	1.02	408.24	1.14	588
0.77	0.30	1.04	0.30	3.5	7	4	6	0.40	1.02	389.10	1.14	588
0.81	0.30	0.99	0.30	3.5	7	4	6	0.55	1.02	375.44	1.14	588
0.90	0.30	0.90	0.30	3.5	7	4	6	1.00	1.02	364.50	1.14	588
0.99	0.30	0.81	0.30	3.5	7	4	6	1.83	1.02	375.44	1.14	588
1.17	0.30	0.63	0.30	3.5	7	4	6	6.41	1.02	462.92	1.14	588
1.26	0.30	0.54	0.30	3.5	7	4	6	12.70	1.02	539.46	1.14	588
0.54	0.30	1.26	0.30	3.5	21	4	6	0.08	3.06	539.46	1.14	1764
0.63	0.30	1.17	0.30	3.5	21	4	6	0.16	3.06	462.92	1.14	1764
0.68	0.30	1.13	0.30	3.5	21	4	6	0.22	3.06	432.84	1.14	1764
0.72	0.30	1.08	0.30	3.5	21	4	6	0.30	3.06	408.24	1.14	1764
0.77	0.30	1.04	0.30	3.5	21	4	6	0.40	3.06	389.10	1.14	1764
0.81	0.30	0.99	0.30	3.5	21	4	6	0.55	3.06	375.44	1.14	1764
0.90	0.30	0.90	0.30	3.5	21	4	6	1.00	3.06	364.50	1.14	1764
0.99	0.30	0.81	0.30	3.5	21	4	6	1.83	3.06	375.44	1.14	1764
1.17	0.30	0.63	0.30	3.5	21	4	6	6.41	3.06	462.92	1.14	1764
1.26	0.30	0.54	0.30	3.5	21	4	6	12.70	3.06	539.46	1.14	1764
0.54	0.30	1.26	0.30	3.5	34	4	6	0.08	4.95	539.46	1.14	2856
0.63	0.30	1.17	0.30	3.5	34	4	6	0.16	4.95	462.92	1.14	2856
0.68	0.30	1.13	0.30	3.5	34	4	6	0.22	4.95	432.84	1.14	2856
0.72	0.30	1.08	0.30	3.5	34	4	6	0.30	4.95	408.24	1.14	2856
0.77	0.30	1.04	0.30	3.5	34	4	6	0.40	4.95	389.10	1.14	2856
0.81	0.30	0.99	0.30	3.5	34	4	6	0.55	4.95	375.44	1.14	2856
0.90	0.30	0.90	0.30	3.5	34	4	6	1.00	4.95	364.50	1.14	2856
0.99	0.30	0.81	0.30	3.5	34	4	6	1.83	4.95	375.44	1.14	2856
1.17	0.30	0.63	0.30	3.5	34	4	6	6.41	4.95	462.92	1.14	2856
1.26	0.30	0.54	0.30	3.5	34	4	6	12.70	4.95	539.46	1.14	2856
0.54	0.30	1.26	0.30	3.5	6	4	12	0.08	0.44	539.46	1.14	1008
0.63	0.30	1.17	0.30	3.5	6	4	12	0.16	0.44	462.92	1.14	1008
0.68	0.30	1.13	0.30	3.5	6	4	12	0.22	0.44	432.84	1.14	1008
0.72	0.30	1.08	0.30	3.5	6	4	12	0.30	0.44	408.24	1.14	1008
0.77	0.30	1.04	0.30	3.5	6	4	12	0.40	0.44	389.10	1.14	1008
0.81	0.30	0.99	0.30	3.5	6	4	12	0.55	0.44	375.44	1.14	1008
0.90	0.30	0.90	0.30	3.5	6	4	12	1.00	0.44	364.50	1.14	1008
0.99	0.30	0.81	0.30	3.5	6	4	12	1.83	0.44	375.44	1.14	1008
1.17	0.30	0.63	0.30	3.5	6	4	12	6.41	0.44	462.92	1.14	1008
1.26	0.30	0.54	0.30	3.5	6	4	12	12.70	0.44	539.46	1.14	1008

Figure A.19: Geometric properties of each model

0.54	0.30	1.26	0.30	3.5	14	4	12	0.08	1.02	539.46	1.14	2352
0.63	0.30	1.17	0.30	3.5	14	4	12	0.16	1.02	462.92	1.14	2352
0.68	0.30	1.13	0.30	3.5	14	4	12	0.22	1.02	432.84	1.14	2352
0.72	0.30	1.08	0.30	3.5	14	4	12	0.30	1.02	408.24	1.14	2352
0.77	0.30	1.04	0.30	3.5	14	4	12	0.40	1.02	389.10	1.14	2352
0.81	0.30	0.99	0.30	3.5	14	4	12	0.55	1.02	375.44	1.14	2352
0.90	0.30	0.90	0.30	3.5	14	4	12	1.00	1.02	364.50	1.14	2352
0.99	0.30	0.81	0.30	3.5	14	4	12	1.83	1.02	375.44	1.14	2352
1.17	0.30	0.63	0.30	3.5	14	4	12	6.41	1.02	462.92	1.14	2352
1.26	0.30	0.54	0.30	3.5	14	4	12	12.70	1.02	539.46	1.14	2352
0.54	0.30	1.26	0.30	3.5	42	4	12	0.08	3.06	539.46	1.14	7056
0.63	0.30	1.17	0.30	3.5	42	4	12	0.16	3.06	462.92	1.14	7056
0.68	0.30	1.13	0.30	3.5	42	4	12	0.22	3.06	432.84	1.14	7056
0.72	0.30	1.08	0.30	3.5	42	4	12	0.30	3.06	408.24	1.14	7056
0.77	0.30	1.04	0.30	3.5	42	4	12	0.40	3.06	389.10	1.14	7056
0.81	0.30	0.99	0.30	3.5	42	4	12	0.55	3.06	375.44	1.14	7056
0.90	0.30	0.90	0.30	3.5	42	4	12	1.00	3.06	364.50	1.14	7056
0.99	0.30	0.81	0.30	3.5	42	4	12	1.83	3.06	375.44	1.14	7056
1.17	0.30	0.63	0.30	3.5	42	4	12	6.41	3.06	462.92	1.14	7056
1.26	0.30	0.54	0.30	3.5	42	4	12	12.70	3.06	539.46	1.14	7056
0.54	0.30	1.26	0.30	3.5	68	4	12	0.08	4.95	539.46	1.14	11424
0.63	0.30	1.17	0.30	3.5	68	4	12	0.16	4.95	462.92	1.14	11424
0.68	0.30	1.13	0.30	3.5	68	4	12	0.22	4.95	432.84	1.14	11424
0.72	0.30	1.08	0.30	3.5	68	4	12	0.30	4.95	408.24	1.14	11424
0.77	0.30	1.04	0.30	3.5	68	4	12	0.40	4.95	389.10	1.14	11424
0.81	0.30	0.99	0.30	3.5	68	4	12	0.55	4.95	375.44	1.14	11424
0.90	0.30	0.90	0.30	3.5	68	4	12	1.00	4.95	364.50	1.14	11424
0.99	0.30	0.81	0.30	3.5	68	4	12	1.83	4.95	375.44	1.14	11424
1.17	0.30	0.63	0.30	3.5	68	4	12	6.41	4.95	462.92	1.14	11424
1.26	0.30	0.54	0.30	3.5	68	4	12	12.70	4.95	539.46	1.14	11424
0.54	0.30	1.26	0.30	3.5	9	4	18	0.08	0.44	539.46	1.14	2268
0.63	0.30	1.17	0.30	3.5	9	4	18	0.16	0.44	462.92	1.14	2268
0.68	0.30	1.13	0.30	3.5	9	4	18	0.22	0.44	432.84	1.14	2268
0.72	0.30	1.08	0.30	3.5	9	4	18	0.30	0.44	408.24	1.14	2268
0.77	0.30	1.04	0.30	3.5	9	4	18	0.40	0.44	389.10	1.14	2268
0.81	0.30	0.99	0.30	3.5	9	4	18	0.55	0.44	375.44	1.14	2268
0.90	0.30	0.90	0.30	3.5	9	4	18	1.00	0.44	364.50	1.14	2268
0.99	0.30	0.81	0.30	3.5	9	4	18	1.83	0.44	375.44	1.14	2268
1.17	0.30	0.63	0.30	3.5	9	4	18	6.41	0.44	462.92	1.14	2268
1.26	0.30	0.54	0.30	3.5	9	4	18	12.70	0.44	539.46	1.14	2268
0.54	0.30	1.26	0.30	3.5	21	4	18	0.08	1.02	539.46	1.14	5292
0.63	0.30	1.17	0.30	3.5	21	4	18	0.16	1.02	462.92	1.14	5292
0.68	0.30	1.13	0.30	3.5	21	4	18	0.22	1.02	432.84	1.14	5292
0.72	0.30	1.08	0.30	3.5	21	4	18	0.30	1.02	408.24	1.14	5292
0.77	0.30	1.04	0.30	3.5	21	4	18	0.40	1.02	389.10	1.14	5292
0.81	0.30	0.99	0.30	3.5	21	4	18	0.55	1.02	375.44	1.14	5292
0.90	0.30	0.90	0.30	3.5	21	4	18	1.00	1.02	364.50	1.14	5292
0.99	0.30	0.81	0.30	3.5	21	4	18	1.83	1.02	375.44	1.14	5292
1.17	0.30	0.63	0.30	3.5	21	4	18	6.41	1.02	462.92	1.14	5292
1.26	0.30	0.54	0.30	3.5	21	4	18	12.70	1.02	539.46	1.14	5292
0.54	0.30	1.26	0.30	3.5	63	4	18	0.08	3.06	539.46	1.14	15876
0.63	0.30	1.17	0.30	3.5	63	4	18	0.16	3.06	462.92	1.14	15876
0.68	0.30	1.13	0.30	3.5	63	4	18	0.22	3.06	432.84	1.14	15876
0.72	0.30	1.08	0.30	3.5	63	4	18	0.30	3.06	408.24	1.14	15876
0.77	0.30	1.04	0.30	3.5	63	4	18	0.40	3.06	389.10	1.14	15876

Figure A.20: Geometric properties of each model

0.54	0.30	1.26	0.30	3.5	14	4	12	0.08	1.02	539.46	1.14	2352
0.63	0.30	1.17	0.30	3.5	14	4	12	0.16	1.02	462.92	1.14	2352
0.68	0.30	1.13	0.30	3.5	14	4	12	0.22	1.02	432.84	1.14	2352
0.72	0.30	1.08	0.30	3.5	14	4	12	0.30	1.02	408.24	1.14	2352
0.77	0.30	1.04	0.30	3.5	14	4	12	0.40	1.02	389.10	1.14	2352
0.81	0.30	0.99	0.30	3.5	14	4	12	0.55	1.02	375.44	1.14	2352
0.90	0.30	0.90	0.30	3.5	14	4	12	1.00	1.02	364.50	1.14	2352
0.99	0.30	0.81	0.30	3.5	14	4	12	1.83	1.02	375.44	1.14	2352
1.17	0.30	0.63	0.30	3.5	14	4	12	6.41	1.02	462.92	1.14	2352
1.26	0.30	0.54	0.30	3.5	14	4	12	12.70	1.02	539.46	1.14	2352
0.54	0.30	1.26	0.30	3.5	42	4	12	0.08	3.06	539.46	1.14	7056
0.63	0.30	1.17	0.30	3.5	42	4	12	0.16	3.06	462.92	1.14	7056
0.68	0.30	1.13	0.30	3.5	42	4	12	0.22	3.06	432.84	1.14	7056
0.72	0.30	1.08	0.30	3.5	42	4	12	0.30	3.06	408.24	1.14	7056
0.77	0.30	1.04	0.30	3.5	42	4	12	0.40	3.06	389.10	1.14	7056
0.81	0.30	0.99	0.30	3.5	42	4	12	0.55	3.06	375.44	1.14	7056
0.90	0.30	0.90	0.30	3.5	42	4	12	1.00	3.06	364.50	1.14	7056
0.99	0.30	0.81	0.30	3.5	42	4	12	1.83	3.06	375.44	1.14	7056
1.17	0.30	0.63	0.30	3.5	42	4	12	6.41	3.06	462.92	1.14	7056
1.26	0.30	0.54	0.30	3.5	42	4	12	12.70	3.06	539.46	1.14	7056
0.54	0.30	1.26	0.30	3.5	68	4	12	0.08	4.95	539.46	1.14	11424
0.63	0.30	1.17	0.30	3.5	68	4	12	0.16	4.95	462.92	1.14	11424
0.68	0.30	1.13	0.30	3.5	68	4	12	0.22	4.95	432.84	1.14	11424
0.72	0.30	1.08	0.30	3.5	68	4	12	0.30	4.95	408.24	1.14	11424
0.77	0.30	1.04	0.30	3.5	68	4	12	0.40	4.95	389.10	1.14	11424
0.81	0.30	0.99	0.30	3.5	68	4	12	0.55	4.95	375.44	1.14	11424
0.90	0.30	0.90	0.30	3.5	68	4	12	1.00	4.95	364.50	1.14	11424
0.99	0.30	0.81	0.30	3.5	68	4	12	1.83	4.95	375.44	1.14	11424
1.17	0.30	0.63	0.30	3.5	68	4	12	6.41	4.95	462.92	1.14	11424
1.26	0.30	0.54	0.30	3.5	68	4	12	12.70	4.95	539.46	1.14	11424
0.54	0.30	1.26	0.30	3.5	9	4	18	0.08	0.44	539.46	1.14	2268
0.63	0.30	1.17	0.30	3.5	9	4	18	0.16	0.44	462.92	1.14	2268
0.68	0.30	1.13	0.30	3.5	9	4	18	0.22	0.44	432.84	1.14	2268
0.72	0.30	1.08	0.30	3.5	9	4	18	0.30	0.44	408.24	1.14	2268
0.77	0.30	1.04	0.30	3.5	9	4	18	0.40	0.44	389.10	1.14	2268
0.81	0.30	0.99	0.30	3.5	9	4	18	0.55	0.44	375.44	1.14	2268
0.90	0.30	0.90	0.30	3.5	9	4	18	1.00	0.44	364.50	1.14	2268
0.99	0.30	0.81	0.30	3.5	9	4	18	1.83	0.44	375.44	1.14	2268
1.17	0.30	0.63	0.30	3.5	9	4	18	6.41	0.44	462.92	1.14	2268
1.26	0.30	0.54	0.30	3.5	9	4	18	12.70	0.44	539.46	1.14	2268
0.54	0.30	1.26	0.30	3.5	21	4	18	0.08	1.02	539.46	1.14	5292
0.63	0.30	1.17	0.30	3.5	21	4	18	0.16	1.02	462.92	1.14	5292
0.68	0.30	1.13	0.30	3.5	21	4	18	0.22	1.02	432.84	1.14	5292
0.72	0.30	1.08	0.30	3.5	21	4	18	0.30	1.02	408.24	1.14	5292
0.77	0.30	1.04	0.30	3.5	21	4	18	0.40	1.02	389.10	1.14	5292
0.81	0.30	0.99	0.30	3.5	21	4	18	0.55	1.02	375.44	1.14	5292
0.90	0.30	0.90	0.30	3.5	21	4	18	1.00	1.02	364.50	1.14	5292
0.99	0.30	0.81	0.30	3.5	21	4	18	1.83	1.02	375.44	1.14	5292
1.17	0.30	0.63	0.30	3.5	21	4	18	6.41	1.02	462.92	1.14	5292
1.26	0.30	0.54	0.30	3.5	21	4	18	12.70	1.02	539.46	1.14	5292
0.54	0.30	1.26	0.30	3.5	63	4	18	0.08	3.06	539.46	1.14	15876
0.63	0.30	1.17	0.30	3.5	63	4	18	0.16	3.06	462.92	1.14	15876
0.68	0.30	1.13	0.30	3.5	63	4	18	0.22	3.06	432.84	1.14	15876
0.72	0.30	1.08	0.30	3.5	63	4	18	0.30	3.06	408.24	1.14	15876
0.77	0.30	1.04	0.30	3.5	63	4	18	0.40	3.06	389.10	1.14	15876

Figure A.21: Geometric properties of each model

	0.81	0.30	0.99	0.30	3.5	63	4	18	0.55	3.06	375.44	1.14	15876
	0.90	0.30	0.90	0.30	3.5	63	4	18	1.00	3.06	364.50	1.14	15876
	0.99	0.30	0.81	0.30	3.5	63	4	18	1.83	3.06	375.44	1.14	15876
	1.17	0.30	0.63	0.30	3.5	63	4	18	6.41	3.06	462.92	1.14	15876
	1.26	0.30	0.54	0.30	3.5	63	4	18	12.70	3.06	539.46	1.14	15876
	0.54	0.30	1.26	0.30	3.5	102	4	18	0.08	4.95	539.46	1.14	25704
	0.63	0.30	1.17	0.30	3.5	102	4	18	0.16	4.95	462.92	1.14	25704
	0.68	0.30	1.13	0.30	3.5	102	4	18	0.22	4.95	432.84	1.14	25704
	0.72	0.30	1.08	0.30	3.5	102	4	18	0.30	4.95	408.24	1.14	25704
	0.77	0.30	1.04	0.30	3.5	102	4	18	0.40	4.95	389.10	1.14	25704
	0.81	0.30	0.99	0.30	3.5	102	4	18	0.55	4.95	375.44	1.14	25704
	0.90	0.30	0.90	0.30	3.5	102	4	18	1.00	4.95	364.50	1.14	25704
	0.99	0.30	0.81	0.30	3.5	102	4	18	1.83	4.95	375.44	1.14	25704
	1.17	0.30	0.63	0.30	3.5	102	4	18	6.41	4.95	462.92	1.14	25704
	1.26	0.30	0.54	0.30	3.5	102	4	18	12.70	4.95	539.46	1.14	25704

Figure A.22: Geometric properties of each model

B | APPENDIX B

ANALYTICAL DERIVATIONS

SHEAR BEAM - ONE FIELD -

```
> restart;
> ODE := GA·diff(w(x), x$2) = -q;
```

$$ODE := GA\left(\frac{d^2}{dx^2}\,w(x)\right) = -q \tag{1}$$

```
> w := rhs(dsolve(ODE));
```

$$w := -\frac{q\,x^2}{2\,GA} + \_C1\,x + \_C2 \tag{2}$$

```
> gammaa := diff(w, x);
```

$$gammaa := -\frac{q\,x}{GA} + \_C1 \tag{3}$$

```
> V := gammaa·GA;
```

$$V := \left(-\frac{q\,x}{GA} + \_C1\right) GA \tag{4}$$

```
> x := 0 : eq1 := w = 0;
```

$$eq1 := \_C2 = 0 \tag{5}$$

```
> x := L : eq2 := V = 0;
```

$$eq2 := \left(-\frac{q\,L}{GA} + \_C1\right) GA = 0 \tag{6}$$

```
> sol := solve({eq1, eq2}, {_C1, _C2}); assign(sol);
```

$$sol := \left\{\_C1 = \frac{q\,L}{GA}, \_C2 = 0\right\} \tag{7}$$

```
> x :='x'; w;
```

$$x := x$$

$$-\frac{q\,x^2}{2\,GA} + \frac{q\,L\,x}{GA} \tag{8}$$

```
> V;
```

$$\left(-\frac{q\,x}{GA} + \frac{q\,L}{GA}\right) GA \tag{9}$$

```
> x :='x'; w := simplify(w);
```

$$x := x$$

$$w := \frac{x\,q\,(-x + 2\,L)}{2\,GA} \tag{10}$$

```
> x :='x'; V := simplify(V);
```

$$x := x$$

$$V := q\,(L - x) \tag{11}$$

SHEAR BEAM - THREE FIELDS -

```
> restart;
>
>
> ODE1 := GA1·diff(w1(x), x$2) = -q;
```

$$ODE1 := GA1\left(\frac{d^2}{dx^2}\, w1(x)\right) = -q \tag{1}$$

```
>
> w1 := rhs(dsolve(ODE1));
```

$$w1 := -\frac{q\,x^2}{2\,GA1} + \_C1\,x + \_C2 \tag{2}$$

```
> w2 := -q*x^2/(2*GA2) + _C3*x + _C4;
```

$$w2 := -\frac{q\,x^2}{2\,GA2} + \_C3\,x + \_C4 \tag{3}$$

```
> w3 := -q*x^2/(2*GA3) + _C5*x + _C6;
```

$$w3 := -\frac{q\,x^2}{2\,GA3} + \_C5\,x + \_C6 \tag{4}$$

```
> gammaa1 := diff(w1, x);
```

$$gammaa1 := -\frac{q\,x}{GA1} + \_C1 \tag{5}$$

```
> gammaa2 := diff(w2, x);
```

$$gammaa2 := -\frac{q\,x}{GA2} + \_C3 \tag{6}$$

```
> gammaa3 := diff(w3, x);
```

$$gammaa3 := -\frac{q\,x}{GA3} + \_C5 \tag{7}$$

```
>
> V1 := gammaa1·GA1;
```

$$V1 := \left(-\frac{q\,x}{GA1} + \_C1\right) GA1 \tag{8}$$

```
> V2 := gammaa2·GA2;
```

$$V2 := \left(-\frac{q\,x}{GA2} + \_C3\right) GA2 \tag{9}$$

```
> V3 := gammaa3·GA3;
```

$$V3 := \left(-\frac{q\,x}{GA3} + \_C5\right) GA3 \tag{10}$$

```
> x := 0 : eq1 := w1 = 0;
```

$$eq1 := \_C2 = 0 \tag{11}$$

```
> x := a : eq2 := w1 = w2; eq3 := V1 = V2;
```

$$eq2 := -\frac{q\,a^2}{2\,GA1} + \_C1\,a + \_C2 = -\frac{q\,a^2}{2\,GA2} + \_C3\,a + \_C4$$

$$eq3 := \left(-\frac{q\,a}{GA1} + \_C1\right) GA1 = \left(-\frac{q\,a}{GA2} + \_C3\right) GA2 \quad \textbf{(12)}$$

> $x := b : eq4 := w3 = w2; eq5 := V3 = V2;$

$$eq4 := -\frac{q\,b^2}{2\,GA3} + \_C5\,b + \_C6 = -\frac{q\,b^2}{2\,GA2} + \_C3\,b + \_C4$$

$$eq5 := \left(-\frac{q\,b}{GA3} + \_C5\right) GA3 = \left(-\frac{q\,b}{GA2} + \_C3\right) GA2 \quad \textbf{(13)}$$

> $x := L : eq6 := V3 = 0;$

$$eq6 := \left(-\frac{q\,L}{GA3} + \_C5\right) GA3 = 0 \quad \textbf{(14)}$$

> $sol := solve(\{eq1, eq2, eq3, eq4, eq5, eq6\}, \{\_C1, \_C2, \_C3, \_C4, \_C5, \_C6\}) : assign(sol) :$

> $x := 'x';$

$$x := x \quad \textbf{(15)}$$

> $w1 := simplify(w1);$

$$w1 := \frac{q\,x\,(-x + 2\,L)}{2\,GA1} \quad \textbf{(16)}$$

> $w2 := simplify(w2);$

$$w2 := -\frac{\left((a - x)\left(-\frac{a}{2} + L - \frac{x}{2}\right) GA1 - a\,GA2\left(L - \frac{a}{2}\right)\right) q}{GA1\,GA2} \quad \textbf{(17)}$$

> $w3 := simplify(w3);$

$$w3 := -\frac{1}{GA1\,GA2\,GA3}\left(\left(\left((b - x)\left(-\frac{b}{2} + L - \frac{x}{2}\right) GA2 + GA3\left(-\frac{a}{2} - \frac{b}{2} + L\right)(a - b)\right) GA1 - GA3\,a\,GA2\left(L - \frac{a}{2}\right)\right) q\right) \quad \textbf{(18)}$$

>

> $V1 := simplify(V1);$

$$V1 := q\,(L - x) \quad \textbf{(19)}$$

> $V2 := simplify(V2);$

$$V2 := q\,(L - x) \quad \textbf{(20)}$$

EULER BERNOULLI - ONE FIELD -

```
> restart :
>
> ODE := EI·diff(w1(x), x$4) = q;
```

$$ODE := EI\left(\frac{d^4}{dx^4}\, w1(x)\right) = q \tag{1}$$

```
>
> w1 := rhs(dsolve(ODE, w1(x)));
```

$$w1 := \frac{q\,x^4}{24\,EI} + \frac{\_C1\,x^3}{6} + \frac{\_C2\,x^2}{2} + \_C3\,x + \_C4 \tag{2}$$

```
> phi1 := -diff(w1, x); kappa1 := diff(phi1, x); M1 := EI*kappa1; V1 := diff(M1, x);
```

$$\phi 1 := -\frac{q\,x^3}{6\,EI} - \frac{\_C1\,x^2}{2} - \_C2\,x - \_C3$$

$$\kappa 1 := -\frac{q\,x^2}{2\,EI} - \_C1\,x - \_C2$$

$$M1 := EI\left(-\frac{q\,x^2}{2\,EI} - \_C1\,x - \_C2\right)$$

$$V1 := EI\left(-\frac{q\,x}{EI} - \_C1\right) \tag{3}$$

```
>
> x := 0 : eq1 := w1 = 0; eq2 := phi1 = 0;
```

$$eq1 := \_C4 = 0$$

$$eq2 := -\_C3 = 0 \tag{4}$$

```
> x := L : eq3 := M1 = 0; eq4 := V1 = 0;
```

$$eq3 := EI\left(-\frac{q\,L^2}{2\,EI} - \_C1\,L - \_C2\right) = 0$$

$$eq4 := EI\left(-\frac{q\,L}{EI} - \_C1\right) = 0 \tag{5}$$

```
> sol := solve({eq1, eq2, eq3, eq4}, {_C1, _C2, _C3, _C4}) : assign(sol) : x :='x';
```

$$x := x \tag{6}$$

```
>
> w1 := simplify(w1);
```

$$w1 := \frac{q\,x^2\left(6\,L^2 - 4\,L\,x + x^2\right)}{24\,EI} \tag{7}$$

```
> V1 := simplify(V1);
```

$$V1 := q\,(L - x) \tag{8}$$

```
> M1 := simplify(M1);
```

$$M1 := -\frac{q\,(L-x)^2}{2} \tag{9}$$

EULER BERNOULLI - TWO FIELDS -

```
> restart;
> EI1 := EI : EI2 := EI2 :
> w1 := q*x^4/(24*EI1) + C1 + C2*x + C3*x^2 + C4*x^3;
```

$$w1 := \frac{q\,x^4}{24\,EI} + C1 + C2\,x + C3\,x^2 + C4\,x^3 \tag{1}$$

```
> w2 := q*x^4/(24*EI2) + D1 + D2*x + D3*x^2 + D4*x^3;
```

$$w2 := \frac{q\,x^4}{24\,EI2} + D1 + D2\,x + D3\,x^2 + D4\,x^3 \tag{2}$$

```
> phi1 := -diff(w1, x) : kappa1 := diff(phi1, x) : M1 := EI1*kappa1 : V1 := diff(M1, x) :
> phi2 := -diff(w2, x) : kappa2 := diff(phi2, x) :
> M2 := EI2*kappa2 : V2 := diff(M2, x) :
> x := 0 : eq1 := w1 = 0 : eq2 := phi1 = 0 :
> x := L : eq3 := V2 = 0 : eq4 := M2 = 0 :
> x := a; eq5 := w1 = w2 : eq6 := V1 = V2 : eq7 := M1 = M2 : eq8 := phi1 = phi2 :
```

$$x := a \tag{3}$$

```
> sol := solve({eq1, eq2, eq3, eq4, eq5, eq6, eq7, eq8},
  {C1, C2, C3, C4, D1, D2, D3, D4}) : assign(sol) :
> x :='x';
```

$$x := x \tag{4}$$

```
> w1 := simplify(w1);
```

$$w1 := \frac{q\,x^2\left(6\,L^2 - 4\,L\,x + x^2\right)}{24\,EI} \tag{5}$$

```
> w2 := simplify(w2);
```

$$w2 := \frac{1}{4\,EI\,EI2}\left(q\left(\left(\frac{EI}{2} - \frac{EI2}{2}\right)a^4 - \frac{4\left(L + \frac{x}{2}\right)(EI - EI2)\,a^3}{3} + L\,(EI - EI2)\,(L + 2\,x)\,a^2 - 2\,L^2\,x\,(EI - EI2)\,a + x^2\,EI\left(L^2 - \frac{2}{3}\,L\,x + \frac{1}{6}\,x^2\right)\right)\right) \tag{6}$$

```
> V1 := simplify(V1);
```

$$V1 := q\,(L - x) \tag{7}$$

```
> V2 := simplify(V2);
```

$$V2 := q\,(L - x) \tag{8}$$

```
> M1 := simplify(M1);
```

$$M1 := -\frac{q\,(L - x)^2}{2} \tag{9}$$

```
> M2 := simplify(M2);
```

$$M2 := -\frac{q\,(L - x)^2}{2} \tag{10}$$

TIMOSHENKO BEAM - ONE FIELD - STATIC DETERMINATE

```
> restart :
> M := -1·(1/2)*q*(x-L)**2; V := diff(M,x);
```

$$M := -\frac{q\,(x-L)^2}{2}$$

$$V := -q\,(x-L) \tag{1}$$

```
> ODE := diff(w(x),x$2) =-q/GA-M/EI;
```

$$ODE := \frac{d^2}{dx^2}\,w(x) = -\frac{q}{GA} + \frac{q\,(x-L)^2}{2\,EI} \tag{2}$$

```
> w := rhs(dsolve(ODE,w(x)));
```

$$w := \frac{q\,(-x+L)^4}{24\,EI} - \frac{q\,x^2}{2\,GA} + \_C1\,x + \_C2 \tag{3}$$

```
> gamma1 := V/GA;
```

$$\gamma 1 := -\frac{q\,(x-L)}{GA} \tag{4}$$

```
> phi := -diff(w,x) + gamma1;
```

$$\phi := \frac{q\,(-x+L)^3}{6\,EI} + \frac{q\,x}{GA} - \_C1 - \frac{q\,(x-L)}{GA} \tag{5}$$

```
> x := 0; eq1 := phi = 0; eq2 := w = 0;
```

$$x := 0$$

$$eq1 := \frac{q\,L^3}{6\,EI} - \_C1 + \frac{q\,L}{GA} = 0$$

$$eq2 := \frac{q\,L^4}{24\,EI} + \_C2 = 0 \tag{6}$$

```
> sol := solve({eq1,eq2},{_C1,_C2}) : assign(sol) : x :='x':
> w := simplify(w);
```

$$w := \frac{q\,x\,\left(6\,GA\,L^2\,x - 4\,GA\,L\,x^2 + GA\,x^3 + 24\,EI\,L - 12\,x\,EI\right)}{24\,GA\,EI} \tag{7}$$

TIMOSHENKO BEAM - THREE FIELDS - STATIC DETERMINATE

```
> restart :
> M0 := q·L·L/2; V0 := q·L;
```

$$M0 := \frac{q\,L^2}{2}$$

$$V0 := q\,L \tag{1}$$

```
> M1 := -M0 - q·x·(x/2) + V0·x : simplify(M1) : M2 := -M0 - q·x·(x/2) + V0·x :
      simplify(M2) : M3 := M2 :
> V1 := diff(M1, x) : V2 := diff(M2, x) : V3 := V2 :
>
```

```
> ODE1 := diff(w1(x), x$2) = -q/GA1 - M1/EI1;
```

$$ODE1 := \frac{d^2}{dx^2}\,w1(x) = -\frac{q}{GA1} - \frac{-\frac{1}{2}\,q\,L^2 - \frac{1}{2}\,q\,x^2 + q\,L\,x}{EI1} \tag{2}$$

```
> ODE2 := diff(w2(x), x$2) = -q/GA2 - M2/EI2;
```

$$ODE2 := \frac{d^2}{dx^2}\,w2(x) = -\frac{q}{GA2} - \frac{-\frac{1}{2}\,q\,L^2 - \frac{1}{2}\,q\,x^2 + q\,L\,x}{EI2} \tag{3}$$

```
> ODE3 := diff(w3(x), x$2) = -q/GA3 - M3/EI3;
```

$$ODE3 := \frac{d^2}{dx^2}\,w3(x) = -\frac{q}{GA3} - \frac{-\frac{1}{2}\,q\,L^2 - \frac{1}{2}\,q\,x^2 + q\,L\,x}{EI3} \tag{4}$$

```
> sol1 := dsolve({ODE1, ODE2, ODE3}, {w1(x), w2(x), w3(x)}) : assign(sol1) :
> w1 := (w1(x)); w2 := (w2(x)); w3 := (w3(x));
```

$$w1 := \_C6 + \_C5\,x + \frac{\frac{1}{4}\,q\,L^2\,x^2 - \frac{1}{6}\,q\,L\,x^3 + \frac{1}{24}\,q\,x^4}{EI1} - \frac{q\,x^2}{2\,GA1}$$

$$w2 := \frac{q\,L^2\,x^2}{4\,EI2} - \frac{q\,L\,x^3}{6\,EI2} + \frac{q\,x^4}{24\,EI2} - \frac{q\,x^2}{2\,GA2} + \_C3\,x + \_C4$$

$$w3 := \frac{q\,L^2\,x^2}{4\,EI3} - \frac{q\,L\,x^3}{6\,EI3} + \frac{q\,x^4}{24\,EI3} - \frac{q\,x^2}{2\,GA3} + \_C1\,x + \_C2 \tag{5}$$

```
> gamma1 := V1/GA1; gamma2 := V2/GA2; gamma3 := V3/GA3; phi1 := -diff(w1, x) + gamma1;
      phi2 := -diff(w2, x) + gamma2; phi3 := -diff(w3, x) + gamma3;
```

$$\gamma 1 := \frac{q\,L - q\,x}{GA1}$$

$$\gamma 2 := \frac{q\,L - q\,x}{GA2}$$

$$\gamma 3 := \frac{q\,L - q\,x}{GA3}$$

$$\phi 1 := -\_C5 - \frac{\frac{1}{2}\,q\,L^2\,x - \frac{1}{2}\,q\,L\,x^2 + \frac{1}{6}\,x^3\,q}{EI1} + \frac{q\,x}{GA1} + \frac{q\,L - q\,x}{GA1}$$

$$\phi 2 := -\frac{q\,L^2\,x}{2\,EI2} + \frac{q\,L\,x^2}{2\,EI2} - \frac{x^3\,q}{6\,EI2} + \frac{q\,x}{GA2} - \_C3 + \frac{q\,L - q\,x}{GA2}$$

$$\phi 3 := -\frac{q\,L^2\,x}{2\,EI3} + \frac{q\,L\,x^2}{2\,EI3} - \frac{x^3\,q}{6\,EI3} + \frac{q\,x}{GA3} - \_C1 + \frac{q\,L - q\,x}{GA3} \qquad (6)$$

>

> $x := 0;\ eq1 := w1 = 0;\ eq2 := phi1 = 0;$

$$x := 0$$

$$eq1 := \_C6 = 0$$

$$eq2 := -\_C5 + \frac{q\,L}{GA1} = 0 \qquad (7)$$

> $x := a;\ eq3 := w1 = w2;\ \ eq4 := phi1 = phi2;$

$$x := a$$

$$eq3 := \_C6 + \_C5\,a + \frac{\frac{1}{4}\,q\,L^2\,a^2 - \frac{1}{6}\,q\,L\,a^3 + \frac{1}{24}\,q\,a^4}{EI1} - \frac{q\,a^2}{2\,GA1} = \frac{q\,L^2\,a^2}{4\,EI2} - \frac{q\,L\,a^3}{6\,EI2} + \frac{q\,a^4}{24\,EI2} - \frac{q\,a^2}{2\,GA2} + \_C3\,a + \_C4$$

$$eq4 := -\_C5 - \frac{\frac{1}{2}\,q\,L^2\,a - \frac{1}{2}\,q\,L\,a^2 + \frac{1}{6}\,a^3\,q}{EI1} + \frac{q\,a}{GA1} + \frac{q\,L - a\,q}{GA1} = -\frac{q\,L^2\,a}{2\,EI2} + \frac{q\,L\,a^2}{2\,EI2} - \frac{a^3\,q}{6\,EI2} + \frac{q\,a}{GA2} - \_C3 + \frac{q\,L - a\,q}{GA2} \qquad (8)$$

> $x := b;\ eq5 := w3 = w2;\ \ eq6 := phi3 = phi2;$

$$x := b$$

$$eq5 := \frac{q\,L^2\,b^2}{4\,EI3} - \frac{q\,L\,b^3}{6\,EI3} + \frac{q\,b^4}{24\,EI3} - \frac{q\,b^2}{2\,GA3} + \_C1\,b + \_C2 = \frac{q\,L^2\,b^2}{4\,EI2} - \frac{q\,L\,b^3}{6\,EI2} + \frac{q\,b^4}{24\,EI2} - \frac{q\,b^2}{2\,GA2} + \_C3\,b + \_C4$$

$$eq6 := -\frac{q\,L^2\,b}{2\,EI3} + \frac{q\,L\,b^2}{2\,EI3} - \frac{b^3\,q}{6\,EI3} + \frac{q\,b}{GA3} - \_C1 + \frac{q\,L - b\,q}{GA3} = -\frac{q\,L^2\,b}{2\,EI2} + \frac{q\,L\,b^2}{2\,EI2} - \frac{b^3\,q}{6\,EI2} + \frac{q\,b}{GA2} - \_C3 + \frac{q\,L - b\,q}{GA2} \qquad (9)$$

>

> $sol := solve(\{eq1, eq2, eq3, eq4, eq5, eq6\}, \{\_C1, \_C2, \_C3, \_C4, \_C5, \_C6\}) : assign(sol) :$
> $x := 'x';$

$$x := x \qquad (10)$$

>

```
> w1 := simplify(w1);
```

$$w1 := \frac{q\,x\,(6\,GA1\,L^2\,x - 4\,GA1\,L\,x^2 + GA1\,x^3 + 24\,L\,EI1 - 12\,x\,EI1)}{24\,GA1\,EI1} \tag{11}$$

```
> w2 := simplify(w2);
```

$$w2 := \frac{1}{4\,EI1\,EI2\,GA1\,GA2}\left(q\left(\left(\left((a-x)^2\left(\frac{a^2}{2} + \left(-\frac{4\,L}{3} + \frac{x}{3}\right)a + L^2 - \frac{2\,L\,x}{3} + \frac{x^2}{6}\right)EI1 - a\,EI2\left(\frac{a^3}{2} + \left(-\frac{4\,L}{3} - \frac{2\,x}{3}\right)a^2 + L\,(L+2\,x)\,a - 2\,L^2\,x\right)\right)GA2 - 4\,EI1\,EI2\,(a-x)\left(-\frac{a}{2} + L - \frac{x}{2}\right)\right)GA1 + 4\,GA2\,a\,EI1\,EI2\left(L - \frac{a}{2}\right)\right)\right) \tag{12}$$

```
> w3 := simplify(w3);
```

$$w3 := \frac{1}{4\,EI1\,EI2\,EI3\,GA1\,GA2\,GA3}\left(q\left(\left(\left(\left(\left(\left((a+b-2\,x)\,L^2 + \left((2\,a+2\,b)\,x - \frac{4\,a^2}{3} - \frac{4\,a\,b}{3} - \frac{4\,b^2}{3}\right)L + \left(-\frac{2}{3}\,a^2 - \frac{2}{3}\,a\,b - \frac{2}{3}\,b^2\right)x + \frac{(a+b)\,(a^2+b^2)}{2}\right)(a-b)\,EI3 + EI2\,(b-x)^2\left(L^2 + \left(-\frac{4\,b}{3} - \frac{2\,x}{3}\right)L + \frac{b^2}{2} + \frac{b\,x}{3} + \frac{x^2}{6}\right)\right)EI1 - EI2\left((a-2\,x)\,L^2 + \left(-\frac{4}{3}\,a^2 + 2\,a\,x\right)L + \frac{\left(a - \frac{4\,x}{3}\right)a^2}{2}\right)EI3\,a\right)GA3 - 4\,EI2\,(b-x)\,EI3\,EI1\left(-\frac{b}{2} + L - \frac{x}{2}\right)\right)GA2 - 4\,GA3\,EI2\,EI3\,EI1\left(-\frac{a}{2} + L - \frac{b}{2}\right)(a-b)\right)GA1 + 4\,GA3\,EI2\,GA2\,EI3\,a\,EI1\left(L - \frac{a}{2}\right)\right)\right) \tag{13}$$

TIMOSHENKO BEAM - ONE FIELD - GENERIC

```
> restart;
> DV1 := EI*diff(phi(x), x$2) - GA*(diff(w(x), x) + phi(x)) = 0;
```

$$DV1 := EI\left(\frac{d^2}{dx^2}\,\phi(x)\right) - GA\left(\frac{d}{dx}\,w(x) + \phi(x)\right) = 0 \tag{1}$$

```
> DV2 := GA*(diff(w(x), x$2) + diff(phi(x), x)) = -q;
```

$$DV2 := GA\left(\frac{d^2}{dx^2}\,w(x) + \frac{d}{dx}\,\phi(x)\right) = -q \tag{2}$$

```
> sol1 := dsolve({DV1, DV2}, {w(x), phi(x)}) : assign(sol1) :
> w := (w(x)); phi := (phi(x));
```

$$w := \frac{q\,x^4}{24\,EI} + \frac{\_C1\,x^3}{6} + \frac{\_C2\,x^2}{2} + \_C3\,x + \_C4$$

$$\phi := -\frac{\_C1\,x^2}{2} - \frac{q\,x^3}{6\,EI} - \_C2\,x - \frac{EI\,\_C1}{GA} - \_C3 - \frac{q\,x}{GA} \tag{3}$$

```
>
```

```
> Gamma := diff(w, x) + phi;  kappa := diff(phi, x);
```

$$\Gamma := -\frac{EI\,\_C1}{GA} - \frac{q\,x}{GA}$$

$$\kappa := -\_C1\,x - \frac{q\,x^2}{2\,EI} - \_C2 - \frac{q}{GA} \tag{4}$$

```
>
```

sectional forces :

```
> V := GA*Gamma; M := EI*kappa;
```

$$V := GA\left(-\frac{EI\,\_C1}{GA} - \frac{q\,x}{GA}\right)$$

$$M := EI\left(-\_C1\,x - \frac{q\,x^2}{2\,EI} - \_C2 - \frac{q}{GA}\right) \tag{5}$$

```
>
```

```
> x := 0 : eq1 := w = 0 : eq2 := phi = 0 :
> x := L : eq3 := V = 0 : eq4 := M = 0 :
> sol2 := solve({eq1, eq2, eq3, eq4}, {_C1, _C2, _C3, _C4}) : assign(sol2); x := 'x':
> w := simplify(w);
```

$$w := \frac{q\,x\left(6\,GA\,L^2\,x - 4\,L\,x^2\,GA + x^3\,GA + 24\,L\,EI - 12\,EI\,x\right)}{24\,EI\,GA} \tag{6}$$

```
> M := simplify(M);
```

$$M := -\frac{q\,(L-x)^2}{2} \tag{7}$$

```
> V := simplify(V);
```

$$V := q\ (L - x) \tag{8}$$

TIMOSHENKO BEAM - THREE FIELDS - GENERIC

```
>
>
> restart;
> DV1 := EI*diff(phi(x),x$2)-GA*(diff(w(x),x)+phi(x))=0;
```

$$DV1 := EI\left(\frac{d^2}{dx^2}\,\phi(x)\right) - GA\left(\frac{d}{dx}\,w(x) + \phi(x)\right) = 0 \tag{1}$$

```
> DV2 := GA*(diff(w(x),x$2)+diff(phi(x),x))=-q;
```

$$DV2 := GA\left(\frac{d^2}{dx^2}\,w(x) + \frac{d}{dx}\,\phi(x)\right) = -q \tag{2}$$

```
> DV3 := EI2*diff(phi2(x),x$2)-GA2*(diff(w2(x),x)+phi2(x))=0;
```

$$DV3 := EI2\left(\frac{d^2}{dx^2}\,\phi2(x)\right) - GA2\left(\frac{d}{dx}\,w2(x) + \phi2(x)\right) = 0 \tag{3}$$

```
> DV4 := GA2*(diff(w2(x),x$2)+diff(phi2(x),x))=-q;
```

$$DV4 := GA2\left(\frac{d^2}{dx^2}\,w2(x) + \frac{d}{dx}\,\phi2(x)\right) = -q \tag{4}$$

```
> DV5 := EI3*diff(phi3(x),x$2)-GA3*(diff(w3(x),x)+phi3(x))=0;
```

$$DV5 := EI3\left(\frac{d^2}{dx^2}\,\phi3(x)\right) - GA3\left(\frac{d}{dx}\,w3(x) + \phi3(x)\right) = 0 \tag{5}$$

```
> DV6 := GA3*(diff(w3(x),x$2)+diff(phi3(x),x))=-q;
```

$$DV6 := GA3\left(\frac{d^2}{dx^2}\,w3(x) + \frac{d}{dx}\,\phi3(x)\right) = -q \tag{6}$$

```
> sol1 := dsolve({DV1,DV2,DV3,DV4,DV5,DV6},{w(x),phi(x),w2(x),phi2(x),w3(x),
      phi3(x)}):assign(sol1):
> w := (w(x)); phi := (phi(x)); w2 := (w2(x)); phi2 := (phi2(x)); w3 := (w3(x)); phi3 :=
      (phi3(x));
```

$$w := \frac{q\,x^4}{24\,EI} + \frac{\_C9\,x^3}{6} + \frac{\_C10\,x^2}{2} + \_C11\,x + \_C12$$

$$\phi := -\frac{\_C9\,x^2}{2} - \frac{q\,x^3}{6\,EI} - \_C10\,x - \frac{EI\,\_C9}{GA} - \_C11 - \frac{q\,x}{GA}$$

$$w2 := \frac{q\,x^4}{24\,EI2} + \frac{\_C5\,x^3}{6} + \frac{\_C6\,x^2}{2} + \_C7\,x + \_C8$$

$$\phi2 := -\frac{\_C5\,x^2}{2} - \frac{q\,x^3}{6\,EI2} - \_C6\,x - \frac{EI2\,\_C5}{GA2} - \_C7 - \frac{q\,x}{GA2}$$

$$w3 := \frac{q\,x^4}{24\,EI3} + \frac{\_C1\,x^3}{6} + \frac{\_C2\,x^2}{2} + \_C3\,x + \_C4$$

$$\phi3 := -\frac{\_C1\,x^2}{2} - \frac{q\,x^3}{6\,EI3} - \_C2\,x - \frac{EI3\,\_C1}{GA3} - \_C3 - \frac{q\,x}{GA3} \tag{7}$$

```
>
```

```
> Gamma := diff(w, x) + phi;  kappa := diff(phi, x); Gamma2 := diff(w2, x) + phi2;
      kappa2 := diff(phi2, x); Gamma3 := diff(w3, x) + phi3;  kappa3 := diff(phi3, x);
```

$$\Gamma := -\frac{EI\_C9}{GA} - \frac{q\,x}{GA}$$

$$\kappa := -\_C9\,x - \frac{q\,x^2}{2\,EI} - \_C10 - \frac{q}{GA}$$

$$\Gamma 2 := -\frac{EI2\_C5}{GA2} - \frac{q\,x}{GA2}$$

$$\kappa 2 := -\_C5\,x - \frac{q\,x^2}{2\,EI2} - \_C6 - \frac{q}{GA2}$$

$$\Gamma 3 := -\frac{EI3\_C1}{GA3} - \frac{q\,x}{GA3}$$

$$\kappa 3 := -\_C1\,x - \frac{q\,x^2}{2\,EI3} - \_C2 - \frac{q}{GA3} \qquad \textbf{(8)}$$

```
>
```

sectional forces :

```
> V := GA*Gamma; M := EI*kappa; V2 := GA2*Gamma2; M2 := EI2*kappa2; V3 := GA3
      *Gamma3; M3 := EI3*kappa3;
```

$$V := GA\left(-\frac{EI\_C9}{GA} - \frac{q\,x}{GA}\right)$$

$$M := EI\left(-\_C9\,x - \frac{q\,x^2}{2\,EI} - \_C10 - \frac{q}{GA}\right)$$

$$V2 := GA2\left(-\frac{EI2\_C5}{GA2} - \frac{q\,x}{GA2}\right)$$

$$M2 := EI2\left(-\_C5\,x - \frac{q\,x^2}{2\,EI2} - \_C6 - \frac{q}{GA2}\right)$$

$$V3 := GA3\left(-\frac{EI3\_C1}{GA3} - \frac{q\,x}{GA3}\right)$$

$$M3 := EI3\left(-\_C1\,x - \frac{q\,x^2}{2\,EI3} - \_C2 - \frac{q}{GA3}\right) \qquad \textbf{(9)}$$

```
>
```

boundary condition, clamped at the left, simply supported at the right :

```
> x := 0 : eq1 := w = 0 : eq2 := phi = 0 :
>
>
>
> x := a : eq3 := w = w2 : eq4 := phi = phi2 : eq5 := M = M2 : eq6 := V = V2 :
> x := b : eq7 := w3 = w2 : eq8 := phi3 = phi2 : eq9 := M3 = M2 : eq10 := V3 = V2 :
```

```
> x := L : eq11 := M3 = 0 : eq12 := V3 = 0 :
> sol2 := solve( {eq1, eq2, eq3, eq4, eq5, eq6, eq7, eq8, eq9, eq10, eq11, eq12}, {_C1, _C2, _C3,
      _C4, _C5, _C6, _C7, _C8, _C9, _C10, _C11, _C12} ) : assign(sol2); x :='x':
> w := simplify(w);
```

$$w := \frac{q\,x\,(6\,GA\,L^2\,x - 4\,L\,x^2\,GA + x^3\,GA + 24\,L\,EI - 12\,EI\,x)}{24\,EI\,GA} \tag{10}$$

```
> w2 := simplify(w2);
```

$$w2 := \frac{1}{4\,EI\,GA\,EI2\,GA2}\left(\left(\left(\left(\left(\frac{a^2}{2} + \left(-\frac{4\,L}{3} + \frac{x}{3}\right)a + L^2 - \frac{2\,L\,x}{3} + \frac{x^2}{6}\right)(a-x)^2\,EI - \left(\frac{a^3}{2} + \left(-\frac{4\,L}{3} - \frac{2\,x}{3}\right)a^2 + L\,(L+2\,x)\,a - 2\,L^2\,x\right)a\,EI2\right)GA2 - 4\,EI\left(-\frac{a}{2} + L - \frac{x}{2}\right)(a-x)\,EI2\right)GA + 4\left(L - \frac{a}{2}\right)GA2\,EI\,a\,EI2\right)q\right) \tag{11}$$

```
> w3 := simplify(w3);
```

$$w3 := \frac{1}{4\,EI\,EI2\,EI3\,GA\,GA2\,GA3}\left(\left(\left(\left(\left(\left((a-b)\left((a+b-2\,x)\,L^2 + \left((2\,a+2\,b)\,x - \frac{4\,a^2}{3} - \frac{4\,a\,b}{3} - \frac{4\,b^2}{3}\right)L + \left(-\frac{2}{3}\,a^2 - \frac{2}{3}\,a\,b - \frac{2}{3}\,b^2\right)x + \frac{(a+b)\,(a^2+b^2)}{2}\right)EI3 + EI2\left(L^2 + \left(-\frac{4\,b}{3} - \frac{2\,x}{3}\right)L + \frac{b^2}{2} + \frac{b\,x}{3} + \frac{x^2}{6}\right)(b-x)^2\right)EI - \left((a-2\,x)\,L^2 + \left(-\frac{4}{3}\,a^2 + 2\,a\,x\right)L + \frac{\left(a - \frac{4\,x}{3}\right)a^2}{2}\right)EI2\,a\,EI3\right)GA3 - 4\,EI\,EI2\,(b-x)\left(-\frac{b}{2} + L - \frac{x}{2}\right)EI3\right)GA2 - 4\,(a-b)\,EI\left(-\frac{a}{2} + L - \frac{b}{2}\right)EI2\,GA3\,EI3\right)GA + 4\left(L - \frac{a}{2}\right)EI\,EI2\,GA2\,a\,GA3\,EI3\right)q\right) \tag{12}$$

```
>
>
> w := simplify(w);
```

$$w := \frac{q\,x\,(6\,GA\,L^2\,x - 4\,L\,x^2\,GA + x^3\,GA + 24\,L\,EI - 12\,EI\,x)}{24\,EI\,GA} \tag{13}$$

```
> w2 := simplify(w2);
```

$$w2 := \frac{1}{4\,EI\,GA\,EI2\,GA2}\left(\left(\left(\left(\left(\frac{a^2}{2} + \left(-\frac{4\,L}{3} + \frac{x}{3}\right)a + L^2 - \frac{2\,L\,x}{3} + \frac{x^2}{6}\right)(a-x)^2\,EI - \left(\frac{a^3}{2} + \left(-\frac{4\,L}{3} - \frac{2\,x}{3}\right)a^2 + L\,(L+2\,x)\,a - 2\,L^2\,x\right)a\,EI2\right)GA2 - 4\,EI\left(-\frac{a}{2} + L\right.\right.\right.\right. \tag{14}$$

$$-\frac{x}{2}\right)(a-x)\,EI2\Bigg)GA+4\left(L-\frac{a}{2}\right)GA2\,EI\,a\,EI2\Bigg)q\Bigg)$$

> $w3 := simplify(w3);$

$$w3 := \frac{1}{4\,EI\,EI2\,EI3\,GA\,GA2\,GA3}\Bigg(\Bigg(\Bigg(\Bigg(\Bigg(\Bigg((a-b)\left((a+b-2x)L^2+\left((2a+2b)x\right.\right. \tag{15}$$

$$\left.-\frac{4a^2}{3}-\frac{4ab}{3}-\frac{4b^2}{3}\right)L+\left(-\frac{2}{3}a^2-\frac{2}{3}ab-\frac{2}{3}b^2\right)x+\frac{(a+b)\left(a^2+b^2\right)}{2}\right)$$

$$EI3+EI2\left(L^2+\left(-\frac{4b}{3}-\frac{2x}{3}\right)L+\frac{b^2}{2}+\frac{bx}{3}+\frac{x^2}{6}\right)(b-x)^2\Bigg)EI-\Bigg((a-2x)L^2$$

$$+\left(-\frac{4}{3}a^2+2ax\right)L+\frac{\left(a-\frac{4x}{3}\right)a^2}{2}\Bigg)EI2\,a\,EI3\Bigg)GA3-4\,EI\,EI2\,(b-x)\left(-\frac{b}{2}$$

$$+L-\frac{x}{2}\right)EI3\Bigg)GA2-4\,(a-b)\,EI\left(-\frac{a}{2}+L-\frac{b}{2}\right)EI2\,GA3\,EI3\Bigg)GA+4\Bigg(L$$

$$\left.-\frac{a}{2}\right)EI\,EI2\,GA2\,a\,GA3\,EI3\Bigg)q\Bigg)$$

> $M := simplify(M);$

$$M := -\frac{q\,(L-x)^2}{2} \tag{16}$$

> $M2 := simplify(M2);$

$$M2 := -\frac{q\,(L-x)^2}{2} \tag{17}$$

> $M3 := simplify(M3);$

$$M3 := -\frac{q\,(L-x)^2}{2} \tag{18}$$

> $V := simplify(V);$

$$V := q\,(L-x) \tag{19}$$

> $V2 := simplify(V2);$

$$V2 := q\,(L-x) \tag{20}$$

> $V3 := simplify(V3);$

$$V3 := q\,(L-x) \tag{21}$$

COMBINED SYSTEM - ONE FIELD

```
>
> restart;
> ODE1 := EI·diff(w1(x), x$4) - GA1·diff(w1(x), x$2) = q;
```

$$ODE1 := EI\left(\frac{d^4}{dx^4}\, w1(x)\right) - GA1\left(\frac{d^2}{dx^2}\, w1(x)\right) = q \tag{1}$$

```
> w1 := rhs(dsolve(ODE1));
```

$$w1 := \frac{\_C2\, EI\, e^{\frac{\sqrt{GA1}\, x}{\sqrt{EI}}}}{GA1} - \frac{q\, x^2}{2\, GA1} + \frac{\_C1\, EI\, e^{-\frac{\sqrt{GA1}\, x}{\sqrt{EI}}}}{GA1} + \_C3\, x + \_C4 \tag{2}$$

```
> phi := diff(w1, x);
```

$$\phi := \frac{\_C2\sqrt{EI}\, e^{\frac{\sqrt{GA1}\, x}{\sqrt{EI}}}}{\sqrt{GA1}} - \frac{q\, x}{GA1} - \frac{\_C1\sqrt{EI}\, e^{-\frac{\sqrt{GA1}\, x}{\sqrt{EI}}}}{\sqrt{GA1}} + \_C3 \tag{3}$$

```
> M := -EI·diff(w1, x$2);
```

$$M := -EI\left(e^{\frac{\sqrt{GA1}\, x}{\sqrt{EI}}}\, \_C2 + e^{-\frac{\sqrt{GA1}\, x}{\sqrt{EI}}}\, \_C1 - \frac{q}{GA1}\right) \tag{4}$$

```
> V := GA1·diff(w1, x) - EI·diff(w1, x$3);
```

$$V := GA1\left(\frac{\_C2\sqrt{EI}\, e^{\frac{\sqrt{GA1}\, x}{\sqrt{EI}}}}{\sqrt{GA1}} - \frac{q\, x}{GA1} - \frac{\_C1\sqrt{EI}\, e^{-\frac{\sqrt{GA1}\, x}{\sqrt{EI}}}}{\sqrt{GA1}} + \_C3\right) - EI\left(\frac{\sqrt{GA1}\, e^{\frac{\sqrt{GA1}\, x}{\sqrt{EI}}}\, \_C2}{\sqrt{EI}} - \frac{\sqrt{GA1}\, e^{-\frac{\sqrt{GA1}\, x}{\sqrt{EI}}}\, \_C1}{\sqrt{EI}}\right) \tag{5}$$

```
> x := 0 :  eq1 := w1 = 0;  eq2 := phi = 0;
```

$$eq1 := \frac{EI\, \_C2}{GA1} + \frac{\_C1\, EI}{GA1} + \_C4 = 0$$

$$eq2 := \frac{\_C2\sqrt{EI}}{\sqrt{GA1}} - \frac{\_C1\sqrt{EI}}{\sqrt{GA1}} + \_C3 = 0 \tag{6}$$

```
> x := L : eq3 := M = 0; eq4 := V = 0;
```

$$eq3 := -EI\left(e^{\frac{\sqrt{GA1}\, L}{\sqrt{EI}}}\, \_C2 + e^{-\frac{\sqrt{GA1}\, L}{\sqrt{EI}}}\, \_C1 - \frac{q}{GA1}\right) = 0$$

$$eq4 := GA1\left(\frac{\_C2\sqrt{EI}\, e^{\frac{\sqrt{GA1}\, L}{\sqrt{EI}}}}{\sqrt{GA1}} - \frac{q\, L}{GA1} - \frac{\_C1\sqrt{EI}\, e^{-\frac{\sqrt{GA1}\, L}{\sqrt{EI}}}}{\sqrt{GA1}} + \_C3\right) \tag{7}$$

$$-EI\left(\frac{\sqrt{GA1}\,e^{\frac{\sqrt{GA1}\,L}{\sqrt{EI}}}\,\_C2}{\sqrt{EI}}-\frac{\sqrt{GA1}\,e^{-\frac{\sqrt{GA1}\,L}{\sqrt{EI}}}\,\_C1}{\sqrt{EI}}\right)=0$$

> $sol := solve(\{eq1, eq2, eq3, eq4\}, \{\_C1, \_C2, \_C3, \_C4\}); assign(sol) : x := 'x';$

$$sol := \left\{\_C1=\frac{q\left(L\,e^{\frac{\sqrt{GA1}\,L}{\sqrt{EI}}}\,GA1^2\,EI^2+EI^{5/2}\,GA1^{3/2}\right)}{EI^{5/2}\,GA1^{5/2}\left(e^{\frac{\sqrt{GA1}\,L}{\sqrt{EI}}}+e^{-\frac{\sqrt{GA1}\,L}{\sqrt{EI}}}\right)},\ \_C2=-\frac{q\left(L\,e^{-\frac{\sqrt{GA1}\,L}{\sqrt{EI}}}\,GA1\,EI-EI^{3/2}\sqrt{GA1}\right)}{EI^{3/2}\,GA1^{3/2}\left(e^{\frac{\sqrt{GA1}\,L}{\sqrt{EI}}}+e^{-\frac{\sqrt{GA1}\,L}{\sqrt{EI}}}\right)},\ \_C3=\frac{q\,L}{GA1},\ \_C4=-\frac{q\left(\sqrt{EI}\,e^{\frac{\sqrt{GA1}\,L}{\sqrt{EI}}}\,\sqrt{GA1}\,L-\sqrt{GA1}\,\sqrt{EI}\,L\,e^{-\frac{\sqrt{GA1}\,L}{\sqrt{EI}}}+2\,EI\right)}{GA1^2\left(e^{\frac{\sqrt{GA1}\,L}{\sqrt{EI}}}+e^{-\frac{\sqrt{GA1}\,L}{\sqrt{EI}}}\right)}\right\}$$

$$x := x \qquad \textbf{(8)}$$

> $w1 := simplify(w1);$

$$w1 := \frac{1}{\sqrt{EI}\,GA1^{5/2}\left(2\,e^{\frac{2\sqrt{GA1}\,L}{\sqrt{EI}}}+2\right)}\left(2\,e^{-\frac{\sqrt{GA1}\,L}{\sqrt{EI}}}\,q\left(EI^{3/2}\sqrt{GA1}\,e^{\frac{\sqrt{GA1}\,(2L-x)}{\sqrt{EI}}}+EI\,GA1\,L\,e^{\frac{\sqrt{GA1}\,(3L-x)}{\sqrt{EI}}}+EI^{3/2}e^{\frac{\sqrt{GA1}\,(x+2L)}{\sqrt{EI}}}\sqrt{GA1}-L\,EI\,GA1\,e^{\frac{\sqrt{GA1}\,(L+x)}{\sqrt{EI}}}+\left(x\sqrt{EI}\left(L-\frac{x}{2}\right)GA1^{3/2}-L\,EI\,GA1\right)e^{\frac{3\sqrt{GA1}\,L}{\sqrt{EI}}}-2\,EI^{3/2}\sqrt{GA1}\,e^{\frac{2\sqrt{GA1}\,L}{\sqrt{EI}}}+\left(x\sqrt{EI}\left(L-\frac{x}{2}\right)GA1^{3/2}+L\,EI\,GA1\right)e^{\frac{\sqrt{GA1}\,L}{\sqrt{EI}}}\right)\right) \qquad \textbf{(9)}$$

> $M := simplify(M);$

$$M := \frac{1}{GA1^{3/2}\left(e^{\frac{2\sqrt{GA1}\,L}{\sqrt{EI}}}+1\right)}\left(e^{-\frac{\sqrt{GA1}\,L}{\sqrt{EI}}}\left(-\sqrt{GA1}\,\sqrt{EI}\,e^{\frac{\sqrt{GA1}\,(2L-x)}{\sqrt{EI}}}-GA1\,L\,e^{\frac{\sqrt{GA1}\,(3L-x)}{\sqrt{EI}}}-e^{\frac{\sqrt{GA1}\,(x+2L)}{\sqrt{EI}}}\sqrt{GA1}\,\sqrt{EI}+L\,GA1\,e^{\frac{\sqrt{GA1}\,(L+x)}{\sqrt{EI}}}\right.\right. \qquad \textbf{(10)}$$

$$+\sqrt{EI}\,\sqrt{GA1}\left(e^{\frac{\sqrt{GA1}\,L}{\sqrt{EI}}}+e^{\frac{3\sqrt{GA1}\,L}{\sqrt{EI}}}\right)\Bigg)\,q\,\sqrt{EI}\Bigg)$$

```
> V := simplify(V);
```

$$V := (L-x)\,q \tag{11}$$

```
>
```